University of Alberta

Fluid Inclusion and Stable Isotopic Study of Precious and Base Metal Veins from the Coeur d' Alene Ag-Pb-Zn district, Idaho, USA

by

Serguey Viktorov Arkadakskiy ©

A thesis submitted to the Faculty of Graduate Studies and Research in partial fulfillment of the requirements for the degree of Master of Science

Department of Earth and Atmospheric Sciences

Edmonton, Alberta

Fall, 2000

National Library
of Canada

Acquisitions and
Bibliographic Services

395 Wellington Street
Ottawa ON K1A 0N4
Canada

Bibliothèque nationale
du Canada

Acquisitions et
services bibliographiques

395, rue Wellington
Ottawa ON K1A 0N4
Canada

Your file Votre référence

Our file Notre référence

The author has granted a non-exclusive licence allowing the National Library of Canada to reproduce, loan, distribute or sell copies of this thesis in microform, paper or electronic formats.

The author retains ownership of the copyright in this thesis. Neither the thesis nor substantial extracts from it may be printed or otherwise reproduced without the author's permission.

L'auteur a accordé une licence non exclusive permettant à la Bibliothèque nationale du Canada de reproduire, prêter, distribuer ou vendre des copies de cette thèse sous la forme de microfiche/film, de reproduction sur papier ou sur format électronique.

L'auteur conserve la propriété du droit d'auteur qui protège cette thèse. Ni la thèse ni des extraits substantiels de celle-ci ne doivent être imprimés ou autrement reproduits sans son autorisation.

0-612-59773-3

Canada

University of Alberta

Library Release Form

Name of Author: Serguey V. Arkadakskiy

Title of thesis: **Fluid Inclusion and Stable Isotopic Study of Precious and Base Metal Veins from the Coeur d' Alene Ag-Pb-Zn district, Idaho, USA**

Degree: Master of Science

Year this Degree was Granted: 2000

Permission is hereby granted to the University of Alberta Library to reproduce single copies of this thesis and to lend or sell such copies for private, scholarly, or scientific purposes only.

The author reserves all other publication and other rights in association with the copyright in the thesis, and except as hereinbefore provided, neither the thesis nor any substantial portion thereof may be printed or otherwise reproduced in any material form whatever without the author's prior written permission.

222^b, app. 15, Borovo
Sofia, Bulgaria
1680

Date: 28.09.2000

ABSTRACT

Ag-Pb-Zn veins at the Coeur d'Alene district precipitated from CO_2-undersaturated ($X_{CO2} < 0.04$) fluids of moderate to high salinities (9 to 23 eq. wt. % NaCl) and uniform $\delta^{18}O_{fluid}$ (8.5 ± 2.4 ‰; n = 69). Microthermometric data and positive $\delta^{18}O$ and $\delta^{13}C$ correlation of vein siderite suggest that fluid mixing caused mineral deposition. Calculated $\delta^{13}C_{fluid}$ (-10.7 ± 2.1 ‰, n = 45) and $\delta^{34}S_{\Sigma S}$ (4.4 ± 1.6 ‰, n = 15) indicate carbon and sulphur derivation from oxidation of organic matter, and from leaching of preexisting sulphides of abiogenic or magmatic origin, respectively. Late $CO_2(N_2, CH_4)$-rich fluids (X_{CO2} 0.14 to 0.23) precipitated unmineralized quartz.

Immiscibility of CO_2-rich fluids caused gold deposition in Au-quartz veins in the district. Similar P-V-T-X properties suggest a common origin for the fluids associated with Au-quartz veins and late stage quartz in the Ag-Pb-Zn veins.

In contrast to previous studies suggesting Precambrian age for some Ag-Pb-Zn veins, similar fluid P-V-T-X properties and mineral stable isotopic compositions suggest that all veins studied formed simultaneously possibly during the Mesozoic.

University of Alberta

Faculty of Graduate Studies and Research

The undersigned certify that they have read, and recommended to the faculty of Graduate Studies and Research for acceptance, a thesis entitled Fluid Inclusion and Stable Isotopic Study of Precious and Base Metal Veins at the Coeur d' Alene Ag-Pb-Zn district, Idaho, USA submitted by Serguey V. Arkadakskiy in partial fulfillment of the requirements for the degree of Master of Science.

Dr. Jeremy P. Richards (supervisor)

Dr. Karlis Muehlenbachs (committee member)

Dr. Murray R. Gray (committee member)

Date: 28/9/00

Dedication

To Galina, Monika, and Nikola for their patience and understanding

TABLE OF CONTENTS

Chapter Page

I. INTRODUCTION 1
Results of previous studies 1
Objectives of the present study 3

II. GEOLOGICAL SETTINGS 5
Regional Geological Settings 5
Proterozoic evolution of the Belt Basin 7
East Kootenay metamorphic event 9
Termination of Belt Sedimentation 10
Grenville metamorphic event 10
Goat River Orogeny 10
Mesozoic Evolution of the Belt Supergroup 10

III. GENERAL GEOLOGY OF COEUR D'ALENE DISTRICT 12
Belt Supergroup 12
Metamorphic grade 13
Magmatic rocks in the district 13
Tectonic Settings 15
Tectonics related to the mineralization 16

IV. MINERAL DEPOSITS AND VEIN GEOLOGY 19
Vein types and classification 19
Age of the Ag-Pb-Zn veins 20
Sample location 24
Geology of silver and lead-zinc veins 25
Siderite-quartz-tetrahedrite (SQT) veins 26
Quartz-siderite-galena (QSG) veins 32
Siderite-quartz-sphalerite (SQS) veins 35
Hydrothermal alteration related to the Ag-Pb-Zn veins 38
Geology of the Coleman Au-quartz vein 39

V. FLUID INCLUSION STUDY 41
Introduction 41
Selection of material 41
Compositional types of fluid inclusions 42
Type 1: Aqueous inclusions 43
Type 2: low-X_{CO_2} fluid inclusions 43
Type 3: Intermediate-X_{CO_2} inclusions 45
Type 4: High-X_{CO_2} (CO_2-rich) inclusions 46
Results of microthermometric study 47
SQT veins (Sunshine Vein) 49
Stage I 49
Stage II 49
Stage II 50
QSG veins (Lucky Friday Main vein) 51

TABLE OF CONTENTS (Continued)

Chapter | Page

Stage II 51
Stage III 53
SQS veins (Gold Hunter mine) 53
Stage I 55
Stage II 55
Stage III 55
Au-quartz Coleman Vein 56
Fluid Compositions and Densities 58
SQT veins 64
Stages I and II 64
Stage III 64
QSG veins 64
Stage II 64
Stage III 64
SQS veins 65
Stages I and II 65
Stage III 65
Coleman Au-quartz vein 65

VI LIGHT STABLE ISOTOPE STUDY 67
Introduction 67
Analytical techniques 67
Oxygen and carbon isotopic composition of siderite 68
SQT veins 68
Stage I 68
Stage II 71
Siderite from the alteration envelope 71
QSG veins Stage I 71
Stage II 71
Siderite from the alteration envelope 72
SQS veins (Gold Hunter mine) 73
Stage I 73
Stage II 73
Siderite from the alteration envelope 74
Oxygen and carbon isotopic variance of stage I siderite 74
Stable isotopic composition of vein ankerite and calcite 74
Oxygen isotopic composition of vein quartz 74
Mineral pair thermometry 76
Choice of equilibrium fractionation expressions 77
Quartz-siderite pairs 77
Quartz–ankerite and quartz-calcite pairs 78
Sulphur Isotopes 79
Mineral Pair Thermometry 80

TABLE OF CONTENTS (Continued)

Chapter — Page

VII SOLUTE THERMOMETRY 82
Analytical methods 83
Results of the Na/K thermometry 83
  SQT veins 83
    Stage I 84
    Stage II 84
  QSG veins 86
    Stage II 86
    Stage III 86
Siderite-quartz-sphalerite (SQS) veins (Gold Hunter mine) 87
    Stage I 87
    Stages II and III 87
Au-quartz vein (Coleman vein) 87

VIII DISCUSSION 89
Estimation of fluid trapping P-T conditions 89
Type 2, low-X_{CO_2} fluid inclusions 89
Type 3, intermediate-X_{CO_2} and type 4, CO_2-rich fluid inclusions Evidence for fluid immiscibility? 90
Trapping P-T conditions in the SQT veins (Sunshine Vein) 93
  Stage I 94
  Stage II 94
  Stage III 94
Trapping conditions in the QSG veins (Lucky Friday main vein) 94
  Stage I 94
  Stage II 95
  Stage III 95
Trapping conditions in the SQS veins (Gold Hunter mine) 96
  Stage I 96
  Stage II 96
  Stage III 96
Trapping conditions in the Coleman Au-quartz vein 97
Summary of P-T-X data 97
Ag-Pb-Zn veins 97
Coleman Au-quartz vein 98
Stable isotope systematics 99
$\delta^{18}O$ and $\delta^{13}C$ variation 100
Fluid Isotopic Signature 108
Origin of Coeur d'Alene Ag-Pb-Zn hydrothermal fluids 112
  Source of water 112
  Source of carbon 114
  Source of sulphur 115
Coleman Au-quartz vein fluid source 116
Synthesis 117

TABLE OF CONTENTS (Continued)

Chapter Page

Conditions of mineral deposition during stage I at the QSG, SQS, and SQT veins 117
Silver mineralization 120
Late stage CO_2-rich fluids and subhorizontal quartz veins 123
Coleman Au-quartz vein 124
A model for Ag-Pb-Zn vein formation 125
Coeur d'Alene and other Ag-Pb-Zn vein deposits 128
Conclusions 130
References 135
Appendix I 146
Appendix II 152
Appendix III 155

LIST OF TABLES

Table | | Page
1.1 Proterozoic Evolution of the Belt Supergroup (modified after Burwash, 1993). 8

4.1 Various vein types at the four Ag-Pb-Zn mines studied (modified after Fryklund, 1964; Wavra et al., 1994; Eaton et al., 1995). 19

4.2 Paragenetic sequence in individual vein types in the Coeur d'Alene district. 26

5.1 Summary of microthermometric data for the principal vein types studied. 48

5.2 Fluid composition, molar volume, and density in Coeur d'Alene. Calculation of particular fluid inclusion compositions (e.g., CH_4 or N_2 as second important gas species in the carbonic phase) based on low temperature measurements and on the results of Fig. 5.9. 63

6.1 Range and average $\delta^{18}O_{SMOW}$ and $\delta^{13}C_{PDB}$ isotopic composition of vein and alteration siderite from the SQT veins at the Sunshine and Coeur mines, and the QSG and SQS veins at the Lucky Friday and Gold Hunter mines respectively. The errors quoted are $\pm 1\sigma$. 69

6.2 Geothermometry results based on $\Delta^{18}O_{QUARTZ\text{-}SIDERITE}$. 78

6.3 Sulphur isotopic data for sulphides and sulphosalts from the Coeur d'Alene district. 81

7.1 Summary of the important element ratios and temperatures obtained from bulk crush-leach analysis of vein quartz, siderite, sphalerite, and tetrahedrite from different precious and base-metal veins at the Coeur d'Alene district 85

8.1 Calculated trapping temperatures and pressures of individual fluid inclusion populations from SQS, QSG, and SQT veins and also from Au-quartz Coleman vein, Coeur d'Alene district 91

LIST OF FIGURES

Table Page

1.1 General features of the Coeur d'Alene mining district. Shown are the locations of the Silver Belt and also on some of the major past and current producers mentioned in the text (Modified after Eaton et al. 1995). 2

1.2 Geological map of the Belt Supergroup in Canada and the USA. (Modified after Harrison and Cressman, 1993). Shown is the outline of Coeur d'Alene mining district as seen on Fig. 3.1 6

1.3 Mineral belts in the Coeur d'Alene district. The first set contains belts No. 1, 2, 3, and 7 (Silver, Sunset, Carlisle-Hercules, and Golconda-Lucky Friday). The second set contains belts No. 4, 5, and 6 (Tamarack-Marsh; Rex-Snowstorm, and Gem-Gold Hunter belts; modified after Fryklund, 1964, and Reid, 1984). 17

5.1 a.Total homogenization temperature (Th_{total}), and b. calculated salinities (eq. wt % NaCl) for type 2 and 3 inclusions from stages I, II, and III at the SQT Sunshine vein. Calculated salinities for type 2 inclusions are not corrected for CO_2. 50

5.2 Total homogenization temperature (Th_{total}) against salinity (eq. wt. % NaCl) for type 2 and 3 fluid inclusion from stages I, II, and III at the SQT Sunshine vein. 50

5.2 a.Total homogenization temperature (Th_{total}), and b. calculated salinities (eq. wt % NaCl) for type 2 and 3 inclusions from stages II, and III at the QSG Lucky Friday main vein. Calculated salinities for type 2 inclusions are not corrected for CO_2. 52

5.4 Total homogenization temperature (Th_{total}) against salinity (eq. wt. % NaCl) for type 2 and 3 fluid inclusion from stages II and III at the QSG Lucky Friday Main vein. 52

5.5 a.Total homogenization temperature (Th_{total}), and b. calculated salinities (eq. wt % NaCl) for type 2 and 3 inclusions from stages I, II, and III in SQS veins at the Gold Hunter mine. Calculated salinities for type 2 inclusions are not corrected for CO_2. 54

LIST OF FIGURES (Continued)

Table Page

5.6 Total homogenization temperature (Th_{total}) against salinity (eq. wt. % NaCl) for type 2 and 3 fluid inclusion from stages I, II, and III in SQS veins at the Gold Hunter mine. 54

5.7 (a). Total homogenization temperature (Th_{total}), and (b). calculated salinities (eq. wt % NaCl) for type 3 inclusions from at the Au-quartz Coleman vein. 57

5.8 Total homogenization temperature (Th_{total}) against salinity (eq. wt. % NaCl) for type 3 fluid inclusion at the Coleman Au-quartz vein. 58

5.9 Plots of Th_{CO2} against Tm_{CO2} present microthermometric data from: a.QST Sunshine vein; b. QSG Lucky Friday Main vein; c. SQS veins in the Gold Hunter mine; d. Au-quartz vein. Fields I and II represent predominantly CO_2-CH_4 and CO_2-N_2 gas phase compositions respectively. The two fields are outlined on the basis of the data of Thiery and van den Kerkhof (1994). 60

6.1 Range of $\delta^{13}C_{PDB}$ (A) and $\delta^{18}O_{SMOW}$ (B) of stage I siderite from SQT veins at the Sunshine and Coeur mines, and QSG and SQS veins at the Lucky Friday and Gold Hunter mines. Two samples of stage III siderite from subhorizontal quartz veins at the Lucky Friday and Gold Hunter mines have $\delta^{18}O$ and $\delta^{13}C_{PDB}$ similar to that and are thus included in the stage II siderite group. 70

6.2 Oxygen and carbon isotopic composition of siderite from the alteration envelopes of the SQT, QSG, and SQS veins from the Sunshine, Lucky Friday, and Gold Hunter mines. Note that the veins at the Sunshine and Lucky Friday mines are hosted by the predominantly quartzitic rocks of the Revett and/or St. Regiss Formations. 72

6.3 Plot of $\delta^{13}C_{PDB}$ vs. $\delta^{18}O_{SMOW}$ of stage I siderite from SQT veins in the Sunshine and Coeur mines, and from QSG and SQS veins in the Lucky Friday and Gold Hunter mines, respectively. 75

LIST OF FIGURES (Continued)

Table Page

6.4 Oxygen isotopic composition of quartz from the SQT veins at the Sunshine and Coeur mines, the QSG and SQS veins at the Gold Hunter and Lucky Friday mines, and from Coleman Au-quartz vein. 76

6.5 Histogram of the sulphur isotopic composition of sphalerite, galena and tetrahedrite from the SQT, QSG, and QSQ veins in Coeur d'Alene district. 80

7.1 A. Graph of $\delta^{18}O$ and Na/K (atomic) against distance across Coleman Au-quartz vein at the surface and approximately 60 m underground (B). Note the V shaped Na/K trends in vein quartz with the lowest values near the vein walls. The lack of correlation between the Na/K and $\delta^{18}O$ values indicates that the variance in the Na/K ratios is not temperature dependent (see text for details). 88

8.1 Plot of $\delta^{13}C$ against $\delta^{18}O$ for vein siderite from stages I, II, and III at the SQT, QSG, and SQS veins. The fields of vein siderite from SQT veins at the Sunshine and Galena mines are from Eaton et al. (1995) and Yates (1987), respectively. The temperature dependent trend is calculated for siderite precipitated from a fluid having an average $\delta^{18}O$ and $\delta^{13}C$ of +8.5 ‰ and −10.7 ‰, respectively. The mixing trend is calculated assuming $\delta^{18}O$ and $\delta^{13}C$ of fluid (a) = +5 and −2; and +9 and −12 per mil for fluid B. The temperatures of the two fluids are assumed to be 150 and 325°C, respectively, and the fluid A is assumed to be dominated by HCO_2^-, whereas fluid B contains H_2CO_3. 101

8.2 Total homogenization temperature (Th_{total}) against salinity for fluid inclusions from different paragenetic stages at the QST, SQS, and QSG veins. 105

LIST OF FIGURES (Continued)

Table		Page
8.3	A. Graph of $\delta^{18}O$ against distance across Sunshine vein, level 3100, Sunshine mine. Note the Π–shaped isotopic trend in stage I siderite with the highest values at the vein centre. This trend is exactly the opposite of what was observed by Eaton et al. (1995) in SQT veins at the Sunshine mine. No evidence for faulting that could have juxtaposed parts of the vein formed at different places and or times were seen in the stope. B. Graph of $\delta^{13}C$ against distance. The $\delta^{13}C$ values of Siderite I show a trend similar to this of the $\delta^{18}O$ values in (A). The only exception is a single stage I siderite near the hanging wall which exhibits an unusually low $\delta^{13}C$	107
8.4	Calculated oxygen and carbon isotopic composition of hydrithermal fluids in equilibrium with vein siderite from stages I, II, and III at the SQS, QSG, and SQT veins.	110

LIST OF PLATES

PLATE		Page
1	SQT veins. (a). Coeur vein in the Coeur Mine (level 1600). (b). Sunshine vein, Sunshine mine (level 3100). Visible are unmineralizaed subhorizontal quartz veins that crosscut the SQT veins and continue in the host metasedimentary rocks.	27
2	Two different types of silver ore in the SQT veins. (a). Brecciated siderite I cemented by massive tetrahedrite and minor quartz, Coeur Mine (level 1600). (b). Megascopic euhedral tetrahedrite associated with irregular blebs of stage II quartz, Sunshine mine (level 3100).	29
3	(a). Transmitted light photomicrograph of stage II siderite filling small cavity in fractured early siderite, Sunshine vein. (b). Transmitted light photomicrograph of tetrahedrite crystal in fracture within stage I siderite, Sunshine mine. The light mineral that surrounds tetrahedrite is stage II siderite. To the left the fracture is filled with stage II quartz.	30
4	(a). SQT Sunshine vein. Reflected light photomicrograph of tetrahedrite, chalcopyrite, and galena in mutual crosscutting relationships. Boulangerite (white arrow) is hosted in tetrahedrite. (b). QSG Lucky Friday main vein. Reflected light photomicrograph of silver-rich tetrahedrite and minor chalcopyrite included in moderately deformed galena.	31
5	QSG veins. (a). Lucky Friday Main vein (level 5560). At this Level the vein consists of almost 90% galena. (b). A sample of QSG vein ore from Gold Hunter mine. The dark mineral is massive galena. High degree of post-ore shearing and deformation is visible in the sample.	34
6	SQS veins. (a). Gold Hunter mine (4900 level). The outcrop contains three vein types, SQS and QSG (labeled and pointed with black arrows), and subhorizontal quartz veins (unlabeled). (b). Sample of fractured crustification banding texture, Gold Hunter mine (4900 level).The dark mineral is sphalerite, the light mineral is early siderite. Mineral zoning is visible in siderite. The fractures in early siderite are filled with stage II sphalerite and siderite.	36

LIST OF PLATES

PLATE Page

7 Coleman Au-quartz vein, approximately 60 m. underground. The vein is brecciated by late tectonic movements along the sinuous vein fracture in the Prichard Formation argillite. 40

8 Photomicrographs of type 2, 3, and 4 fluid inclusions in SQT and QSG veins taken at room temperature (~25oC); A. (SQT) Field of small type 2 inclusions in sample SSM-11 B. - stage I siderite; B. (SQT) Relatively large type 2 fluid C. inclusions in SSM-9, stage II siderite. C. (SQT). Type 2 fluid inclusions in SSM-9 stage II siderite; D. (QSG)Type 3 fluid inclusions in stage III quartz (LF-14); E.(QSG) Type 3 inclusions with different degrees of fill in stage III quartz (LF-10). F. (QSG) Coexisting type 3 and type 4 fluid inclusions in stage III quartz (LF-10). 44

I. INTRODUCTION

The Coeur d'Alene mining district is located in Northern Idaho, approximately 100 km east of Spokane, Washington. Since the discovery of placer gold in 1879 the 37 mines in the district have yielded 7.3 Mt of lead, 3.0 Mt of zinc, 0.2 Mt of copper, 519 748 ounces of gold, and 1 091 362 000 ounces of silver (Wavra et al., 1994; White, 1998; Long, 1998). This establishes the district as one of the largest silver producers in the world, comparable only to Potosi in Bolivia (White, 1998).

Almost all of Coeur d'Alene production has come from precious- and base metal-rich veins hosted in the Mesoproterozoic marine and nonmarine clastic metasedimentary rocks of the Belt Supergroup that have been regionally metamorphosed to sub-greenschist facies. The mineralized veins comprise steeply dipping tabular bodies of simple mineralogy. The important ore minerals are galena, sphalerite, and silver-rich tetrahedrite. Pyrite, pyrrhotite, arsenopyrite, and chalcopyrite, as well as copper and silver sulphosalts and scheelite are locally abundant. Typical gangue minerals are quartz, siderite, and ankerite (Hobbs and Fryklund, 1968).

Major past producers in the district were the Star-Morning, Hecla, Hercules, and Gold Hunter mines. Mining still continues in the Sunshine, and Galena mines located in the so-called Silver Belt (Fig. 1.1), and also at the Lucky Friday mine, near the town of Mullan. Until 1997 the Coeur mine was also in production. Limited operations continue at the Bunker Hill mine, and recent discoveries in the Gold Hunter mine have added major new ore reserves that have created an opportunity for reopening the mine (Fig. 1.1; White, 1998).

Results of previous studies

The Coeur d'Alene district has been the subject of a great number of geological studies since the beginning of the century. The earlier works have been focused primarily on field relations (e.g., Ransome and Calkins, 1908;

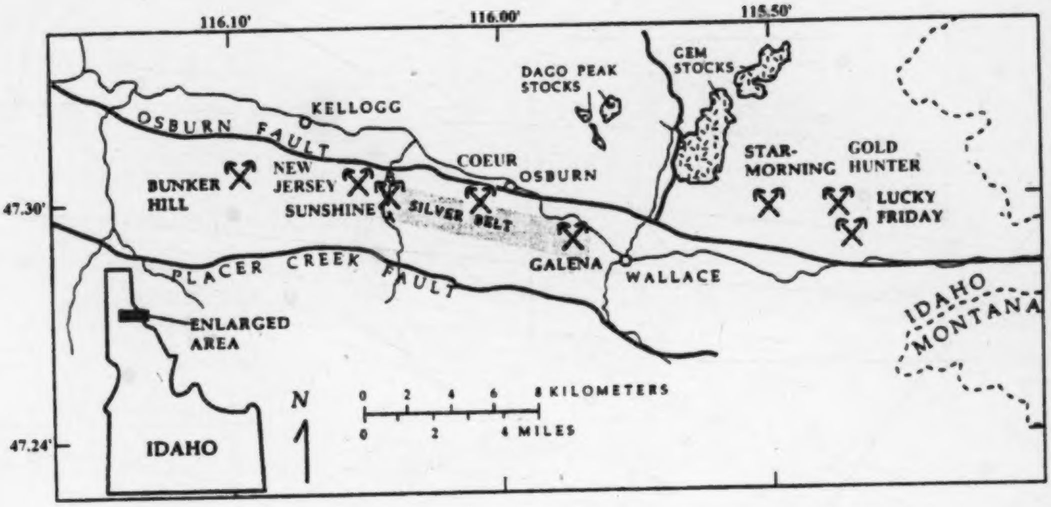
116.10'
116.00'
115.50'
47.30'
47.24'
KELLOGG
OSBURN FAULT
BUNKER HILL
NEW JERSEY
SUNSHINE
SILVER BELT
COEUR
OSBURN
DAGO PEAK STOCKS
GEM STOCKS
STAR-MORNING
GOLD HUNTER
LUCKY FRIDAY
GALENA
WALLACE
PLACER CREEK FAULT
ENLARGED AREA
IDAHO
IDAHO
MONTANA
N
0 2 4 6 8 KILOMETERS
0 2 4 MILES

Fig. 1.1. General features of the Coeur d'Alene mining district. Shown are the locations of the Silver Belt and also some of the major past and current producers mentioned in the text (Modified after Eaton et al.,1995).

Hershey, 1916; Umpleby and Jones, 1923; Crosby, 1959). Later studies continued with radiogenic isotopes (Kerr and Kulp, 1952; Zartman and Stacey, 1971; Fleck et al., 1991; Beaudoin, 1997; Leach et al., 1998), fluid inclusion (Norman and Bijak, 1982; Leach et al., 1983, 1988; Yates and Ripley, 1985), and stable isotope studies (Harris et al., 1981; Yates and Ripley, 1983, 1985; Fleck et al., 1991; Constantopoulus and Larson, 1991; Constantopoulus, 1994; Eaton et al., 1995).

The results of the recent studies suggested that the Ag-Pb-Zn veins in the district are of metamorphic origin (Leach et al., 1988, 1998; Criss and Fleck, 1990; Constantopoulus and Larson, 1991; Constantopoulus, 1994; Eaton et al., 1995; White, 1998). On the basis of vein mineralogy, P-T conditions of deposition, and stable isotopic composition of vein minerals Beaudoin and Sangster (1992) classified Coeur d' Alene veins as Ag-Pb-Zn veins in clastic metasedimentary terranes. Similar Ag-Pb-Zn veins are found in the North

American Cordillera and the Variscan orogen in Europe (Lynch, 1987; Beaudoin and Sangster, 1992; Hein, 1993). Several features such as the location of the veins in diffuse shear zones, and the sub-greenschist metamorphic grade of the host metasedimentary rocks also bear similarities to those of mesothermal Au-quartz veins (Lange, 1992; White, 1994; Reid et al., 1995).

Objectives of the present study

Despite the great number of studies there is still a general disagreement about the age and certain aspects of the origin of the Coeur d'Alene Ag-Pb-Zn veins. Under the influence of the classic works of Fryklund (1964) and Hobbs and Frykund (1968) structural and mineralogical differences between the Ag-Pb-Zn veins have largely been neglected, and the veins have long been considered the product of a single stage mineralization event related to the emplacement of the Cretaceous monzonite stocks (Fig. 1.1). However, in a recent study, Leach et al. (1998) subdivided the Ag-Pb-Zn veins to low-silver (lead- and zinc-rich), and high-silver type and on the basis on $^{40}Ar/^{39}Ar$ and K/Ar data, and Pb-isotopic signature of vein minerals suggested that the low-silver veins formed during a Late Proterozoic metamorphic event, whereas the high-silver veins formed in Late Cretaceous-early Tertiary times. In contrast, Fleck et al. (1991); Eaton et al. (1995), and Criss and Eaton (1999) argued on the basis of $^{87}Sr/^{86}Sr$ and $\delta^{18}O$ data that all Ag-Pb-Zn veins in the Coeur d'Alene district are of Mesozoic age.

The primary objective of this study is to compare the paragenetic, fluid inclusion, and stable isotope characteristics of three different Ag-Pb-Zn vein types in the Coeur d'Alene district. Two of these vein types, e.g. quartz-siderite-galena (QSG) veins at the Lucky Friday and Gold Hunter mines, and siderite-quartz-sphalerite (SQS) veins an the Gold Hunter mine, are of suggested Late Proterozoic age (Leach et al., 1998, 1999). The third type, siderite-quartz-tetrahedrite (SQT) veins at the Sunshine and Coeur mines, are suggested to be of Late Cretaceous-early Tertiary age (Leach et al., 1998, 1999). Also included are fluid inclusion and stable isotopic data from a small mesothermal Au-quartz vein system at the New Jersey mine, which is of unknown age. The comparative approach has been chosen to highlight the differences and similarities between these vein types. Although no direct methods for age dating have been applied in this study, some of the results presented here may have important implications for the age of the vein deposits in the Coeur d'Alene district.

II. GEOLOGICAL SETTINGS

Regional Geological Settings

The Coeur d'Alene mining district is hosted by metasedimentary rocks of the Mesoproterozoic Belt Supergroup, a 20-km-thick sequence of siliciclastic and carbonate sediments that accumulated in a large extensional intracratonic basin about 1.5 - 1.2 Ga ago (Burwash, 1993). The Belt Supergroup in northern Idaho and Montana and its stratigraphic equivalent the Purcell Supergroup in southern British Columbia and Alberta crops out over an area of 125 000 km^2 and is the most extensive and least disturbed sequence of Mesoproterozoic sediments in North America (Ghosh, 1986; Fig. 2.1).

In northern Idaho and Montana the Belt Supergroup is divided into four major divisions: the lower Belt (Prichard Formation), middle Belt quartzite or Ravalli Group, middle Belt carbonate (Wallace and Helena Formations), and the upper Belt or Missoulla Group (Harrison, 1972). The lower Belt contains a thick sequence of deep-water turbidites and dark colored argillites deposited in a marine environment. It is overlain by the shallow-water quartzites and argillites of Ravalli Group and by the carbonate-bearing clastic sediments, limestones, and dolomites of middle Belt carbonate. The upper Belt comprises a sequence of siliciclastics and carbonate beds deposited in shallow shelf and tidal to subaerial environments.

Several Proterozoic and Mesozoic tectonic events have disturbed the original position of the sedimentary sequences in the Belt basin. This has made the accurate restoration of lithofacieses to their initial sites of deposition difficult and has largely obscured the size and the geometry of the basin. The gradual transition from deep-water sediments to the southwest to tidal-flat, deltaic, and shallow-water deposits to the northeast was considered to be evidence that the Belt basin formed in a miogeocline setting along the continental margin of the North American Craton (Aitiken and McMechan, 1992). Recent studies, however,

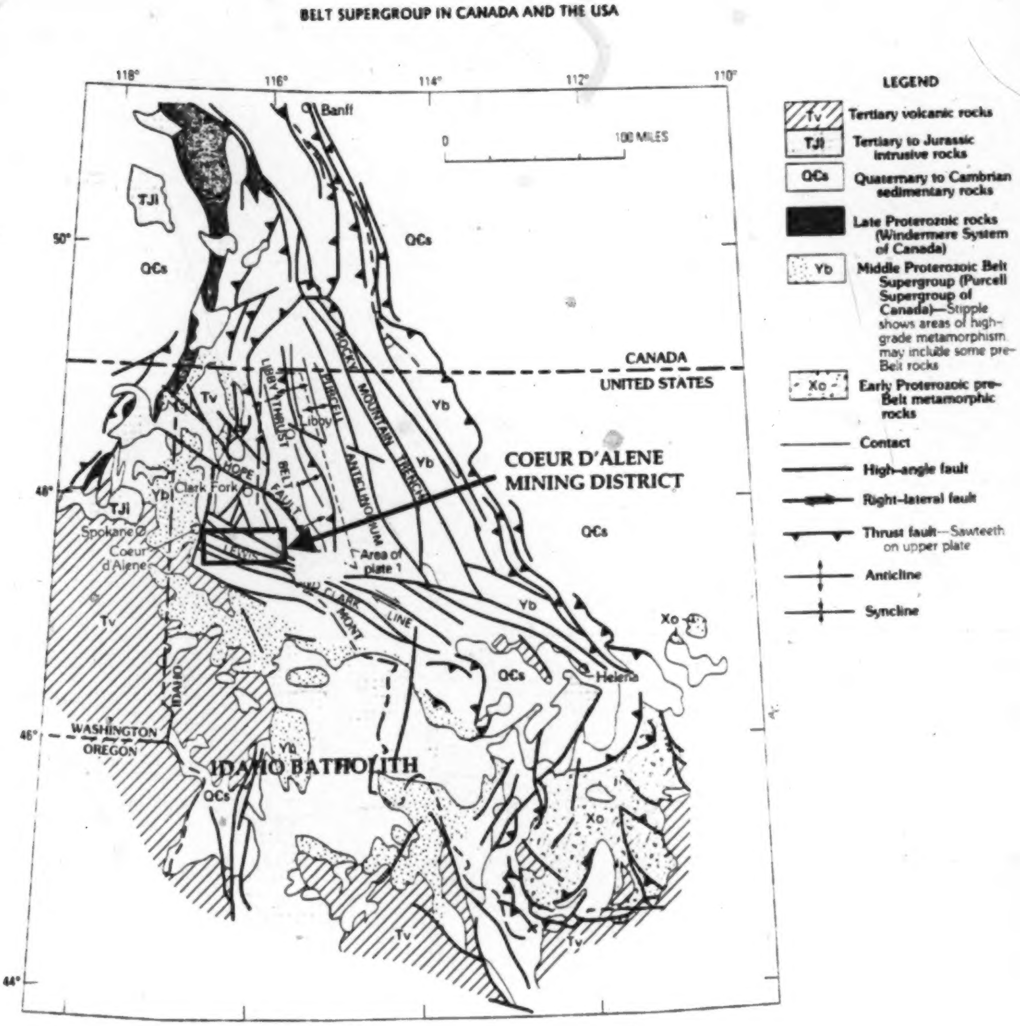
BELT SUPERGROUP IN CANADA AND THE USA
118°
116°
114°
112°
110°
50°
48°
46°
44°
Banff
0
100 MILES
TJi
QCs
Yb
Tv
CANADA
UNITED STATES
Libby
PURCELL
ROCKY MOUNTAIN TRENCH
ANTICLINORIUM
LIBBY THRUST BELT
HOPE FAULT
Clark Fork
Ybl
Spokane
Coeur d'Alene
COEUR D'ALENE MINING DISTRICT
Area of plate 1
LEWIS AND CLARK LINE
MONT.
IDAHO
WASHINGTON
OREGON
IDAHO BATHOLITH
Helena
Xo
LEGEND
Tv Tertiary volcanic rocks
TJi Tertiary to Jurassic intrusive rocks
QCs Quaternary to Cambrian sedimentary rocks
Late Proterozoic rocks (Windermere System of Canada)
Yb Middle Proterozoic Belt Supergroup (Purcell Supergroup of Canada)—Stipple shows areas of high-grade metamorphism, may include some pre-Belt rocks
Xo Early Proterozoic pre-Belt metamorphic rocks
Contact
High-angle fault
Right-lateral fault
Thrust fault—Sawteeth on upper plate
Anticline
Syncline

Fig. 2.1. Geological map of the Belt Supergroup in Canada and the USA. Modified after Harrison and Cressman (1993). Shown is the outline of Coeur d'Alene mining district as seen on Fig. 1.1.

suggest that the Belt sediments were most likely deposited in a remnant oceanic basin similar to the Black and Caspian seas (Ross et al., 1992; Hoffman, 1989) or in an elongate open seaway similar to the Gulf of California (Anderson and Davis, 1995). According to the paleotectonic reconstruction of Ross et al. (1992) the Belt basin was situated in the interior of the Laurentian Supercontinent, and was bordered by the Australian Albany-Fraser belt to the west and by the North American craton to the east (Ross et al., 1992; Anderson and Davis, 1995).

The Belt Supergroup was intruded by voluminous diabase sills and granitoid intrusions during the Middle and Late Proterozoic. In the Mesozoic the metasediments were affected by thrusting, regional metamorphism, and a pulse of felsic magmatism related to the emplacement of the Cretaceous Idaho batholith. Felsic and intermediate plutons and porphyry dikes intruded the sequence in Tertiary time (Harrison and Cressman, 1993).

Proterozoic evolution of the Belt Basin

Sm-Nd isotopic data for intrusive rocks from east-central Idaho (Doughty and Chamberlain, 1996) and K-Ar ages for biotite (Burwash, 1993) from the eastern edge of the Belt basin constrained the age of the underlying Pre-Belt basement to 1.7 Ga. Although most of the basement is not exposed and could have been tectonically displaced during the Mesozoic, an exposure of Archean rocks has recently been reported from the core of the Priest River metamorphic complex, approximately 150 km to the east of the Coeur d'Alene district (Doughty et al., 1998). U-Pb zircon data constrained the age of this part of the basement to ~2.65 Ga, which is coeval with the 2.55 – 2.65 Ga old Gawler craton on the eastern margin of Australia (Doughty et al., 1998).

Paleomagnetic and isotope data indicate that incipient rifting and transgressive clastic sedimentation in the basin began ca. 1500 Ma (Anderson and Davis 1995; Burwash, 1993; Table 1). Lower Belt deep-water turbidites and argillites (Prichard Formation, correlative Aldridge Formation) accumulated in a rapidly subsiding basin. The voluminous tholeiitic Moyie sills intruded into the

Table 1. Proterozoic Evolution of the Belt Supergroup (modified after Burwash, 1993)

Age (Ma)	Important events in the Proterozoic evolution of the Belt Supergroup.
800 - 900	Goat River Orogeny: uplift, block faulting, mild metamorphism. (McMechan and Price, 1982).
1100 - 1000	Grenville event: metamorphism and tectonism (Anderson and Davis, 1995).
~1250	Termination of Belt sedimentation (Anderson and Davis, 1995).
~1310	Renewed clastic sedimentation – Upper Belt deposition (?).
>1370 - 1310	Basin extension. Widespread shallow marine water clastic and carbonate sedimentation – middle Belt quartzite and carbonate deposition. Formation of strata-bound copper-silver deposits. East Kootenay metamorphic event: burial metamorphism; deformation (formation of folds and N trending cleavage); bimodal magmatism; (Anderson and Davis, 1995; Doughty and Chamberlain, 1996).
1480 - 1430	Extensional tectonics; deep water sedimentation; Moyie sills intrusion; formation of stratiform SEDEX Pb-Zn-(Ag) deposits (Hoy, 1989; Anderson and Davis, 1995). End of lower Belt deep water sedimentation.
1500	Incipient rifting triggers the onset of transgressive clastic sedimentation.
1700	Stabilization of the 2.65 Ga old Pre-Belt crystalline basement.

base of the lower Belt at 1468 ± 3 Ma (Anderson and Davis, 1995). Gradational contacts, and large scale dewatering features associated with some sills indicate that mafic magmas were emplaced in weak, water-saturated sediments possibly at their level of neutral buoyancy (Hoy, 1989). On the basis of sill geochronology, Anderson and Davis (1995) estimated sedimentation rates for the middle part of the Aldridge Formation of ca. 0.25-0.4 km/Ma. Such rapid rates explain the lack of dewatering features near many sills which were emplaced at greater depths with respect to the sea floor level (Hoy, 1989; Anderson and Davis, 1995).

The lower Belt hosts several large syngenetic SEDEX deposits including the Sullivan Pb-Zn-Ag deposit located at the boundary between the lower and middle divisions of Aldridge Formation (correlative Prichard Formation). The close spatial and possible temporal relationship between the Moyie sills and the

SEDEX deposits implies a genetic link between the two (Anderson and Davis, 1997). Massive Pb-Zn-Ag deposits are not found in or near the Coeur d'Alene district. However, parts of the lower Prichard Formation that crop out in Montana are known to contain anomalous zinc and lead (White, 1989).

East Kootenay metamorphic event

The Belt strata were affected by mild regional metamorphism during the poorly defined East Kootenay event ca. 1370 - 1320 Ma. According to McMechan and Price (1982) the East Kootenay orogeny was a compressional event that created gentle folding and north trending cleavage. Anderson and Davis, (1995) and Doughty and Chamberlain, (1996) however, argued that the East Kootenay orogeny was associated with rifting, renewed basin subsidence, and local mafic and felsic magmatism superimposed on static burial metamorphism (greenschist facies) in the lower Belt at 1370 Ma. In the Salmon River arch, south-central Idaho, intrusion of mafic sills near the base of the basin induced partial melting of Belt strata at 1370 ± 2 Ma. Felsic plutons of similar age intruded metamorphosed and deformed sediments and mafic sills in various parts of the basin (cf. Doughty and Chamberlain, 1996). At the Sullivan deposit peak metamorphic conditions during the East Kootenay event reached 450 ± 50°C and 380 ± 100 MPa (De Paoli and Pattison, 1995).

According to Anderson and Davis (1995), middle and parts of upper Belt were deposited prior to 1370 Ma. Basin subsidence and sediment accumulation however continued during the East Kootenay event which is evident from the 6 km increase in the sediment thickness recorded in south-central Idaho (Doughty and Chamberlain, 1996). Volcanic zircons from the St. Regis formation have constrained the age of middle Belt quartzite sedimentation to ~1350 Ma (Leach et al., 1998).

Middle Belt quartzite hosts a number of copper-silver stratabound deposits including the large Spar Lake deposit in western Montana (Haynes and Einaudi, 1986). These deposits are syndiagenetic in origin and therefore not much younger than 1350 Ma (Haynes and Einaudi, 1986; Haynes et al., 1989).

Bennett and Venkatakrishnan (1982) suggested that the National and Snowstorm mines in the district, were in fact stratabound copper-silver deposits.

Termination of Belt Sedimentation

The timing of the termination of Belt sedimentation is controversial. McMechan and Price (1992) and Doughty and Chamberlain (1996) suggested that the sedimentation was terminated before the East Kootenay metamorphism ca. 1350-1370 Ma, whereas Burwash (1993) and Anderson and Davis (1995) argue that a hiatus during or after the East Kootenay event was followed by renewed clastic sedimentation that continued until 1260 Ma. The former hypothesis is in agreement with a major tectonic adjustment in the basin in early upper Belt (Missoula Formation, Harrison, 1972).

Grenville metamorphic event

Widespread Grenville age metamorphism in the Belt Supergroup is supported largely by geochronological data summarized in Anderson and Davis (1996). Very little is known, however, about the nature and the extent of this metamorphic event.

Goat River Orogeny

The Goat River Orogeny ca. 800 - 900 Ma is the third Proterozoic metamorphic event to affect the Belt metasediments. According to McMechan and Price (1982) this event involved uplift, block faulting, and low-grade metamorphism in the north-eastern parts of the basin.

Mesozoic Evolution of the Belt Supergroup

The Mesozoic Evolution of the Belt Supergroup reflects the complex plate tectonic history of the western continental margin of the North American craton in Jurassic and Cretaceous times. Crustal thickening, high-grade regional metamorphism, and deformation related to the accretion of the allochthonous Wallowa-Seven Devils terrane affected the rocks in the southwestern parts of the

Belt Supergroup between 130 and 100 Ma (Snee, 1995; Criss and Fleck, 1987). Conservative estimates indicate more than 160 km of eastward thrusting of Belt metasediments along ramp-and-flat and listric thrust faults in northern Idaho and Montana during the Cretaceous/Tertiary compression (Harrison, 1993). Preexisting Proterozoic structures were largely deformed and displaced by the thrusting which continued until about 60 Ma and was followed by uplift and extension in the Eocene (Harrison, 1993). The granitoid plutons of the Idaho batholith intruded the Belt metasediments between 90 and 50 Ma (Snee, 1995). Recent data from Northern Idaho show that peak metamorphism in the Priest River metamorphic complex and movement along the Spokane dome mylonite zone located some 150 km to the east of the Coeur d'Alene district took place ca. 72 Ma (Doughty et al., 1998). Widespread crustal extension associated with formation of metamorphic core complexes and abundant felsic magmatism at the Bitterroot lobe of the Idaho batholith affected Belt rocks from 50 to 40 Ma (Doughty et al., 1998).

III. GENERAL GEOLOGY OF COEUR D' ALENE DISTRICT

Belt Supergroup

The thickness of the Mesoproterozoic Belt metasedimentary rocks in the Coeur d'Alene district is estimated to be greater than 9000 m (Reid, 1995). The base of the Lower Belt (Prichard Formation) which is a stratigraphic equivalent of the rocks that host the massive sulphide Pb-Zn-Ag deposits in British Columbia is not exposed in the district (Hobbs and Fryklund, 1968). Syndepositional slump folds, fluid escape textures, ripple marks, and mud cracks indicative of shallow water origin are locally preserved in the middle and upper Belt metasediments (Hobbs et al., 1995).

The Belt metasedimentary rocks are composed of variable amounts of quartz and sericite with subordinate carbonate (calcite, ferroan dolomite, ankerite, and siderite) and chlorite (Hobbs et al., 1995). Quartz is mostly detrital, although it is locally overgrown by metamorphic silica. Metamorphic sericite is very fine-grained, interstitial to quartz and to other detrital minerals, and is oriented parallel to cleavage (Wavra et al., 1995). Recrystallized carbonates are abundant only in the Middle Belt where they locally reach 20% by volume of the rock. Near the Ag-Pb-Zn veins syngenetic calcite and ferroan dolomite are replaced by ankerite and siderite introduced during vein formation (Fryklund, 1964; White, 1998). Chlorite is mostly of metamorphic origin, although some chlorite is associated with hydrothermal alteration. Common accessory minerals are detrital muscovite, plagioclase, potassium feldspar, and zircon, and metamorphic hematite, tourmaline, and rutile (Fryklund, 1964). The dark-colored argillites of the Prichard Formation contain as much as 5% diagenetic pyrite. Some pyrrhotite in the Prichard argillites in the vicinity of the Gem stocks is probably of contact metamorphic origin (Fryklund, 1964).

Metamorphic grade

The metamorphic grade of the Belt metasedimentary rocks in the Coeur d'Alene district is very low. In a recent study White (1998) argues that the burial metamorphism of the metasediments never reached greenschist facies, and that typical metamorphic minerals such as chlorite and iron- and magnesium-poor sericite developed only in the vicinity of the Ag-Pb-Zn veins. To the south of the district the metamorphic grade increases significantly reaching 625ºC and 6 kb in the sillimanite zone along the contacts with the Idaho batholith (Mora and Valley, 1991).

Magmatic rocks in the district

The Belt metasedimentary rocks in the central part of the Coeur d'Alene district are intruded by the Early Cretaceous Gem stocks. The stocks crop out as two small masses of monzonitic rock referred to as the North and the South Stock (Fig 1.1). Their compositions vary from syenite to diorite depending on microcline phenocryst abundance (Crosby, 1959). The Dago peak stocks that crop out approximately 7 km northeast of the town of Osburn comprise the sliced tops of the Gem stocks that were displaced along the low-angle Dobson Pass fault (Hobbs et al., 1995). The absence of cleavage and schistosity from the contact metamorphic zone around the stocks indicates low pressures during emplacement (Ransome and Calkins, 1923). Large xenoliths of country rock in monzonite suggest stoping as a dominant process of emplacement (Crosby, 1959).

A genetic link between the Ag-Pb-Zn veins and the monzonitic stocks has long been suggested mainly on the basis of crosscutting relationships (Crosby, 1959; Frylkund 1964, and references therein). However, recent studies have demonstrated that the lead- and zinc-rich veins near the stocks contain typical contact metamorphic minerals such as magnetite, gahnite, garnet, Fe-rich biotite, grunerite, and recrystallized sulphides (Leach et al., 1988, 1998; 1999; Constantopoulus, 1994). In contrast to early interpretations that linked the Ag-Pb-Zn veins to magmatic-hydrothermal activity associated with the monzonite (e.g., Crosby 1959; Fryklund, 1964), Leach et al. (1998) attributed the rare occurrences of sulphide veins in the stocks to "mechanical emplacement...by late structural events". Radiogenic isotope studies, however, demonstrated that most sulphide-bearing veins in the stocks contain galena with lead isotopic composition which is significantly more radiogenic than the "Coeur d'Alene" type of lead commonly found in the lead- and zinc-rich veins outside the stocks (Zartman and Stacey, 1971). Therefore, those sulphide veins are most likely associated with the monzonite emplacement.

The monzonite stocks cut across major fold structures and were thus intruded after the main folding in the district (McKinstry and Swendsen, 1942; Hobbs et al., 1995). Folding and faulting associated with movement along the Osburn fault, however, continued after monzonite emplacement (McKinstry and Swendsen, 1942; Hobbs et al., 1995). According to Bennett and Venkatakrishnan (1982) the stocks played an important role in the tectonic framework in the district by acting as a structural buttress that affected the kinematics of fault movements to the north of the Osburn fault. K-Ar analyses on hornblende from the stocks yielded ages of 128 ± 4 and 134 ± 4 Ma (McDowel, 1971). These data indicate that monzonite is unrelated to the Idaho batholith (90 to 50 Ma; Criss and Fleck, 1987; Snee, 1995). It is noteworthy that the monzonite emplacement age broadly corresponds to the onset of metamorphism along the Salmon River suture zone (ca. 130 Ma) which marked the beginning of the accretion of the exotic Wallowa-Seven Devils terrane to the North American Craton (Snee et al., 1995).

The metasedimentary rocks in the district are also intruded by diabase sills and diabase and lamprophyre dikes of undetermined age. The diabase sills are most likely of Proterozoic age as are many similar sills in the Belt metasediments (Anderson and Davis, 1995). Some diabase dikes postdate the zinc- and lead-rich veins on the basis of crosscutting relationships. Lamprophyre dikes crosscut monzonite and are emplaced along the Osburn fault (Hobbs and Fryklund, 1968) which indicates that they are clearly younger than ca. 50 Ma. Diabase and lamprophyre dikes are possibly of common origin, although

Fryklund (1964) argued that there is a distinct group of lamprophyres with contrasting chemistry and structural relationships that is genetically related to the Columbia River Basalt, and is therefore Tertiary in age.

Tectonic Settings

The Coeur d'Alene district is situated in the north-western segment of the Lewis and Clark line, a regional west-northwest trending zone of high-angle faults that extends from Wallace, Idaho, to near Helena, Montana (Fig. 2.1). The line is a 400 km-long structural lineament which ranges from about 40-km wide in the west to as much as 80 km-wide in the east. Individual faults of the Lewis and Clark line extend up to 250 km along strike (Wallace et al., 1990). Rapid facies and thickness changes in the Belt metasediments suggest that faulting within the line was active as early as the Middle Proterozoic (Hobbs et al., 1965; Wallace et al., 1990). Recent paleotectonic studies suggest that the Lewis and Clark line was an active tectonic boundary between the northwestern Montana and Colorado Plateau-Southern Rockies plates during Late Cretaceous-Paleocene times (Sears, 1997). The metasedimentary rocks within the Lewis and Clark line exhibit more intense deformation than elsewhere in the Belt basin (Bennett and Venkatakrishnan, 1982). The Coeur d'Alene district is located in a segment of the line that had experienced highly complex folding, shearing and faulting (Hobbs and Fryklund, 1968). A major structure of the Lewis and Clark line in the district is the Osburn fault (Fig. 1.1). During the Tertiary the fault experienced 24 km of post ore dextral strike-slip movement that separated the district into two parts with contrasting tectonic features (Hobbs and Fryklund, 1968). The area to the north of the Osburn fault is moderately deformed and is characterized by large, open, north- to northwest-trending folds and faults. To the south folds are much more tightly compressed and in some places are overturned with fold axes and most faults trending east. According to Hobbs et al. (1965), and Bennett and Venkatakrishnan (1982) the northwest-trending folds were produced by a Precambrian tectonic event. Precambrian age for the folding to the south of the Osburn fault was initially supported by brannerite dating (erroneously identified as uraninite by Kerr and Kulp, 1952). The results indicated that discordant brannerite-bearing quartz-hematite veins that crosscut the overturned northern limb of the Big Creek anticline at the Sunshine mine formed ca. 1,100-1,200 Ma (Eckelman and Kulp, 1953). However, a recent reexamination of brannerite from the same quartz-hematite veins yielded a U-Th-Pb age of 136 ± 3 Ma (Zartman and Smith, 1995). This age is close to or within the analytical uncertainty of the K-Ar monzonite ages (e.g., 128 ± 4, 134 ± 4 Ma; McDowel, 1971), and is in agreement with the earlier hypothesis of Juras (1982), who suggested a Mesosoic age for the east-northeast-trending folds to the south of the Osburn fault. These data are also in agreement with the suggestion of Kell and Childs (1993) that eastward-directed thrusting during the Mesozoic produced all major folds in the district. Kell and Childs (1993) also argued that Coeur d'Alene Ag-Pb-Zn veins formed at that time by metamorphic fluid migration into fault zones.

Tectonics related to the mineralization

All major Ag-Pb-Zn vein deposits in the Coeur d'Alene district occur within well defined zones of preferred vein occurrence called mineral belts (Fryklund, 1964; Fig. 3.1). The mineral belts are structurally controlled features independent from the stratigraphy and major folds in the district. The belts are elongated to the NW and are between 2 and 20 km long. Individual silver and base metal veins tend to be parallel to the trend of the belt they occur in, and in most cases may be part of the same vein system (Bennett and Venkatakrishnan, 1982). The mineral belts also contain veins of different orientation and mineralogy.

Two major sets of belts have been recognized in the district (Reid et al., 1995; Fig. 3.1). The first set trends ~290°, and includes the largest silver producing mines to the south of the Osburn fault such as the Sunshine and Galena mines. The veins within this set strike mainly west-northwest to northeast, plunge from the southwest to the southeast, and intersect down dip (Reid, 1995).

The second set lies within the Terror fault, a major zone of ductile deformation in the footwall of the Osburn fault. The veins within this set trend

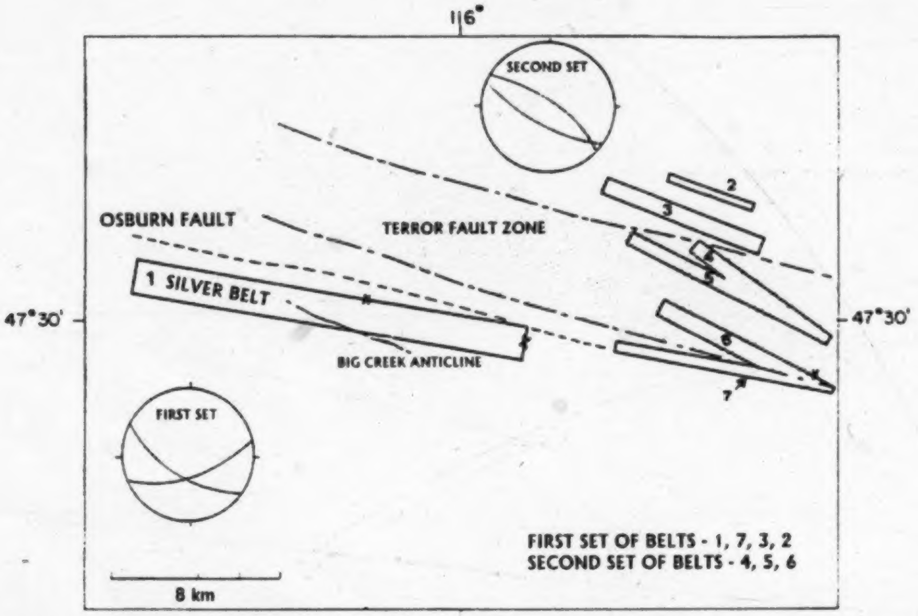
116°
SECOND SET
OSBURN FAULT
TERROR FAULT ZONE
1 SILVER BELT
2
3
4
5
6
7
47°30'
47°30'
BIG CREEK ANTICLINE
FIRST SET
FIRST SET OF BELTS - 1, 7, 3, 2
SECOND SET OF BELTS - 4, 5, 6
8 km

Figure 3.1. Mineral belts in the Coeur d'Alene district. The first set contains belts No. 1, 2, 3, and 7 (Silver, Sunset, Carlisle-Hercules, and Golconda-Lucky Friday). The second set contains belts No. 4, 5, and 6 (Tamarack-Marsh; Rex-Snowstorm, and Gem-Gold Hunter belts). Modified after Fryklund (1964) and Reid (1995).

~300°. The geometry and the structural relationships of these veins are not well studied (Reid, 1995).

Hobbs et al. (1965) suggested that the main stage mineralization in the district was contemporaneous with a strike slip faulting along the Lewis and Clark line. Recent studies however, demonstrated that most mineralized veins are hosted in steeply dipping fractures with relatively minor reverse and normal displacement (White, 1989; Bond et al., 1991; Wavra et al., 1994, Reid, 1995). The reverse and normal faults in the Coeur d'Alene district have relatively consistent dip but vary in strike. Their dominant trend is to the northwest (Reid, 1995). Studies at the Sunshine and Galena mines demonstrated lack of evidence for earlier, pre-ore movement along the fault planes. Minor post-mineral overprinting was attributed to a late strike-slip movement related to the Osburn fault (Reid, 1995). Further evidence supporting dip slip during vein formation is provided by locally developed cleavage subparallel to the trend of the ore-bearing fractures (White, 1992, Wavra et al., 1994). A steeply dipping shearing lineation within the cleavage planes parallels the long axes of the ore bodies and indicates dip slip during vein formation (Hobbs et al., 1995; Wavra et al., 1994; White, 1998). In the Sunshine mine the late cleavage is characterized by the development of thin mylonite selvages in the metasedimentary rocks along the vein walls. The stretching and recrystallization of quartz grains within these mylonitic selvages is consistent with greenschist facies metamorphic conditions (Wavra et al., 1994).

IV. MINERAL DEPOSITS AND VEIN GEOLOGY

Vein types and classification

As mentioned in chapter I the Ag-Pb-Zn vein deposits in Coeur d'Alene district have recently been subdivided to high-silver or low-silver type (Leach et al., 1998). The high-silver deposits ($Ag_{[ppm]}$ /$Pb_{[\%]}$ >> 50) are confined to the Silver Belt which lies to the south of the Osburn fault (Figs. 1.1 and 3.1), and contain mainly massive siderite veins with subordinate amounts of quartz and silver-rich tetrahedrite and occur in the steeply dipping, overturned north limb of the Big Creek anticline, at the transition between the dominantly quartzitic Revett and the more argillic St. Regis Formations (Fryklund, 1964; Bennett and Venkatakrishnan, 1982).

Table 4.1. Various vein types at the four Ag-Pb-Zn mines studied (modified after Fryklund, 1964; Wavra et al., 1994; Eaton et al., 1995).

Mine	Vein type	Host Formation (s)	Suggested Vein Age[1]
Sunshine	Siderite-quartz-tetrahedrite (SQT) veins	Revett/St. Regis	Late Cretaceous-early Tertiary
Coeur	Siderite-quartz-tetrahedrite (SQT) veins	Revett/St. Regis	Late Cretaceous-early Tertiary
Lucky Friday	Quartz-siderite-galena (QSG) veins	Revett/St. Regis	Late Proterozoic
Gold Hunter	Siderite-quartz-sphalerite (SQS) veins	Wallace	Late Proterozoic

---

[1] Vein ages are inferred on the basis of K/Ar and $^{39}Ar/^{40}Ar$ dating of sericite, and Pb isotopic composition of vein sulphides and siderite (Leach et al., 1988, 1998), and $^{87}Sr/^{86}Sr$ of vein siderite (Eaton et al., 1995; Leach et al., 1998, 1999).

The low-silver deposits ($Ag_{[ppm]}$/$Pb_{[\%]}$ < 50) are further subdivided into zinc- and lead -rich type (Leach et al., 1998). The zinc-rich veins contain sphalerite as a major ore mineral, whereas the lead-rich veins are galena-dominant. Both types contain variable amounts of quartz, siderite, pyrite, and/or pyrrhotite.

To avoid ambiguous terms and to simplify the presentation the silver and base metal veins are classified on the basis of their dominant gangue and ore mineralogy as follows: (1) siderite-quartz-tetrahedrite or SQT veins, (2) quartz-siderite-galena or QSG veins, and (3) siderite-quartz-sphalerite or SQS veins (Table 4.1).

Age of the Ag-Pb-Zn veins

One of the most controversial aspects of the Coeur d' Alene district has been the age of the Ag-Pb-Zn veins. Arguments about the vein age date back to the early nineteen fifties when the first Pb-isotopic analyses from the district became available (Long et al., 1959; see also Fryklund, 1964, and references therein). These and later studies suggested that the lead in the veins had a Precambrian isotopic signature, which was in conflict with contemporary models that linked Coeur d'Alene Ag-Pb-Zn veins to the emplacement of the Cretaceous monzonitic stocks (Fryklund 1964; Zartman and Stacey, 1971).

As mentioned in chapter I, currently there are two conflicting theories about the age of the Ag-Pb-Zn veins. The first theory implies two mineralization events with a Proterozoic lead- and zinc-rich event during which the SQS and QSG veins were deposited, followed by a Late Cretaceous-early Tertiary silver-antimony event (Leach et al.,1998). In support of this theory Leach et al. (1998) presented numerous Pb-isotopic analyses of sulphides, sulphosalts, and carbonates which according to their interpretation fall into two distinctive groups, a "Proterozoic" one and a "Mesozoic" one. Sulphides and sulphosalts from the QSG and SQS veins fall within the Proterozoic group whereas tetrahedrite and siderite from the SQT veins fall within the Mesozoic group. To explain the Proterozoic Pb-isotopic signature of galena in some SQT veins Leach et al. (1998) argued that silver- and antimony- rich fluids penetrated into older zinc- and lead-rich vein fractures in the Late Cretaceous-early Tertiary. Leach et al.

(1998) also presented ^{39}Ar/^{40}Ar analyses of three sericite samples from three different mines in the district. One of these samples, from the QSG Lucky Friday main vein, yielded a disturbed pseudo plateau of Late Proterozoic age (> 1.0 Ga), which according to Leach et al. (1998) reflects the age of all QSG and SQS veins in the district. The disturbed argon signature was attributed to thermal overprinting during the Mesozoic (Leach et al., 1998). In addition, Leach et al. (1998) argued that previously published K/Ar data of 876 ± 43 Ma and 829 ± 40 Ma from sericite at the Lucky Friday and Bunker Hill mines (Leach et al., 1988) also support a Late Proterozoic "age" for the QSG and SQS veins. In contrast, two other sericite samples from SQT veins in the district yielded Late Cretaceous-early Tertiary ages (~86 and 64.4 ± 0.2 Ma). These results were interpreted to reflect the age of the silver mineralization in the district. However, the sericite sample from the Lucky Friday main vein dated by Leach et al. (1998) was collected not from the vein but from the host metasedimentary rock proximal to the vein (R. Anderson, pers. commun., 2000); this information casts doubt on the primary hydrothermal origin of the mineral. The closure temperature (Tc) for Ar diffusion in muscovite is 350 ± 50°C (Hanes, 1991). Therefore, it is possible that the >1.0 Ga ^{39}Ar/^{40}Ar date reflects the original age of Proterozoic wall rock sericite. In addition, petrographic observations (this chapter) demonstrate the presence of partially recrystallized sericitic wall rock fragments in the Ag-Pb-Zn veins studied. Such fragments could have easily been mistaken for "vein" sericite. Thus, the "old" K/Ar ages from the Lucky Friday and Bunker Hill mines (Leach et al., 1988), could also reflect inheritance of Proterozoic wall rock sericite.

To support their argument about a mineralization event of Proterozoic age, Leach et al. (1998) also referred to 1018 ± 7 and 946 ± 7 Ma ^{39}Ar/^{40}Ar isochron ages of fluorphlogopite in ankerite veins from the district (Rosenberg and Larson, 1996), However, the ankerite veins at the Coeur d'Alene district have distinct mineralogy and in contrast to the Ag-Pb-Zn veins are largely barren of economic mineralization (Fryklund, 1964). In addition, none of the Ag-Pb-Zn veins studied contains vein phlogopite. Thus, it seems unreasonable to suggest

Proterozoic age for the Ag-Pb-Zn veins on the basis of results obtained from the ankerite veins.

A Proterozoic Ag-Pb-Zn vein age is also inconsistent with the deformation style of the Belt metasediments. For example if the SQS and the QSG veins in the district are associated with a metamorphic event of Grenville age, as suggested by Leach et al. (1998, 1999), major folding which precedes vein formation in the district, must also be at least 1.0 Ga old. However, there is little evidence of a major Precambrian deformation outside the district (Harrison and Cressman, 1993). Very small (<7.0 degrees) angular unconformities between Precambrian and Cambrian strata measured some ~100 km northeast of the Coeur d'Alene district indicate that Precambrian folds were large open structures (Harrison and Cressman, 1993). Harrison and Cressman (1993) also argued that these structures were subjected to major re-folding in the Mesozoic. In addition, White (1998) noted that the structural style of the two generations of folds in the Coeur d'Alene district is similar to that of Mesozoic folds elsewhere in the Belt basin, and also suggested that folding in the district may be Phanerozoic.

The second theory for the age of the Ag-Pb-Zn veins implies that the origin of all Coeur d'Alene Ag-Pb-Zn veins is linked to a giant metamorphic-hydrothermal system driven by the emplacement of the Idaho batholith (Fleck et al., 1991; Eaton et al., 1995; Criss and Eaton, 1998). This theory is based mainly on highly radiogenic strontium contents of siderite from SQT veins at the Sunshine mine, and also of siderite samples from nine other unspecified mines at the district (Fleck et al., 1991; Criss and Eaton, 1998). According to Fleck et al. (1991) the high $^{87}Sr/^{86}Sr$ of vein siderite could have only been inherited from the Belt metasediments in the last 200 million years, which requires the veins to be of Mesozoic age. In addition, Criss and Fleck (1990) used regional $\delta^{18}O$ trends and evidence for oxygen stable isotopic homogenization of the Belt rocks near the district in support of their theory for a link between the veins and a metamorphic-hydrothermal system associated with the Idaho batholith. Criss and Eaton (1998) dismissed the Pb-isotopic data of Leach et al. (1998) arguing that the Pb-isotopic signature can not be used as conclusive evidence for Proterozoic vein formation. They also rejected the K/Ar and ^{39}Ar/^{40}Ar data of Leach et al. (1988, 1998), but failed to provide convincing arguments why the data were deemed invalid.

However, Metz et al. (1985) noted that the high ^{87}Sr/^{86}Sr of calcite and ankerite from the REE Snowbird deposit in Montana, which is hosted in Belt strata, could also be acquired from the metamorphic basement that underlies the metasediments. Therefore, due to the old age of the basement rocks (2651 ± 20 Ma; Doughty et al., 1998) the highly radiogenic strontium content of vein siderite may not be evidence for a Mesozoic origin. In addition, Leach et al. (1999) reported a strontium isotopic ratio of 0.750 for siderite at the SQT Baychief vein. The Pb-isotopic composition of the siderite sample falls within the Mesozoic lead group and sericite from this vein yielded a ^{39}Ar/^{40}Ar plateau age of 64.4 ± 0.2 Ma. Leach et al. (1998) noted that such a discrepancy questions the use of Sr isotopic compositions of vein minerals in the district for dating purposes. In addition, Mora and Valley (1989, 1991) provided convincing evidence that the oxygen stable isotope homogenization of the Belt metasedimentary rocks resulted from metamorphic devolatilization, and can not be consistent with pervasive metamorphic fluid flow in the Belt metasediments as suggested by Criss and Fleck (1990).

Contact metamorphism of SQS and QSG veins in the vicinity of the monzonite stocks indicates that the veins are at least ~130 Ma or older (Leach et al., 1988; 1998). This date, although still permissive of Mesosoic vein age, renders any association of the SQS and QSG veins with the emplacement of the Idaho batholith (90 to 50 Ma) unlikely. It is consistent, however, with a possible relationship between the SQS and QSG veins and regional deformation and metamorphism related to the docking of the Walowa-Seven Devils terrane to the North American Craton. ^{39}Ar/^{40}Ar spectra of metamorphic and magmatic hornblende from the Salmon River suture zone, which lies several hundred kilometres southwest of the district, indicate that the accretion began at ca. 130 Ma (Snee et al., 1995).

The absence of convincing geochronological and geological evidence for

Ag-Pb-Zn vein mineralization of Proterozoic age in the district implies that most Ag-Pb-Zn veins most likely formed during the Mesozoic/Cenozoic. However, as mentioned above, geochronological evidence is also not consistent with a possible involvement of the Idaho Batholith in the formation of the QSG and SQS veins as suggested by Criss and Fleck (1990). Therefore, it is most likely that the Ag-Pb-Zn veins in the Coeur d'Alene district formed between ca. 130 Ma and 40 Ma as a result of a regional metamorphism and deformation associated with the docking of the Wallowa-Seven Devils terrane to the North American Craton.

Sample location

Samples for this study are collected from underground workings at the Sunshine, Coeur, Lucky Friday, and Gold Hunter mines, and also from underground and surface outcrops at the New Jersey mine (Fig. 1.1).

Approximate locations including the vein name and mining level at which the samples were collected are given Appendix III along with vein type and a brief sample description.

Table 4.2. Paragenetic sequence in individual vein types in the Coeur d'Alene district.

Stage	Characteristic Features	Principal ore minerals	Accessory ore minerals	Gangue minerals
Siderite-quartz-tetrahedrite (SQT) veins at the Sunshine and Coeur Mines				
Stage I	Massive tabular veins	None	Pyrite, arsenopyrite	Siderite, quartz (?)
Stage II	Breccias, veins, stockworks, disseminations	Ag-rich tetrahedrite, galena (?)	Chalcopyrite, pyrite, arsenopyrite, boulangerite, sphalerite	Quartz, siderite, white coarse-grained muscovite
Stage III	Subhorizontal quartz veins, some fibrous	None	None	Quartz, siderite, vug filling calcite
Quartz-siderite-galena (QSG) veins at the Lucky Friday and Gold Hunter mines				
Stage I	Fragments of veins with crustification banding textures (?)	Galena (?), sphalerite	Pyrite, arsenopyrite, tetrahedrite (?)	Siderite
Stage II	Irregular pods, stringers and veinlets	Tetrahedrite (?)	Coarse-grained sphalerite, galena, pyrite, chalcopyrite, tetrahedrite	Quartz, ankerite kutnahorite, minor siderite
Stage III	Same as stage II	None	Rare sphalerite, galena	Clear transparent quartz, and/or euhedral vug filling quartz, siderite
Siderite-quartz-sphalerite (SQS) veins at the Gold Hunter mine				
Stage I	Veins with primary crustification banding and mineral growth zoning textures	Dark brown sphalerite, galena.	Pyrite, arsenopyrite	Siderite
Stage II	Irregular veinlets, and stringers	None	Pale yellow sphalerite, galena, pyrite, rare tetrahedrite, meneghinite, boulangerite (?)	Siderite, quartz, muscovite (?)
Stage III	Subhoriznztal quartz veins, some fibrous.	None	Rare sphalerite	Quartz, siderite

Siderite-quartz-tetrahedrite (SQT) veins

The Sunshine and Coeur mines lie in the east-central parts of the Silver Belt approximately 5 km away from each other (Fig. 1.1). The SQT veins at the two mines comprise discordant, steeply dipping tabular bodies hosted in the highly deformed overturned limb of the Big Creek anticline. The veins are largely confined to the quartzites and argillites of the Revett and St. Regis Formations, with only minor Ag-mineralization hosted in the carbonate-bearing Wallace formation. Most veins at the Sunshine mine are west-northwest trending. In contrast SQT veins at the Coeur mine have a predominantly northeastern trend (Fryklund, 1964). Similarities in the mineralogy and structural position of the veins suggest that they most likely belong to a single large siderite-quartz-tetrahedrite vein system.

The mineralogy of the SQT veins in the Sunshine and Coeur mines is simple: the veins consists almost entirely (>80%) of creamy, massive siderite with minor quartz, pyrite, and arsenopyrite and locally silver-rich tetrahedrite and rarely galena (Plate 1). Minor chalcopyrite, boulangerite, and sphalerite also occur. Ore bodies are confined within the veins and have dip lengths several times their strike lengths. Outside the ore bodies the veins grade into barren siderite with subordinate quartz. Rare quartz-dominant veins with little siderite and tetrahedrite occur at the Coeur mine. These veins occupy fractures with structural orientation similar to the SQT veins and are most likely contemporaneous.

Petrographic observations are consistent with the paragenetic sequence described by Harris et al. (1981) for the lower Chester vein at the Sunshine mine. Massive siderite, pyrite, arsenopyrite, and/or quartz were deposited during an early stage of mineralization referred here to as stage I (Table 4.2). Stage II is characterized by shearing and brecciation of stage I minerals followed by precipitation of silver-rich tetrahedrite, minor chalcopyrite, boulangerite, galena, sphalerite, muscovite, quartz, and siderite.

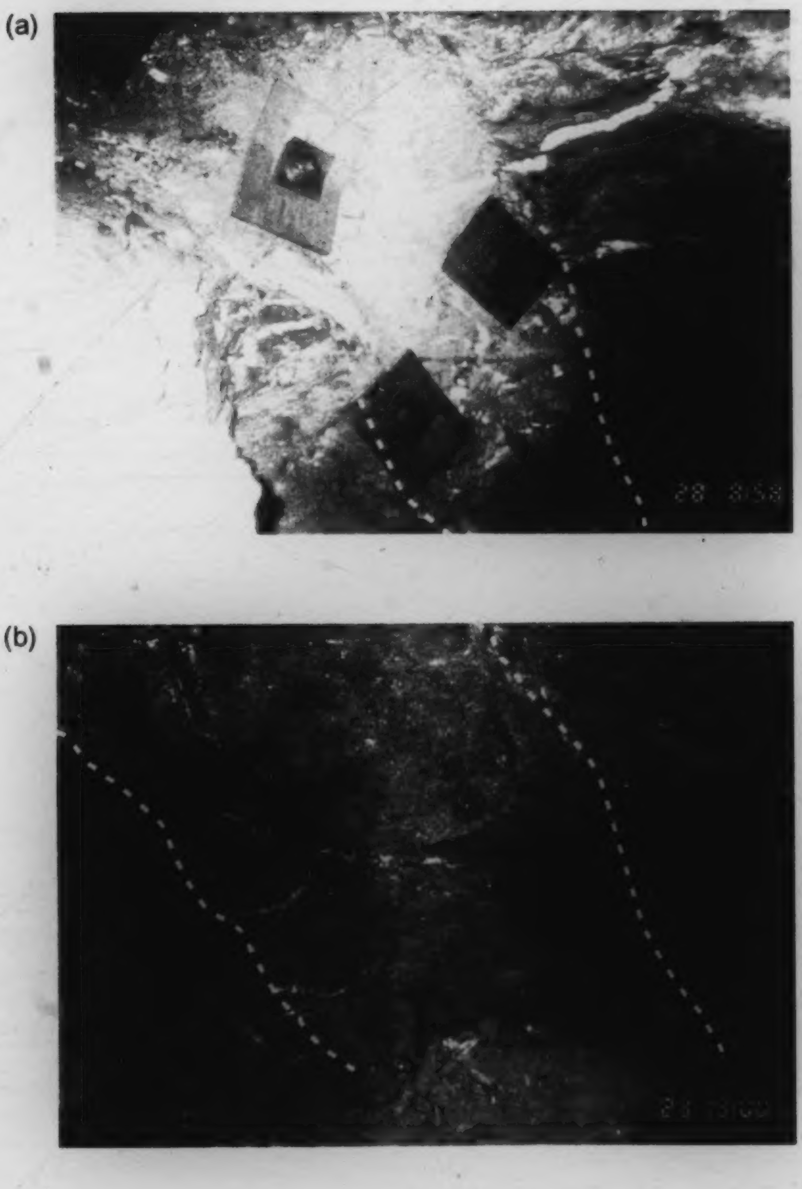

Plate 1. SQT veins. (a). Coeur vein in the Coeur Mine (level 1600). (b). Sunshine vein, Sunshine mine (level 3100). The vein contacts are outlined with yellow dashed line. Visible are unmineralized subhorizontal quartz veins that crosscut the SQT veins and continue in the host metasedimentary rocks.

Individual stage I siderite crystals reach 4-5 cm and are often strained and deformed. The degree of deformation varies from undulatory extinction and slight bending along cleavage, to matrix supported brecciation, with breccia matrix consisting of clear secondary siderite and quartz. Late syntaxial siderite veinlets locally fill millimetre size fractures within stage I siderite indicating that violent episodes of brecciation were followed by periods of slow opening along the vein fractures allowing for fibrous mineral growth. Pyrite is locally abundant and forms segregations within massive siderite. It is often brecciated and/or partially replaced by late sulphides and sulphosalts (Harris et al., 1981). Rare arsenopyrite occurs with pyrite and siderite. It is possible that some quartz also precipitated in stage I as suggested by Harris et al. (1981).

Silver-rich tetrahedrite fills fracture networks or forms large tabular masses in the central parts of the SQT veins (Plate 2). Most tetrahedrite is fine-grained and deformed indicating that deformation continued during stage II. Individual megascopic tetrahedrite crystals of millimetre to centimetre size occur in quartz stringers or in cavities lined by prismatic quartz and euhedral siderite (Plate 2, 3). Chalcopyrite is rare and forms blebs and veinlets that crosscut tetrahedrite, galena, and siderite. Minor sphalerite and galena are deposited in fractures that locally crosscut the Ag-mineralization. Galena is anhedral, deformed, and contains rounded inclusions of tetrahedrite and other sulphides (Plate 4). Boulangerite occurs as rare inclusions in tetrahedrite. The quartz associated with tetrahedrite is largely unstrained and contains clusters of primary fluid inclusions. Local deformation has resulted in serrated grain boundaries and rare sub-grain development. Trails of secondary inclusions are seen along grain boundaries and healed fractures in these areas. Rare clear medium- to coarse-grained muscovite occurs along sinuous fractures cutting across early siderite. Its association with late quartz and tetrahedrite suggests that muscovite may be coeval with the silver mineralization. Small, deformed fragments of recrystallized host argillite and quartzite also occur in the SQT veins and their abundance

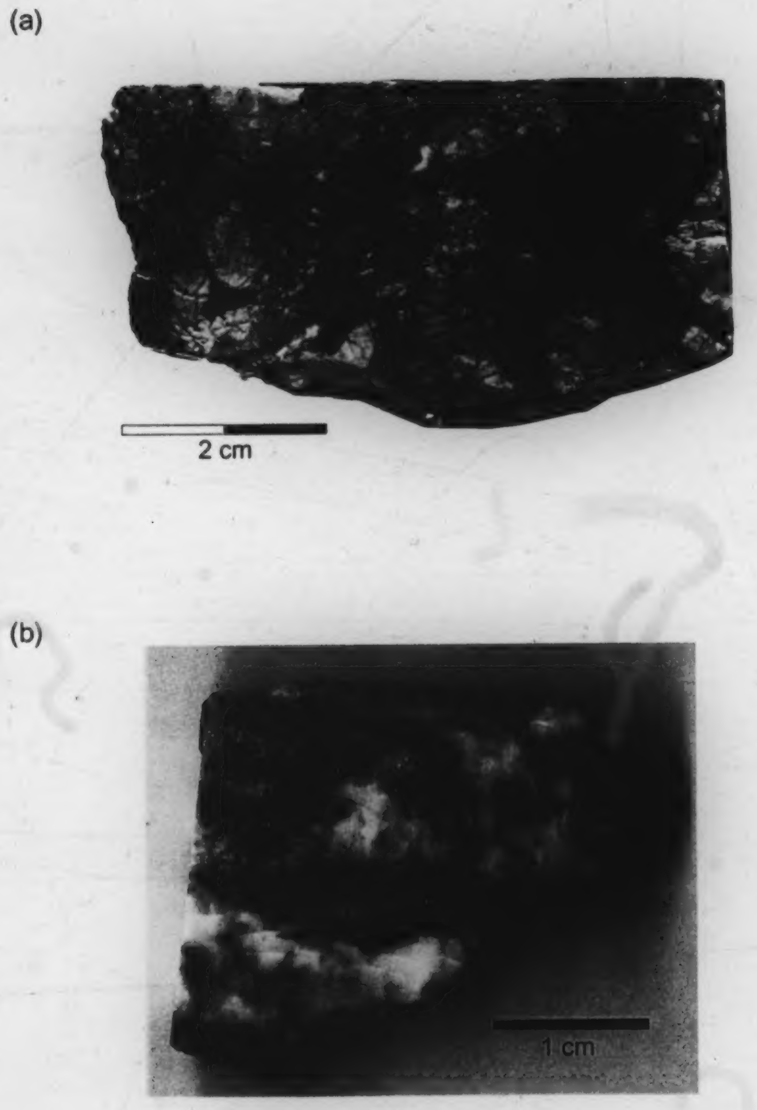

Plate 2. Two different types of silver ore in the SQT veins. (a). Brecciated siderite I cemented by massive tetrahedrite and minor quartz, Coeur Mine (level 1600).
(b). Megascopic euhedral tetrahedrite associated with irregular blebs of stage II quartz, Sunshine mine (level 3100).

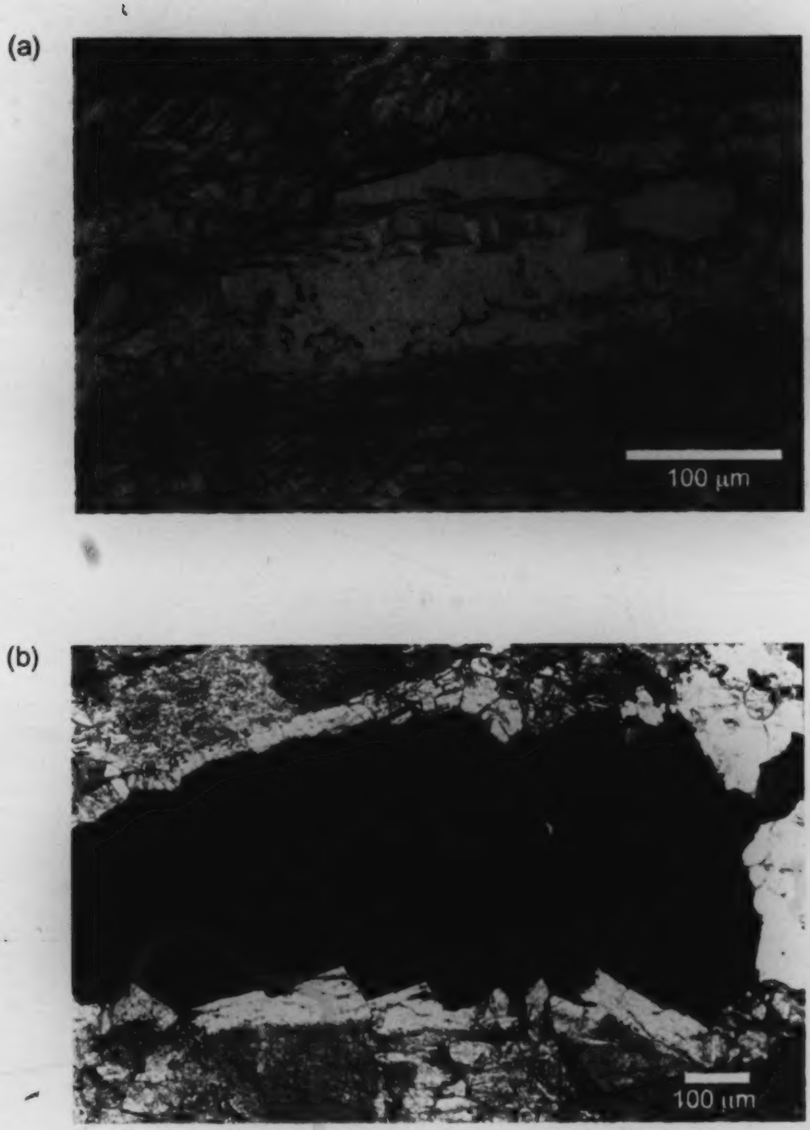

Plate. 3. (a). Transmitted light photomicrograph of stage II siderite filling small cavity in fractured early siderite, Sunshine vein. (b). Transmitted light photomicrograph of tetrahedrite crystal in fracture within stage I siderite, Sunshine mine. The light mineral that surrounds tetrahedrite is stage II siderite. To the right the fracture is filled with stage II quartz.

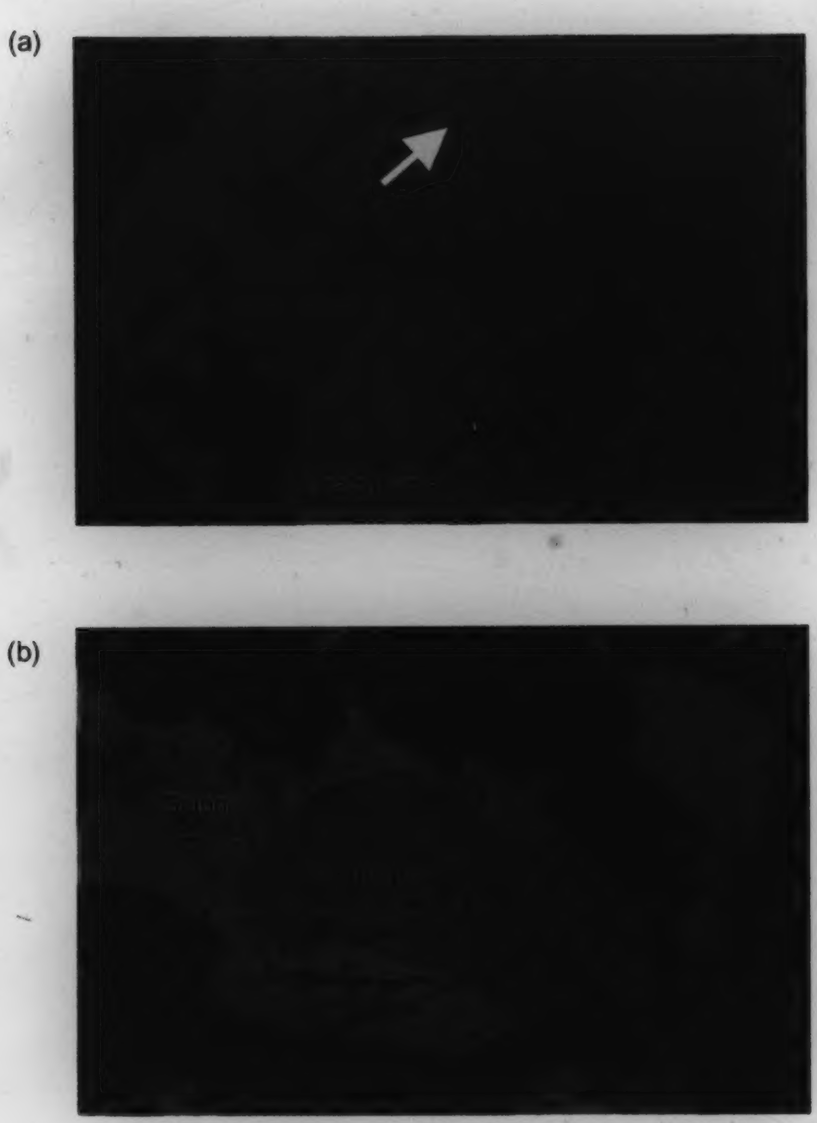

Plate 4. (a). SQT Sunshine vein. Reflected light photomicrograph of tetrahedrite, chalcopyrite, and galena in mutual crosscutting relationships. Boulangerite (white arrow) is hosted in tetrahedrite. (b). QSG Lucky Friday main vein. Reflected light photomicrograph of silver-rich tetrahedrite and minor chalcopyrite included in moderately deformed galena.

increases near the vein walls. These fragments consist of partly recrystallized fine-grained sericite with or without pyrite and are distinctly different from the white muscovite from the sinuous fractures.

The latest event in the evolution of siderite-quartz-tetrahedrite veins (stage III) is characterized by the development of sub-horizontal fractures filled with barren quartz and rarely siderite (Plate 1). The flat veins cut across the steeply dipping SQT veins and host metasedimentary rocks. Their thickness rarely exceeds 10 cm. The subhorizontal veins are mostly localized along the SQT veins and are rarely seen as independent occurences. Quartz from the sub-horizontal veins is largely undeformed or exhibits only slight undulatory extinction. Centimetre to millimetre wide sub-horizontal antitaxial veinlets with sigmoidal quartz fibers also indicate minor deformation during the late stages of sub-horizontal quartz vein formation.

Quartz-siderite-galena (QSG) veins

The Lucky Friday and Gold Hunter mines occur approximately 30 km to the east of the Sunshine and Coeur mines. Palinspastic reconstructions demonstrate that the veins in the four mines were originally a few kilometres apart, and their present position resulted from 24 km of dextral strike-slip displacement along the Osburn fault in the late Tertiary (Bennett and Venkatakrishnan, 1982).

The large quartz-siderite-galena (QSG) Lucky Friday main vein is confined mostly to the quartzitic strata of the Revett Formation. The vein is "S" shaped in plan, and is bounded by two subparallel faults that strike west-northwest. In contrast to most SQT veins at the Sunshine mine which trend NW, the Lucky Friday main vein strikes ~065° and dips steeply to the south (Fryklund, 1964). The QSG veins at the Gold Hunter mine are thinner than the Lucky Friday main vein, and are hosted in the argillaceous strata of the Wallace Formation.

Despite their unusually high silver content (most zinc- and lead-rich veins in the district are silver-poor) the QSG veins at the Lucky Friday and Gold Hunter mines are mineralogically indistinguishable from the "J" or "Link" veins at the

Bunker Hill, and Star-Morning mines, and also to the Lead vein in the Galena mine (Fryklund, 1964; Reid et al., 1975).

The QSG veins contain variable amounts of quartz, siderite, ankerite, kutnahorite, galena, sphalerite, pyrite, tetrahedrite, and chalcopyrite. A notable feature of the QSG veins is that galena locally reaches more than 90% by volume (Plate 5). The main mineral of economic interest, silver-rich tetrahedrite, occurs as small, millimetre to sub-millimetre-size irregular inclusions in galena. The QSG veins at Gold Hunter contain visible segregations of fine-grained tetrahedrite within strongly deformed and sheared "schistose" galena (Plate 5).

Zones of disseminated sulphides extend outside the vein walls at the Lucky Friday mine and also at several other mines in the district (White, 1998). Some authors have interpreted these zones as evidence for mobilization of sulphides from the host metasedimentary rocks into the veins (Ramalingaswamy, 1976). White (1998), however, demonstrated that the irregular zones of disseminated carbonates and sulfides in the vicinity of the Lucky Friday main vein are products of the hydrothermal fluids associated with vein formation, and concluded that all such zones in the district are of epigenetic origin.

Intense deformation has obliterated most of the primary features in the QSG veins at the Lucky Friday and Gold Hunter. Four separate post-ore tectonic events were recognized in samples from the similar "J" vein at the Bunker Hill mine (Caddey, 1975). Petrographic observations demonstrate that siderite at the Lucky Friday main vein often occurs in association with sphalerite as irregular fragments with locally preserved crustification banding texture "floating" in massive galena, which is usually very fine-grained and includes angular fragments of other vein minerals and wall-rock. Caddey (1975) suggested that the fine-grained galena possibly resulted from shearing and subsequent annealing. Large portions of the Lucky Friday main vein, however, consist of

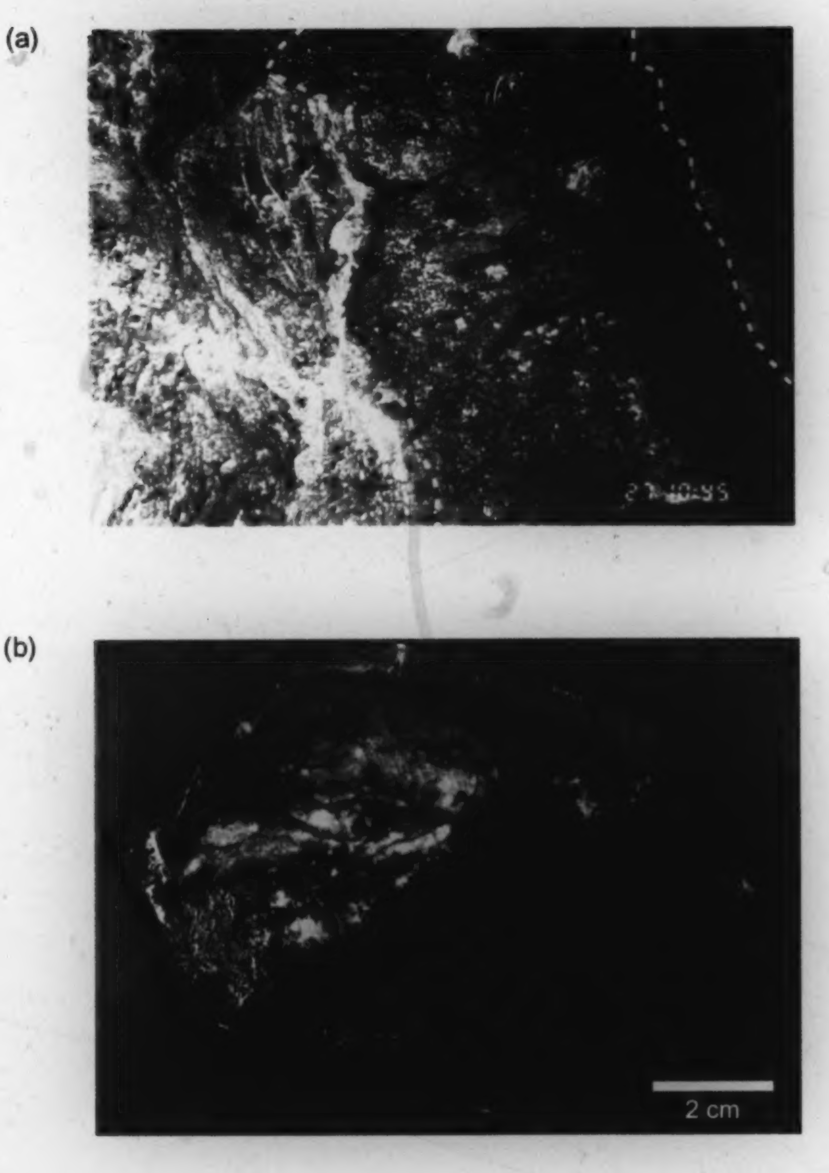

Plate 5. QSG veins. (a). Lucky Friday Main vein (level 5560). At this level the vein consists of almost 90% galena. (b). A sample of QSG vein ore from Gold Hunter mine. The dark mineral is massive galena. High degree of post-ore shearing and deformation is visible in the sample.

irregular masses of coarse-grained galena (Plate 5). The degree of deformation of coarse-grained galena varies from minor bending along cleavage to the development of schistosity. The convoluted contacts between the coarse- and fine-grained galena at the Lucky Friday main vein are not consistent with shearing as a mechanism of formation of the latter.

Although the high degree of deformation precludes unequivocal determination of the paragenetic sequence at the QSG veins the bulk of the galena was most likely deposited in an early stage (i.e. stage I) along with siderite and sphalerite. Thin continuous slivers of sheared siderite-sphalerite with preserved crustification banding along the footwall of the Lucky Friday main vein at level 5660 however, indicate that sphalerite and siderite could have preceded the bulk of galena deposition.

Textural relationships of the QSG veins indicate that the deposition of early siderite, sphalerite, and galena was followed by the introduction of pods and stringers of milky quartz, associated with minor tetrahedrite, chalcopyrite, galena, sphalerite, siderite, and ankerite. The quartz exhibits variable degrees of deformation with local undulatory extinction, serrated grain boundaries, and subgrain formation. Syn- to post-depositional shearing has resulted in plastic flow of galena along fractures within some quartz stringers.

The last stage (stage III), is characterized by the deposition of irregular blebs of undeformed subhedral to euhedral clear quartz, which at places lines small cavities within stage II quartz. Stage III quartz occurs mainly in coarse-grained galena and may contain rare inclusions of galena, and/or sphalerite.

Siderite-quartz-sphalerite (SQS) veins

In contrast to the discordant SQT and QSG veins at the Sunshine, Coeur, and Lucky Friday mines, SQS veins at the Gold Hunter mine are concordant to semi-concordant to the steeply dipping argillite of the host Wallace Formation. The SQS veins at Gold Hunter are relatively thin (from 50 to 10 cm) and occur as en echelon veins parallel to QSG and barren siderite veins (Plate 6). The

(a)

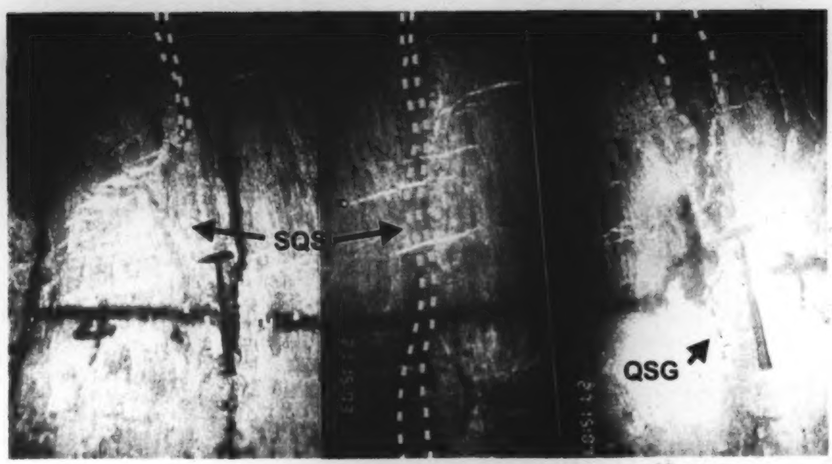

(b)

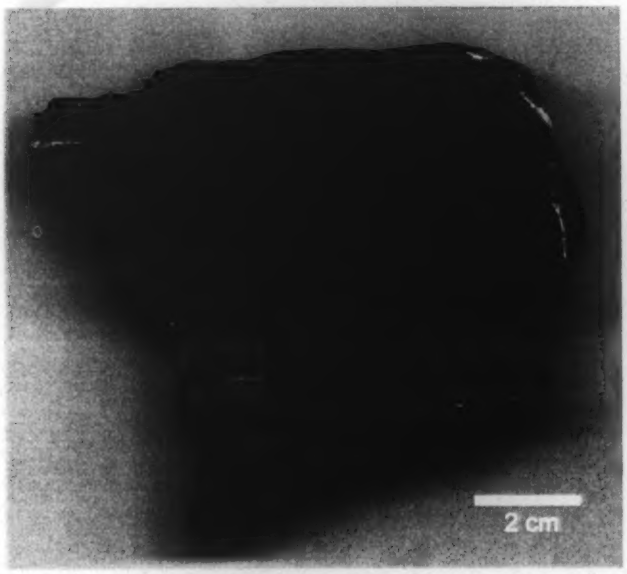

Plate 6. SQS veins. (a). Gold Hunter mine (4900 level). The outcrop contains three vein types, SQS and QSG (labeled and pointed with black arrows), and subhorizontal quartz veins (unlabeled). (b). Sample of fractured crustification banding texture, Gold Hunter mine (4900 level).The dark mineral is sphalerite, the light mineral is early siderite. Mineral zoning is visible in siderite. The fractures in early siderite are filled with stage II sphalerite and siderite.

contacts of the SQS veins are sinuous and are often coated with thin quartz-sericite selvages that contain slickenfibers indicative of dip slip. Structural studies at the Bunker Hill mine demonstrate that the SQS veins are developed parallel to the axial plane of a west-northwest trending fold system, whereas QSG veins are associated with east-northeast trending folds of presumably younger age (Juras, 1982). Although no clear crosscutting relationships are reported, mixtures of minerals of the two vein types occur at the intersection of the SQS and QSG veins. At other mines of the district, however, the two vein types have sub-parallel orientation (Leach et al., 1988; this study).

The ratio of sphalerite to galena in the SQS veins is 2/1 or higher. Along with the principal ore and gangue minerals the SQS veins contain subordinate amounts of quartz, galena, pyrite, tetrahedrite, arsenopyrite, and meneghinite ($CuPb_{13}Sb_7S_{24}$).

Fragments of preserved crustification banding textures in the SQS veins in the Gold Hunter mine indicate simultaneous precipitation of siderite, sphalerite, and possibly galena in an early stage I (Plate 6). Individual crystals of massive siderite from the crustification bands exhibit preserved mineral zoning. Siderite at Gold Hunter reaches up to 2 cm in diameter and exhibits similar deformation features to siderite at the SQT veins. Locally, fine-grained sphalerite and galena, associated with pyrite, and chalcopyrite indicate that a relatively high degree of post depositional shearing followed mineral deposition in stage I.

Stage II in the SQS veins is characterized by the introduction of minor honey colored sphalerite and clear siderite along fractures in the early siderite and sphalerite. The honey colored sphalerite and siderite have grown after the deformation. Medium- to fine-grained euhedral pyrite occurs in deformed sphalerite. Small amounts of meneghinite and tetrahedrite also occur as irregular, millimetre to sub-millimetre size inclusions in the early minerals.

Precipitation of discordant veins of massive and fibrous quartz characterizes the latest stage (stage III) in the development of the siderite-quartz-sphalerite SQS veins at the Gold Hunter mine. Some pods and stringers of milky or transparent quartz may contain inclusions of coarse-grained sphalerite and galena.

Hydrothermal alteration related to the Ag-Pb-Zn veins

Hydrothermal alteration at Coeur d'Alene has produced zones of bleaching, which are prominent in the hematite bearing Belt metasedimentary strata (Fryklund, 1964; White, 1998) especially in the Sunshine and Coeur mines. At the Sunshine mine these zones extend 10 to 30 m away from the vein walls and their outward boundaries are rimmed by narrow bands of pyrite (White, 1998). Bleaching sometimes extends hundreds of meters away from the veins, and is also found in the Belt metasedimentary rocks outside of the district (White, 1998). Petrographic observations demonstrate that bleaching resulted mainly from alteration of hematite, magnetite, and/or pyrite to goethite, replacement of green chlorite with a colorless variety, and also from leaching of carbonaceous material (Fryklund, 1964; Weiss, 1964). Fryklund (1964) noted that detrital feldspar was preserved, and attributed this to a near neutral pH and/or low temperature of the hydrothermal fluid related to bleaching.

The hydrothermal alteration in Coeur d'Alene is also characterized by the replacement of syngenetic ferroan dolomite and ankerite by siderite near the vein walls (Fryklund, 1964, White, 1998). The siderite zone extends tens to hundreds of meters away from the veins and is surrounded by a narrow zone of ankerite and calcite which grades into unaltered rock (White, 1998). The mineralogical change is consistent with the geochemical evidence that bleached rocks are significantly depleted in Ca (Tibbs, 1972). Unlike the Archean mesothermal Au-quartz deposits which are surrounded by large haloes of carbonate alteration caused by the high CO_2 content of the hydrothermal fluids, whole rock analyses of altered and unaltered metasedimentary rocks at the Coeur d' Alene district demonstrated a lack of net CO_2 contribution in the alteration zones surrounding the Ag-Pb-Zn veins (Fryklund et al., 1964) which implies low CO_2 content of the mineralizing fluids.

Geology of the Coleman Au-quartz vein

The Coleman vein is a part of a small Au-quartz vein system that lies approximately 3 km to the northwest of the Sunshine mine (Fig. 1.1). Recent estimates indicate resources of approximately 35000 ounces of gold at 0.15 ounces per ton (New Jersey Mining Company Ltd., press release, 1999). The Au-quartz veins in the district are hosted mainly by the argillites of the Prichard Formation. The aggregated strike length of the vein system is about 450 m. The main Au-quartz vein strikes approximately to the north and dips steeply to the west, and is between 1.5 and 3 meters thick. The vein contacts are sharp with little or no visible alteration. Red-brown staining with iron oxides and hydroxides produced by supergene processes is seen in the vein and in the immediate host rocks both at the surface and underground (Plate 7).

The Au-quartz vein consists of >99% milky quartz, which is brecciated and deformed to a variable degree. The deformation has locally resulted in sub-grain development, and also in the development of trails of submicroscopic secondary fluid inclusions. Minor amounts of sulphides and sulphosalts such as galena, tetrahedrite and sphalerite occur as isolated inclusions within massive quartz. A thin (sub-millimetre size) rim of clear quartz is seen along the contact between the sulphides and the milky quartz. Gold is fine-grained and is either associated with sulphides, or occurs as individual irregular grains within vein quartz (F. Brakebush, personal communication). No carbonates were seen in the vein.

The Au-quartz Coleman vein displays a similar paragenetic sequence to other Mesozoic Au-quartz veins from the North American Cordillera, such as the the veins at Alleghany in California (Böhlke and Kistler, 1986), or the mesothermal Au-quartz veins in the Yukon (Rushton et al., 1996). The initial bulk quartz deposition in the Coleman vein was followed by precipitation of minor amounts of sulphides and gold. The lack of sulphide mineralization along the vein walls indicates that sulphidation was not an important depositional mechanism. The absolute age of Au-quartz veins in the district has not been determined.

Plate 7. Coleman Au-quartz vein, approximately 60 m underground. The vein is brecciated by late tectonic movements along the sinuous vein fracture in the Prichard Formation argillite.

V. FLUID INCLUSION STUDY

Introduction

A fluid inclusion study of various vein minerals from the Coeur d'Alene district was undertaken in order to define the pressure, temperature, and chemical composition of fluids during various stages of vein formation. Another important objective was to determine the nature of the fluid inclusions and their suitability for bulk crush-leach analysis. Analyses by bulk methods provide greater information on the chemistry of the fluids than microthermometry alone but a major drawback is that the average fluid composition obtained could represent a mixture of various fluids present as different generations of fluid inclusions in the sample (Roedder 1984; Yardley et al., 1993). Over 280 fluid inclusions in 20 doubly-polished sections of siderite, quartz and sphalerite were examined in order to determine the type and relative abundance of various fluid inclusion populations, and their possible impact on the solute chemistry results.

Most microthermometric analyses were carried out on a modified Fluid Inc. gas-flow heating-freezing stage which was calibrated using deionized water-ice bath, and natural pure CO_2 inclusions in Alpine vein quartz. The accuracy of the microthermometric measurements was ± 0.2° C within the low-temperature range (0.0 to -60.0° C) and ± 2.0° C for heating to 350° C. The small size (1-10 µm) of most of the fluid inclusions in siderite and the generally poor optical quality of the mineral necessitated the use of an Olympus BX-50 microscope equipped with a Linkam THMSG 600 heating-freezing stage. The stage was calibrated using synthetic fluid inclusion standards from Syn Flinc®. The accuracy of the measurements was ± 0.1° C below 31.1°C (the critical point of CO_2), and ± 1.0° C for the high temperature range.

Selection of material for microthermometric study

Samples of siderite, quartz, and sphalerite were selected for fluid inclusion study from vein material collected in underground workings, mining dumps, and surface outcrops at the Sunshine, Lucky Friday, Gold Hunter, and New Jersey mines. Most veins in the Coeur d'Alene district have experienced variable syn- to post-mineral shearing and deformation, which has made large sections of the veins unsuitable for microthermometric analysis. Where possible, vein samples were selected for their good optical quality and unstrained nature. Late undeformed quartz closely associated or post-dating the deposition of silver-rich tetrahedrite or galena and sphalerite yielded particularly good quality material. Late siderite was also of good quality but contained fewer fluid inclusions. As a result of this selection microthermometric data from certain veins (i.e. the Lucky Friday main vein) were obtained mainly from stage II and III quartz.

Compositional types of fluid inclusions

Classification of fluid inclusion types is relative and is based on fluid inclusion compositions inferred by the number of phases present at or slightly below room temperature, and the nature of the phase changes observed during heating and freezing experiments. Four compositional types of fluid inclusions were identified in this study: CO_2-free aqueous inclusions (type 1), low-X_{CO2} aqueous inclusions (type 2), intermediate-X_{CO2} aqueous inclusions (type 3), and high-X_{CO2} or CO_2-dominant inclusions (type 4). Fluid inclusions were also classified as primary, pseudosecondary, or secondary, based on the criteria of Roedder (1984), and Shepherd et al. (1985). Unequivocal determination of the origin the fluid inclusions, however, has been difficult especially in siderite. Partial to total reequilibration and migration of fluid inclusions in quartz, fluorite, and carbonates, has been widely recognized (Vityk and Bodnar, 1998; Audetat, 1999), and microthermometric data from fluid inclusions in strained minerals have to be regarded with caution. Thus, efforts were focused on obtaining microthermometric data from the least deformed domains of the vein minerals. The fairly homogeneous microthermometric properties of the fluid inclusions from stage I and II siderite indicate that no significant stretching, necking down, or leakage had occurred.

Type 1: Aqueous inclusions

Aqueous inclusions are rare in samples from the Ag-Pb-Zn veins and absent in the Au-quartz Coleman vein. Most type 1 inclusions occur along healed fractures in sphalerite and late quartz from the QSG Lucky Friday main vein, and very rarely in stage II siderite from the SQT Sunshine vein. The aqueous inclusions contain H_2O liquid and vapour. At room temperature the vapour phase occupies between 5 and 10 volume % of the inclusion. Low temperature phase changes indicate that most type 1 inclusions are of moderate to low salinity (5 to 10 eq. wt. % NaCl), and low Th_{total} (150 to 200°C). Aqueous inclusions range in size from less than 5 to 15 µm and are oblate to irregular in shape. The absence of gas hydrate (clathrate) formation at low temperatures constrains the concentration of CO_2 and/or other volatiles dissolved in inclusion fluids to less that 1.6 mol % (Hedenquist and Henley, 1985). Low salinity aqueous inclusions (<1 eq. wt. % NaCl) were also reported from healed fractures in quartz from other vein deposits the district (Leach et al., 1988). The inclusions were considered to be late and not related to the mineral deposition (Leach et al., 1988). Due to their small number and mostly secondary nature aqueous inclusions are not considered further.

Type 2: low-X_{CO2} fluid inclusions

The results from the microthermometric study indicate that type 2 inclusions are the dominant fluid inclusion type in stage I and II siderite and quartz from the SQT Sunshine vein, and in siderite from SQS veins at the Gold Hunter mine (Plate 8). Low-X_{CO2} inclusions also dominate stage II quartz and sphalerite from the QSG Lucky Friday main vein. They are two phase (L-V) with apparent salinity of ~12 eq. wt. % NaCl and vapour phase of slightly larger average volume (~12%) than the aqueous inclusions. Type 2 inclusions are between 5 and 10 µm in size. Although most low-CO_2 fluid inclusions in siderite are negative crystal shaped, oblate and irregular shapes are also common. In contrast to type 1 inclusions all type 2 inclusions nucleate clathrate upon cooling. The absence of a second liquid phase constrains CO_2 concentration in type 2

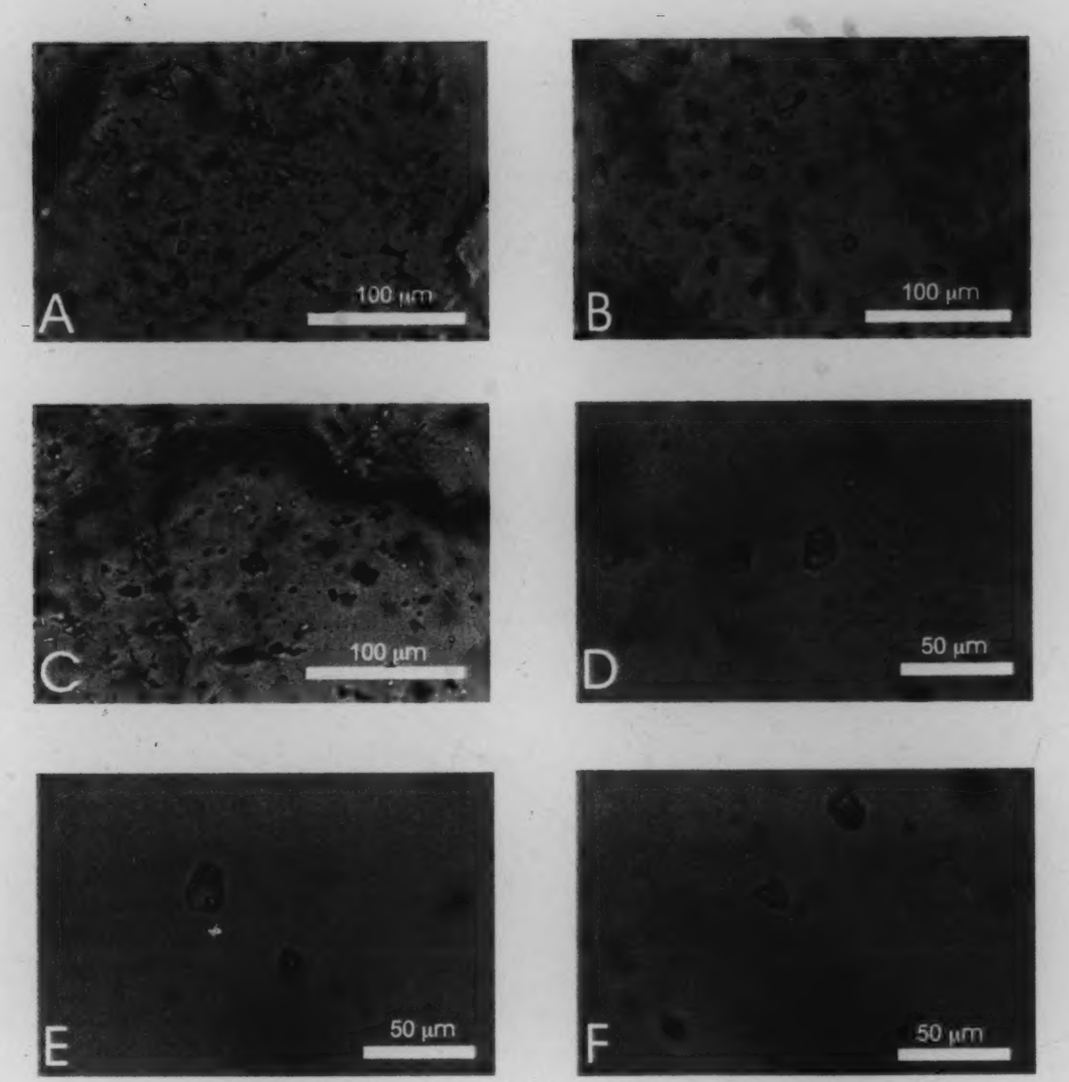

Plate 8. Photomicrographs of type 2, 3, and 4 fluid inclusions in SQT and QSG veins taken at room temperature (~25°C); A. (SQT) Field of small type 2 inclusions in sample SSM-11 - stage I siderite; B. (SQT) Relatively large type 2 fluid inclusions in SSM-9, stage II siderite. C. (SQT) Type 2 fluid inclusions in SSM-9, stage II siderite; D. (QSG) Type 3 fluid inclusions in stage III quartz (LF-14); E.(QSG) Type 3 inclusions with different degrees of fill in stage III quartz (LF-10). F. (QSG) Coexisting type 3 and type 4 fluid inclusions in stage III quartz (LF-10).

inclusions to less than ~4 mol %, and precludes meaningful interpretation of clathrate melting temperatures (Hedenquist and Henley, 1985).

The effect of the presence of dissolved CO_2 on the melting point of ice (Tm_{ice}) is well known (Collins, 1979; Hedenquist and Henley, 1985). The structure of clathrate involves substantial amounts of H_2O and the enrichment of the residual aqueous fluid with NaCl would result in depression of the ice-melting temperature in type 2 inclusions (Tm_{ice}). Even small amounts of dissolved volatiles not sufficient to form clathrate can depress ice-melting temperatures with as much as 1.5°C (Hedenquist and Henley, 1995). Published gas analyses indicate the presence of at least 2.5 wt. % gas which contains roughly equal amounts of CO_2 and N_2, lesser CH_4, and short-chain hydrocarbons in liquid-rich fluid inclusions from zinc-rich veins at the Bunker Hill mine (Bijak and Norman, 1982). Thus, if a maximum concentration of 4 mol % CO_2 is assumed for type 2 inclusions, according to the data of Collins (1979) their apparent salinities as calculated from Tm_{ice} will be overestimated by as much as 2 eq. wt. % NaCl. The lack of quantitative data on the fluid inclusion volatile content, however, does not allow corrections of the estimated salinities to be made.

Type 3: Intermediate-X_{CO2} inclusions

Type 3 inclusions occur predominantly in stage III quartz from all Ag-Pb-Zn veins studied and also in main stage quartz from the Au-quartz veins. The intermediate-X_{CO2} inclusions are mostly two phase and rarely three phase at room temperature ($H_2O[L]+CO_2[V]$, or $H_2O[L]+CO_2[L]+CO_2[V]$). The two-phase inclusions nucleate a liquid CO_2 phase upon cooling, sometimes as low as -2.0°C. Intermediate-X_{CO2} inclusions are typically larger (10 to 20 μm) than type 2 inclusions and often exhibit irregular shapes (Plate 8). Negative crystal shape is rarely seen and is characteristic for secondary type 3 inclusions observed along healed fractures in stage III quartz. The carbonic phase of the intermediate-X_{CO2} inclusions occupies from 10 to 50 % of the inclusion volume, although in most cases it is ~30 vol. %. Clathrate melting temperatures indicate that type 3 inclusions from the Ag-Pb-Zn and Au-quartz veins in the district are of moderate to low salinity (14.0 to 0.1 eq. wt. % NaCl).

Leach et al. (1988) suggested that intermediate-X_{CO2} fluid inclusions which contain 5 to 15 mol % gas (CO_2; C_nH_n, CH_4, N_2) and 5 to 10 eq. wt. % NaCl are the most common fluid inclusion type, which is closely associated with the Ag-Pb-Zn and Au mineralization in Coeur d'Alene. The volatile composition of those fluid inclusions varies from CH_4-light hydrocarbon-dominated in the "older" zinc-rich veins, to CO_2 or CO_2-N_2 dominated in the "younger" silver- and gold-rich veins (Leach et al., 1988). This study, however, demonstrates that not type 3, intermediate-CO_2 fluid inclusions but type 2, low-CO_2 fluid inclusions are closely related to main stage precious- and base-metal mineralization in the veins studied. The study also shows that type 3 fluid inclusions are parageneticaly late and probably not related to the Ag-Pb-Zn mineralization in the district.

Type 4: High-X_{CO2} (CO_2-rich) inclusions

Primary, pseudosecondary and secondary CO_2-rich inclusions occur in stage III quartz from all studied Ag-Pb-Zn veins, and also in main stage quartz from the Coleman Au-quartz vein. They contain a liquid CO_2 (N_2, CH_4) phase at room temperature and nucleate a vapour bubble upon cooling. Almost all type 4 inclusions homogenize to liquid at a temperature range of –43° to +18°C. On the basis of visual estimates type 4 inclusions appear to contain more than 90% CO_2(CH_4, N_2; Plate 7). An aqueous phase was recognized in only one type 4 inclusion. Aqueous fluid may have been present, however, as a thin film wetting the inclusion walls in all CO_2-rich inclusions. Average Tm_{CO2} of type 4 inclusions varies between -56.6 and -60.0°C and indicates variable presence of volatiles other than CO_2. Published data from gas-rich fluid inclusions in quartz from various veins in the Coeur d'Alene district indicate that volatile compositions vary in a manner similar to the intermediate X_{CO2}-(C_nH_n, CH_4, N_2) inclusions as described above (Leach et al., 1988). Upon cooling below -160°C the CO_2-rich inclusions with the most depressed Th_{CO2} contain solid, liquid, and vapour phases (S+L+V). A partial homogenization ([Th_s]; a homogenization of liquid and vapour in the presence of solid CO_2) to gas and/or liquid (e.g., S+L+V → S+L, or S+V) is observed upon warming the inclusions between -160 to -147°C. These phase transitions indicate that N_2 comprises significant part of the fluid inclusion volume (Touret, 1982; van den Kerkhof, 1990). According to van den Kerkhof (1990) these inclusions can be classified as an H type, because they exhibit homogenization instead of sublimation as a final phase transition. N_2-dominant, gas-rich fluid inclusions that homogenize to a liquid phase in the presence of solid CO_2 between -180° and –150°C were reported from the Kennedy Creek mine (Leach et al., 1988).

Results of microthermometric study

A summary of the microthermometric results is presented in Table 5.1. The results for the principal vein types are also presented as histograms and PT plots on Figures 5.1 trough 5.8. The entire data set is presented in Appendix 1. The apparent salinities of the aqueous and the low-X_{CO2} fluid inclusions based on Tm_{ice} were calculated using the equation of Bodnar and Vityk (1994). The salinities of the CO_2 saturated inclusions were determined from the melting point of clathrate ($Tm_{clathrate}$) using the equation of Darling et al. (1991). The errors quoted in Table 5.1 and in the following section represent plus/minus one standard deviation from the average values.

Table 5.1. Summary of microthermometric data for the principal vein types studied.

Vein Type	Host Min.	Stage	Incl. type	Volume % vapour	$\mathrm{Tm_{CO_2}}$ (°C)	$\mathrm{Tm_{ice}}$ (°C)	$\mathrm{Tm_{clath.}}$ (°C)	$\mathrm{Th_{CO_2}}$ (°C) (to liquid)	$\mathrm{Th_{total}}$ (°C)	Eq. wt. % NaCl
SQT veins (Sunshine Vein)										
	siderite	I	2	11 ± 5		8.9 ± 3.4			239 ± 11	12.6 ± 2.1
		II	2	13 ± 5		6.8 ± 2.1			285 ± 24	10.6 ± 1.3
	siderite /quartz									
	quartz	III	3	46 ± 10*	-57.3 ± 0.8		9.6 ± 0.6	19.6 ± 6.0	289 ± 24	0.5 ± 0.8
	quartz		4	>90	-57.4 to -58.2			11.9 to -24.5		
QSG veins (Lucky Friday main Vein)										
	quartz	II	2	10 ± 7		7.1 ± 2.0			261 ± 20	10.9 ± 1.5
	quartz	III	3	41 ± 12*	-58.7 ± 1.2		7.6 ± 0.8	12.4 ± 3.0	305 ± 24	4.0 ± 2.3
	quartz,	III	3s**	37 ± 15*	-58.0 ± 0.8		9.2 ± 0.3	16.1 ± 3.6	277±6	1.6 ± 0.3
	siderite		4a	>95	-58.0 ± 1.5			1.4 ± 11.4		
			4b	>95	-60.0 ± 0.2			-30.6 ± 11.0		
SQS veins (Gold Hunter mine)										
	siderite	I	2	10 ± 3		12.5 ± 0.7			164 ± 21	16.7 ± 3.0
	siderite	II	2	15 ± 6		7.7 ± 1.3			229 ± 17	11.5 ± 0.9
	quartz	III	3	37 ± 10*	-57.0 ± 0.4			24.1 ± 1.7	280 ± 15	4.0 ± 0.7
	quartz	III	4	>90	-57.4 ± 0.4			12.2 ± 1.1		
Coleman Au-quartz vein										
	quartz	n.a.	3	41 ± 12*	-57.3 ± 0.4		8.9 ± 0.5	21.6 ± 3.4	269 ± 8	2.1 ± 1.2
	quartz	n.a.	4	>95	-57.3 ± 0.1			10.9 ± 3.3		

*The carbonic phase volume was corrected using the method of Brown and Lamb (1989).

** type 3 secondary fluid inclusions.

SQT veins (Sunshine Vein)

The siderite-quartz-tetrahedrite Sunshine vein at the Sunshine mine, was examined in detail. Type 2, low-X_{CO2} fluid inclusions are the dominant inclusion type at the Sunshine vein. Microthermometric data demonstrated the presence of two groups of type 2 inclusions with different Th and apparent salinities which belong to two different paragenetic stages (Fig. 5.1)

Stage I

The first group of type 2 inclusions dominates stage I siderite and exhibits average Th_{total} of 239 ± 11°C (n = 49). The apparent salinities vary from 9.5 to 17.5 eq. wt. % (average 12.6 ± 2.1 eq. wt. % NaCl; n = 76) and define a subhorizontal trend suggestive of mixing of fluids with similar temperatures but different salinities (Fig. 5.2)

Stage II

The second group of type 2 inclusions occurs in paragenetically late siderite and quartz associated with or postdating the deposition of silver-rich tetrahedrite. Fluid inclusions from this group exhibit higher average Th_{total} and slightly lower apparent salinities of 285 ± 24°C (n = 31), and 10.6 ± 1.3 eq. wt. % NaCl (n = 35) respectively (Fig. 5.1A, B; Fig. 5.2). Eutectic melting temperatures (Te) in the majority of stage I and II, type 2 inclusions average -23.3 ± 2.8°C (n = 14), which is close to the eutectic temperature of the H_2O-NaCl-KCl system (~-23°C; Shepherd et al., 1985). Only a few stage I, type 2 high-salinity inclusions of uncertain origin exhibit lower Te (~-52.0°C; n = 4) and brown colored ice diagnostic of the presence of $CaCl_2$ (Shepherd et al., 1985). These inclusions also exhibit high apparent salinities of 16.9 to 20.2 eq. wt. % NaCl and lower homogenization temperatures from 173° to 221°C.

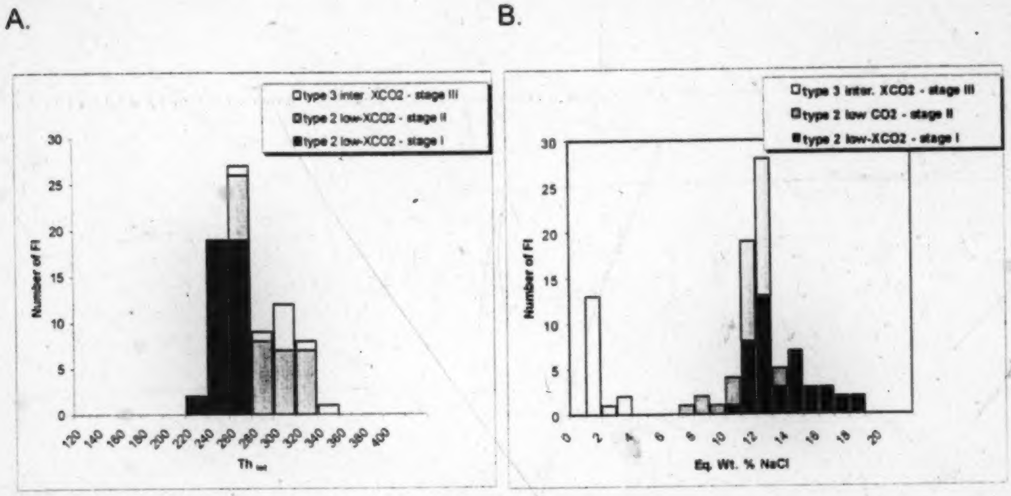

Fig. 5.1. A. Total homogenization temperature (Th_{total}), and B. calculated salinities (eq. wt. % NaCl) for type 2 and 3 inclusions from stages I, II, and III at the SQT Sunshine vein. Calculated salinities for type 2 inclusions are not corrected for CO_2.

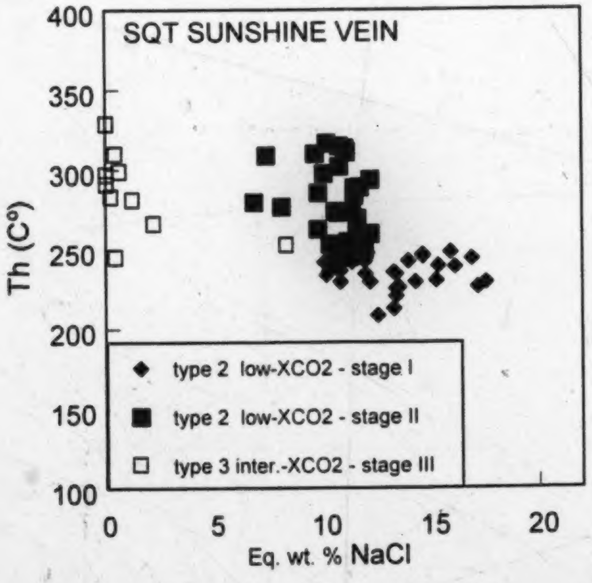

Fig. 5.2. Total homogenization temperature (Th_{total}) against salinity (eq. wt. % NaCl) for type 2 and 3 fluid inclusion from stages I, II, and III at the SQT Sunshine vein.

Stage III

Stage III subhorizontal quartz veins contain coexisting type 3, intermediate-X_{CO_2} and type 4, CO_2-rich fluid inclusions. The inclusions are primary and pseudosecondary and are particularly abundant in small enclaves of undeformed milky quartz. Type 3 inclusions exhibit an average Tm_{CO_2} of -57.5 ± 0.5°C (n = 11) which indicates the presence of N_2 and/or CH_4. Th_{CO_2} varies from 26.0 to 13.3°C. Type 3 fluid inclusions at the Sunshine vein have very low average salinity of 0.5 ± 0.7 eq. wt. % NaCl, (n = 11), and Th of 289 ± 42°C; (n = 11; Fig. 5.1a, b; Fig. 5.2).

On the basis of their microthermometric properties CO_2-rich inclusions measured in this study exhibit contrasting microthermometric properties with Tm_{CO_2} ranging from –57.4 to –58.2°C and Th_{CO_2} from 11.9 to –24.5°C. All CO_2-rich inclusions homogenize to liquid. A few type 4 inclusions exhibit partial homogenization (Th_s) to vapour in the presence of solid CO_2 at around -147°C which indicates the presence of significant amounts of N_2.

QSG veins (Lucky Friday main vein)

Microthermometric data were obtained from milky stage II quartz and sphalerite at the Lucky Friday main vein. Data were also obtained from clear stage III quartz. No data are available from stage I siderite and sphalerite due to the high degree of shearing and deformation of the vein.

Stage II

Stage II sphalerite and quartz associated with tetrahedrite and chalcopyrite are dominated by primary, pseudosecondary, and secondary type 2 inclusions with average Th and salinity of 261 ± 21°C and 10.9 ± 1.5 eq. wt. % NaCl, respectively (n = 17; Fig. 5.3A, B; Fig. 5.4). Secondary type 3 inclusions of higher Th and lower salinities (277 ± 6°C and 1.6 ± 0.3 eq. wt. % NaCl, respectively; n = 6).

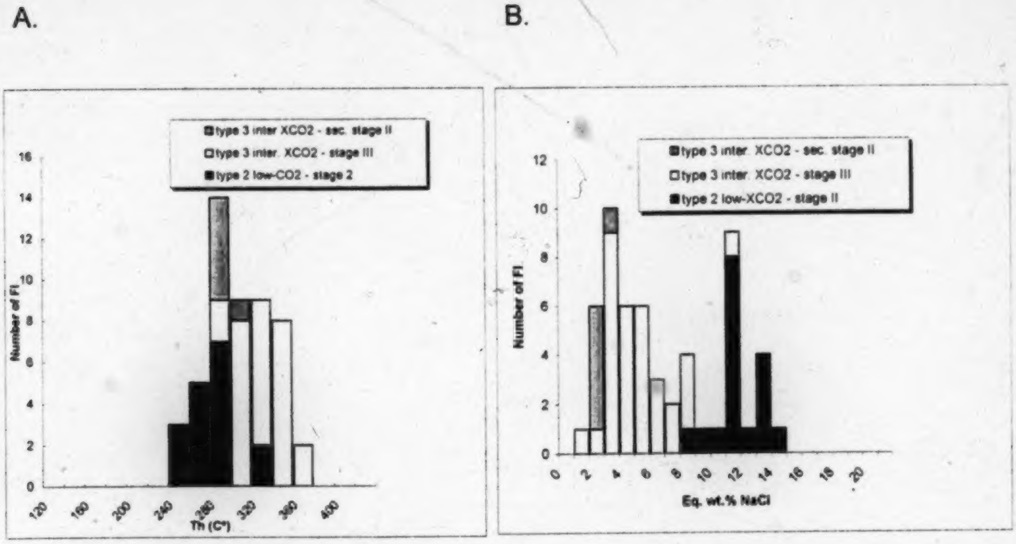

Fig. 5.3. A.Total homogenization temperature (Th_{total}), and B. calculated salinities (eq. wt. % NaCl) for type 2 and 3 inclusions from stages II, and III in the QSG Lucky Friday main vein. Calculated salinities for type 2 inclusions are not corrected for CO_2.

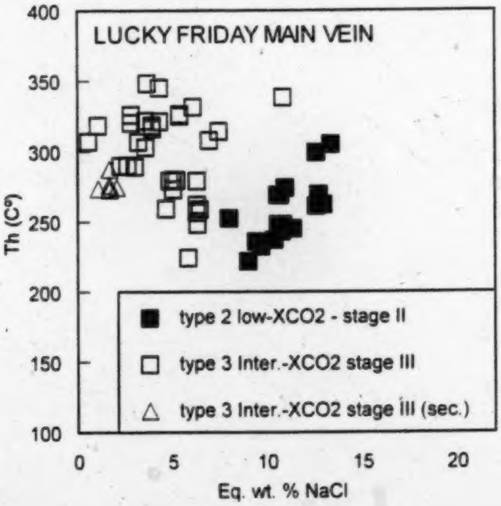

Fig. 5.4. Total homogenization temperature (Th_{total}) against salinity (eq. wt. % NaCl) for type 2 and 3 fluid inclusion from stages II and III in the QSG Lucky Friday main vein.

occur in stage III siderite. Trails of secondary aqueous inclusions of moderate salinity (6.2 ± 0.6 eq. wt. % NaCl) and low average Th (207 ± 37°C, n = 9) occur along healed fractures in sphalerite.

Stage III

Stage III quartz associated with minor galena and sphalerite contains large (up to 30 μm) primary and pseudosecondary type 3, intermediate-X_{CO2} inclusions. Trails of secondary type 3 inclusions with microthermometric properties similar to those of the primary inclusions occur in the same quartz crystals and indicate minor brittle deformation during or immediately after stage III quartz precipitation. Type 3 inclusions have high average Th (305° ± 24° C; n = 21) and variable salinities (0.5 to 10.8 eq. wt. % NaCl, average: 4.0 ± 2.3 eq. wt. % NaCl; n = 26, Fig. 5.3A, B; Fig. 5.4). The average Tm_{CO2} and Th_{CO2} are -58.7 ± 0.6°C and 12.2 ± 1.5°C respectively (n = 26). Primary and pseudosecondary type 4 fluid inclusions also occur in late undeformed quartz in close association with type 3 inclusions (Plate 8). Type 4 fluid inclusions in quartz III at the Lucky Friday main vein are divided into type 4a, which exhibits an average Th_{CO2} of 1.4 ± 11.4°C (n = 14), and type 4b which is characterized by values as low as -30.0 ± 11.0°C, (n = 5). The Tm_{CO2} of type 4a and b inclusions varies from -56.9 to -60.1°C with the most depressed values typical for 4b (Table 5.1). Partial homogenization (Th_s) to liquid and gas was observed in 3 CO_2 rich inclusions from both groups. Protracted melting at Tm_{CO2} coupled with disappearance of the gas bubble in one CO_2-rich inclusion indicates presence of CH_4 (van den Kerkhof and Thiery, 1994).

SQS veins (Gold Hunter mine)

Detailed microthermometric studies were conducted on stage I and stage II siderite from one SQS vein at the Gold Hunter mine (Table 5.1). Data were also collected from stage III quartz which sometimes associates with minor sphalerite and/or galena. The poor optical quality and small size of the fluid

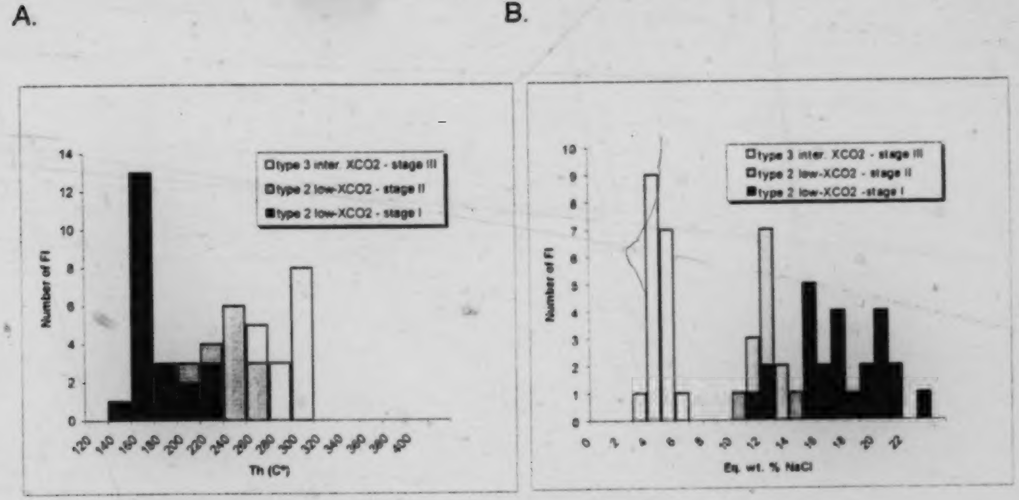

Fig. 5.5. A.Total homogenization temperature (Th_{total}), and B. calculated salinities (eq. wt. % NaCl) for type 2 and 3 inclusions from stages I, II, and III in SQS veins at theGold Hunter mine. Calculated salinities for type 2 inclusions are not corrected for CO_2.

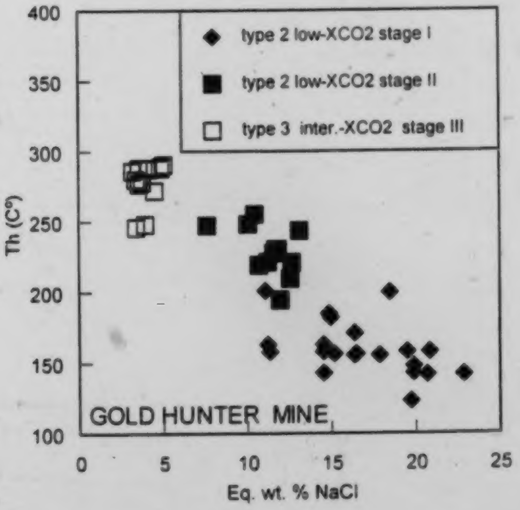

Fig. 5.6. Total homogenization temperature (Th_{total}) against salinity (eq. wt. % NaCl) for type 2 and 3 fluid inclusion from stages I, II, and III in SQS veins at the Gold Hunter mine.

inclusions did not permit microthermometric data to be obtained from samples of zoned stage I siderite from crustification bands with sphalerite.

Stage I

Early siderite is dominated by primary type 2, low-X_{CO2} fluid inclusions with low Th_{total} and generally high apparent salinity. The Th_{total} of stage I inclusion vary from 125 to 206°C, average: 164 ± 21° C (n = 22), and their apparent salinity vary from 11.0 to 22.8 eq. wt. % NaCl, average 16.7 ± 3.0 eq. wt. % NaCl (n = 22; Fig. 5.5 A, B). The Th_{total} and salinity of stage I, type 2 inclusions define negative correlation suggestive of fluid mixing (Fig. 5.6). This group of fluid inclusions exhibits Te of -23.8 ± 0.5°C (n = 5), characteristic of NaCl-dominated compositions (Shepherd et al., 1985). Low temperature phase changes at around -28°C observed in some stage I siderite inclusions are interpreted as initial melting at the metastable NaCl eutectic.

Stage II

Stage II siderite contains fluid inclusions of higher Th_{total} and lower apparent salinities to stage I (229 ± 17°C, n = 11; 11.5 ± 0.9 eq. wt. % NaCl, n = 14; Fig. 5.5 a, b; Fig. 5.6). Fluid inclusions in stage II siderite exhibit average Te of -33.5 ± 3.0°C (n = 3) suggesting presence of $MgCl_2$ and/or $FeCl_2$ (Shepherd et al., 1985).

Stage III

Late stage III quartz is dominated by type 3, intermediate-X_{CO2} inclusions with an average Th_{total} of 280 ± 15°C (n = 14) and salinity of 4.0 ± 0.7 eq. wt. % NaCl (n = 18). Tm_{CO2} of -57.0 ± 0.3°C (n = 18) indicates the presence of small amounts of volatiles other than CO_2. The average Th_{CO2} is 24.1 ± 1.7°C with slightly lower values for the fluid inclusions in euhedral quartz associated with minor sphalerite. Primary and pseudosecondary type 4 inclusions with generally homogeneous microthermometric properties also occur in stage III quartz. They exhibit average Tm_{CO2} and Th_{CO2} of -57.2 ± 0.2°C and 12.2 ± 0.8°C (n = 5) respectively.

Au-quartz Coleman Vein

Fluid inclusion data from the Au-bearing Coleman vein were obtained from relatively unstrained quartz associated with minor disseminated galena, chalcopyrite and sphalerite, and also from late post-mineralization vug quartz. Primary, pseudosecondary, and secondary type 3, intermediate X_{CO2} inclusions are the dominant fluid inclusion type in the Au-bearing Coleman vein. They are usually three phase (H_2O[L]-CO_2[L]-CO_2[V]) at room temperature and exhibit various degrees of fill with carbonic fluid (10 - 50 vol. %). $Tm_{clathrate}$ indicates that type 3 inclusions contain low salinity aqueous fluid that ranges between 0.6 to 5 eq. wt. % NaCl (average: 2.1 ± 1.2; n = 31). The inclusions exhibit an average Th_{total} of 269 ± 8°C (n = 10; Fig. 5.7 A, B, Fig. 5.8). A single fluid inclusion, which homogenizes to liquid at about 70°C lower than the average Th_{total} and 60°C lower than the lowest homogenization temperature in the group (Fig. 5.7) was excluded from the calculations. Type 4, CO_2-rich inclusions also occur in the Coleman vein. They exhibit average Tm_{CO2} of -57.3 ± 0.1°C and Th_{CO2} of 10.9 ± 3.3°C (n = 5) respectively. One type 4 inclusion has Th_{CO2} of -12.0°C. All type 4 inclusions homogenize to liquid CO_2. Partial homogenization and/or other low temperature phase changes were not observed in type 4 inclusions from the Coleman vein.

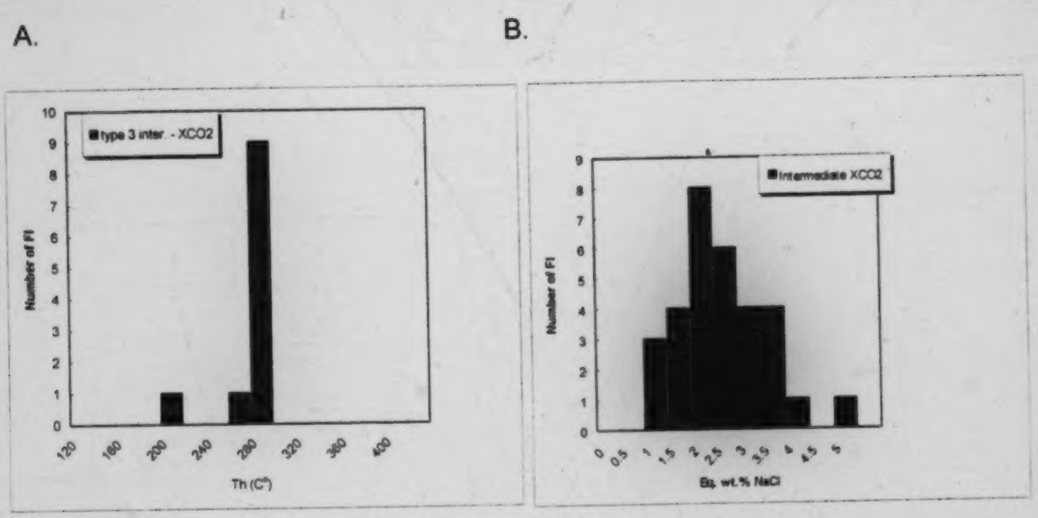

Fig. 5.7. (a). Total homogenization temperature (Th_{total}), and (b). calculated salinities (eq. wt. % NaCl) for type 3 inclusions from at the Au-quartz Coleman vein.

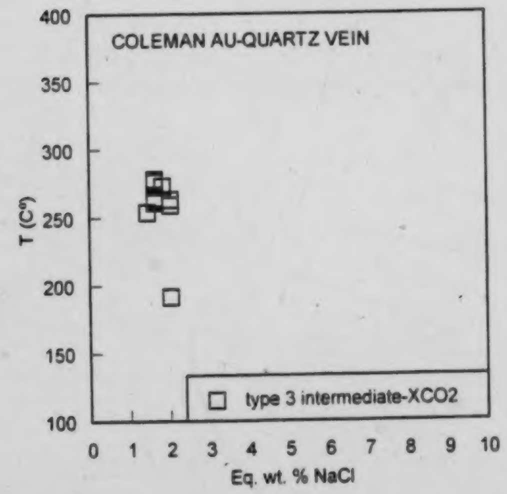

Fig. 5.8. Total homogenization temperature (Th_{total}) against salinity (eq. wt. % NaCl) for type 3 fluid inclusion at the Coleman Au-quartz vein.

Fluid Compositions and Densities

The results of the microthermometric studies and bulk crush-leach analyses (Chapter VII) indicate that the P-V-T-X properties of type 1 and type 2 fluid inclusions are best approximated by the H_2O-NaCl-KCl-$CaCl_2$ system of Zhang and Frantz (1987). Molar volumes and bulk densities of type 1 and 2 inclusion fluids were calculated using MacFlincor 0.93 (Brown and Hagemann, 1994) assuming that the fluid inclusions have negligible gas contents. However, the presence of small amounts of CO_2 (CH_4, N_2, etc.) indicated by the nucleation of clathrate affects the bulk density of the fluid and, although this effect is small calculated densities and molar volumes for type 2 inclusions must be regarded as minimum values.

The lack of quantitative data on the gas composition of the fluid inclusions creates difficulties in choosing an appropriate system that could best describe type 3 and 4 fluid inclusions. Published laser Raman and bulk quadrupole mass spectrometric data from the district indicated the presence of significant amounts of CH_4 and N_2 in some type 3 and 4 fluid inclusions. Minor amounts of short-chain hydrocarbons were also reported (Bijak and Norman 1982; Hofstra et al., 1985; Leach et al., 1988). These data, along with the significant depression of Tm_{CO2} observed in most type 3 and 4 inclusions, do not permit the gas phase of these inclusions to be regarded as pure CO_2. Due to the strong impact which relatively small amounts of N_2 and CH_4 have on Th_{CO2} erroneously high carbonic phase densities and low molar volumes for type 3 and 4 fluid inclusions will be calculated if the presence of N_2 and CH_4 is not accounted for (Touret, 1982; van den Kerkhof et al., 1991). For example, if the carbonic phase of a CO_2-rich inclusion contains 10 mol % N_2, Th_{CO2} will be 7° C lower than that of inclusions which contain pure CO_2. In the meantime the Tm_{CO2} of such inclusions would be only slightly depressed (-1.5 to -2.0°C). Thus, if the N_2 content of the inclusions is neglected calculated density will be approximately 25 % higher than the real density (van den Kerkhof et al., 1991). Overestimated density will result in significant errors in calculating trapping pressure and would affect the overall estimation of the conditions of mineral deposition. Therefore, knowledge of the volatile compositions of type 3 and 4 fluid inclusions is essential for proper interpretation of the microthermometric data.

Although gas compositional data are usually obtained by analytical methods it is theoretically possible to constrain the composition of the carbonic phase of gas-rich inclusions on the basis of microthermometric observations (van den Kerkhof and Thiery, 1994). The method, however, is not without limitations because the observation of the necessary low temperature phase transitions is only possible if at least 10 vol. % liquid, and/or 1 vol. % solid phases are presented in the inclusions (van den Kerkhof, 1990). The presence of water also creates difficulties because the formation of clathrate lowers gas concentrations in the vapour phase even further. As mentioned above, a number of type 4, CO_2-rich fluid inclusions from stage III quartz at the Sunshine and Lucky Friday mines exhibit low temperature phase transitions typical for the CO_2-N_2 system. Partial homogenization (Th_s) to liquid or vapour occurs in these inclusions on warming between -160 and -147° C with only one inclusion from the Lucky Friday main vein exhibiting phase transitions typical for the CO_2-CH_4 system. Thus, on the basis of the microthermometric results the carbonic phase composition of these CO_2-rich inclusions is considered a mixture of CO_2 and N_2. In an attempt to constrain the volatile composition of type 3 inclusions and also of type 4 inclusions for which no low-temperature data are available, the critical curve of the CO_2-N_2 mixture is plotted on a Tm_{CO2} vs. Th_{CO2} diagram (Fig. 5.9). The coordinates of the critical curve are determined from the data of van den Kerkhof and Thiery (1994). The curve separates the diagram in two fields (field I and field II) and allows relatively less dense CO_2-CH_4 compositions to be distinguished from CO_2-N_2 dominated mixtures, and also from more dense CO_2-CH_4 mixtures. The carbonic phase of type 3 and 4 fluid inclusions that plot in field I on Fig. 5.9 is expected to be predominantly CO_2-CH_4. In contrast, fluid inclusions that plot on field II are assumed to be CO_2-N_2-bearing. Because N_2-bearing, CO_2-rich fluid inclusions which homogenize to vapour may also plot on field II, the Tm_{CO2} vs. Th_{CO2} diagram must be used only for inclusions that homogenize to liquid.

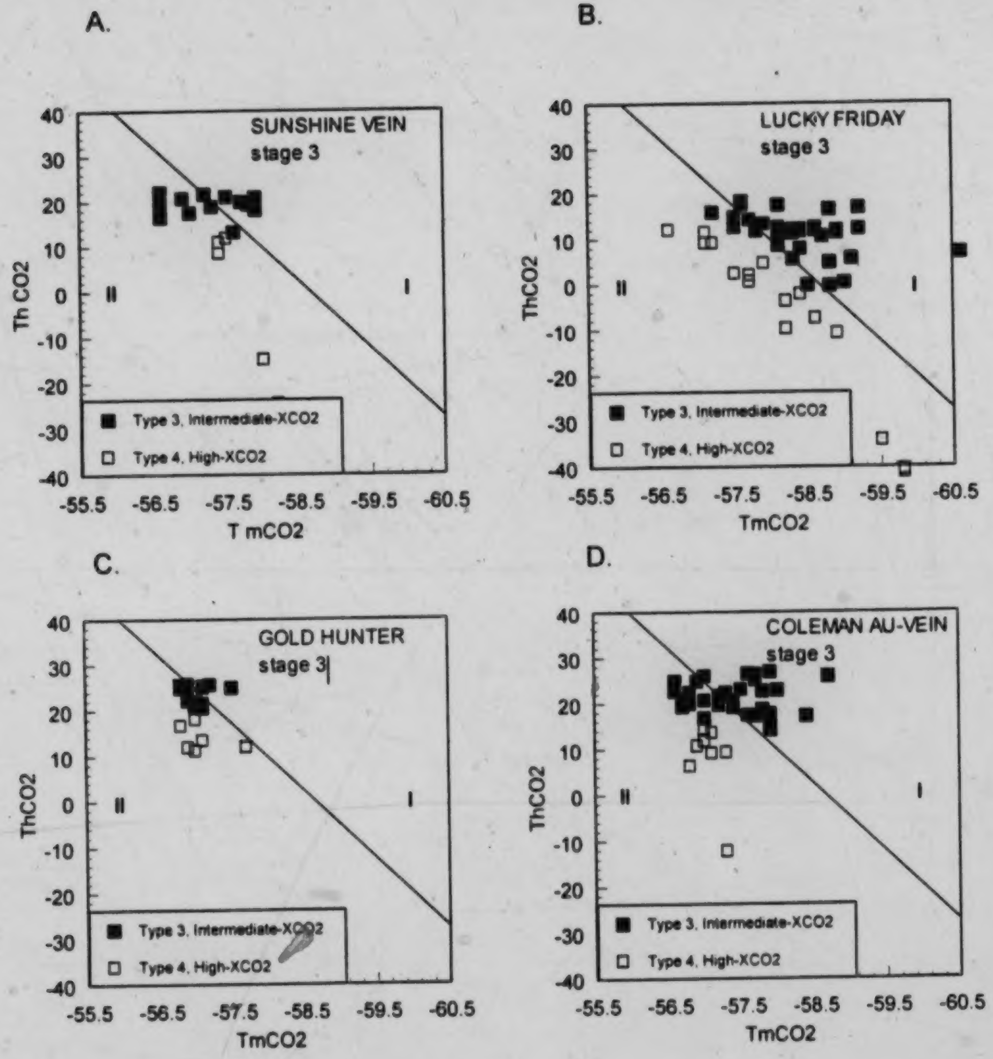

Fig. 5.9. Plots of Th$_{CO_2}$ against Tm$_{CO_2}$ present microthermometric data from: A.SQT Sunshine vein; B. QSG Lucky Friday main vein; C. SQS veins in the Gold Hunter mine; D. Au-quartz vein. Fields I and II represent predominantly CO_2-CH_4 and CO_2-N_2 gas phase compositions respectively. The two fields are separated by the critical curve of the CO_2-N_2 mixture determined from the data of van den Kerkhof and Thiery (1994).

However, although dense CO_2-CH_4 mixtures could plot in field II, no N_2–bearing inclusions will plot in field I, provided that they homogenize to liquid. Although in the absence of low temperature data the Tm_{CO2} against Th_{CO2} plots must be used as qualitative guides only it is suggested that they provide reasonable evidence for the dominance of CH_4, and/or possibly N_2 in the gas phase of most type 3 and 4 inclusions. Several studies demonstrate that mixtures of roughly equal amounts of CO_2, N_2, and CH_4 are rare in natural inclusions (van den Kerkhof 1990; van den Kerkhof and Thiery, 1994). Previous studies in Coeur d'Alene also demonstrated that the carbonic phase of the majority of the fluid inclusions comprises a binary CO_2-CH_4 or CO_2-N_2 system (Landis and Hofstra, 1991). Thus, for the sake of simplicity the volatile compositions of individual type 3 and 4 fluid inclusion populations have been considered binary CO_2-CH_4 or CO_2-N_2 mixtures. However, it may be possible that some type 3 and 4 inclusions contain variable small amounts of both N_2 and CH_4 (cf. Diamond, 1990). This would explain why inclusions from the same fluid inclusion population plot close to the CO_2-N_2 critical curve or straddle both fields on the diagram (Fig. 5.9). Due to the comparable P-V-T characteristics of N_2 and CH_4 errors introduced by assuming binary rather than ternary mixtures would not be significant, however. As seen from Fig. 5.9 C most type 3 inclusions from the Gold Hunter mine plot in field II, which indicates that they are CO_2-N_2-bearing. In contrast, microthermometric data suggest that type 3 inclusions from stage III quartz at the Lucky Friday main vein contain predominantly CH_4 (Fig. 5.9 B). These results are in agreement with the laser-Raman and quadrupole mass spectrometry results of Leach et al. (1988). However, according to Fig 5.9 D the carbonic phase of most type 3 fluid inclusions at the Au-quartz Coleman vein is CH_4-bearing, which contradicts the findings of Leach et al. (1988) who argue that type 3 and 4 fluid inclusions from the Au-quartz veins in the district contain either pure CO_2, or a mixture of CO_2 and N_2. Data from the Sunshine mine where a few type 3 inclusions plot in field I, which indicates that they are CH_4-bearing, also contradict the argument of Leach et al (1988) that Ag-rich veins contain pure CO_2 or CO_2-N_2 mixtures.

Volatile compositions for type 3 and 4 inclusions, and molar volumes for type 4 fluid inclusions were estimated using the graphical method of van den Kerkhof and Thiery (1994) and information from Fig. 5.9. Bulk densities were calculated using MacFlincor 0.93 (Brown and Hagemann, 1994) with the equation of state of Holloway (1977). A substantial disadvantage of the procedure of calculating bulk compositions, molar volumes, and densities of type 3, intermediate-X_{CO2} inclusions, however, is that it is reliant upon the visual estimates of the relative proportion of the phases present in the inclusions. The uncertainty introduced by visually estimating the phase volumes is beyond doubt the major source of error in such calculations (Shepherd et al., 1985; Brown and Lamb, 1989; Boiron and Dubessy, 1994). Due to the general homogeneity of the microthermometric properties (Table 5.2) the average data for each individual fluid inclusion population was used to minimize the error introduced by the use of visual estimations of the phase volumes in density and molar volume calculations (cf. Brown and Hagemann, 1994). To further minimize the error a correction procedure developed by Brown and Lamb (1989) based on the Th_{CO2} of type 3 inclusions was applied. The necessary microthermometric data are Th_{CO2} and Th_{tot}. The method requires the use of P-X diagrams which combine the position of the experimentally derived solvi in the H_2O-CO_2-NaCl system and lines defined by CO_2 density. The intersection of the solvi and the density lines allows a rapid determination of the mole fraction of CO_2 in the inclusion fluid. Than X_{CO2} is converted to volume fraction by the equation:

$$\mathbf{Vol\ Frac\ CO_2 = 1 - (18\rho CO_2)(1\text{-}XCO_2)/(44XCO_2)+(18\rho\ CO_2)(1\text{-}XCO_2)}$$

However, due to the effect of CH_4 and N_2 on Th_{CO2} and the estimated fluid densities of type 3 fluid inclusions the correction procedure of Brown and Lamb (1989) would give best results only for those type 3 fluid inclusions which contain lesser amounts of gases other than CO_2. Therefore, corrected phase volumes of type 3 inclusions must be regarded as approximated values. It is noteworthy however, that the difference between the optically determined and corrected values was less than 10 vol. %, which indicates that the optical determination was relatively accurate. Calculated average fluid compositions, molar volumes, and densities are presented in Table 5.2.

Table. 5.2. Fluid composition, molar volume, and density in Coeur d'Alene. Calculation of gas phase compositions is based on low temperature measurements and on the results of fig. 5.9.

Vein	Stage	Incl. Type	X_{H2O}	X_{CO2}	X_{CH4}	X_{N2}	Molar Volume (cm^3 mole^{-1})	Density (g/cm^3)
SQT vein - Sunshine vein, Sunshine mine								
	I	2					21.4 ± 0.8	0.929 ± 0.036
	II	2					22.7 ± 1.3	0.858 ± 0.065
	III	3	0.754 ± 0.09	0.229 ± 0.08		0.016 ± 0.011	28.1 ± 5.1	0.831 ± 0.076
		4		0.925 ± 0.06		0.07 ± 0.06	50.0 ± 4.0	0.866 ± 0.12
QSG veins - Lucky Friday main vein, Lucky Friday mine								
	II						22.0 ± 1.5	0.889 ± 0.03
	III	3a	0.820 ± 0.01	0.162 ± 0.01	0.013 ± 0.002		25.2 ± 0.24	0.881 ± .020
	III	3s	0.844 ± 0.005	0.148 ± 0.004	0.08 ± 0.02		24.3 ± 0.2	0.899 ± 0.01
	III	4a		0.900 ± 0.07		0.10 ± 0.07	53.0 ± 1.0	0.810 ± 0.02
	III	4b		0.770 ± 0.02		0.23 ± 0.02	45 ± 1.5	0.896 ± 0.03
SQS veins - Gold Hunter mine								
	I	2					20.1 ± 1.1	1.013 ± 0.073
	II	2					21.1 ± 5.8	0.928 ± 0.014
	III	3	0.851 ± 0.032	0.143 ± 0.03		0.006 ± 0.003	25 ± 1.7	0.872 ± 0.03
	III	4		0.936 ± 0.014		0.064 ± 0.035	57.2 ± 3.	0.753 ± 0.048
Au-quartz vein - Coleman Vein								
	n. a	4		0.950 ± 0.010		0.05 ± 0.01	55.0 ± 3.0	0.766 ± 0.043
	n. a.	3	0.821±0.02	0.172 ± 0.005	0.007 ± 0.001		24.6 ± 6.0	0.867 ± 0.01

SQT veins

Stages I and II

Type 2, low-X_{CO2} fluid inclusions from stage I siderite exhibit slightly higher average fluid densities (0.93 ± 0.04 g/cm^3) and lower molar volumes (21 ± 1 cm^3 mole^{-1}) than type 2 fluid inclusions from stage II siderite and quartz from the Sunshine vein (0.86 ± 0.07 g/cm^3, and 23 ± 1 cm^3 mole^{-1}, respectively).

Stage III

Type 3, intermediate X_{CO2} inclusions yield lower average densities (0.83 ± 0.08 g/cm^3) and higher molar volumes (29 ± 5 cm^3 mole^{-1}) than type 2 inclusions (Table 5.2). Calculated average X_{CO2} and X_{N2} values for type 3 inclusions are 0.23 ± 0.08 and 0.02 ± 0.01, respectively. In contrast, type 4a and 4b inclusions contain from 0.07 to 0.15 mole fraction N_2, respectively. The densities of type 4 CO_2-rich inclusions range from 0.73 to 0.96 g/cm^3. Type 4 inclusions, however, have molar volumes ranging from 44 to 58 cm^3 mole^{-1}, which are significantly higher than the molar volumes of all other fluid inclusion populations in the Sunshine vein.

QSG veins

Stage II

Type 2 fluid inclusions from stage II quartz, siderite, and sphalerite at the Lucky Friday main vein have average densities (0.89 ± 0.03 g/cm^3) and molar volumes (22 ± 2 cm^3 mole^{-1}) similar to stage II fluid inclusions at the Sunshine mine (Table 5.2). This is not surprising because the two fluid inclusion populations also have very similar microthermometric properties (Table 5.1).

Stage III

Calculated fluid densities of primary and secondary type 3 fluid inclusions from the Lucky Friday main vein range from 0.86 to 0.90 g/cm^3. The molar volumes of the inclusions range from 24 to 25 cm^3 mole^{-1}. The intermediate-X_{CO2}

inclusions contain from 0.14 to 0.16 mole fraction CO_2 and from 0.01 to 0.1 mole fraction CH_4 (Table 5.2). In contrast, type 4a and 4b, CO_2-rich inclusions are N_2 bearing with average X_{N2} values of 0.10 ± 0.07 and 0.26 ± 0.02. The two groups have average fluid densities of 0.81 ± 0.02 and 0.90 ± 0.03 g/cm^3, respectively, and molar volumes of 53 ± 1 and 46 ± 1 cm^3 mole^{-1}, respectively. These values are similar to that of those two groups CO_2-rich inclusions from the Sunshine vein (Table 5.2).

SQS veins

Stages I and II

Type 2 inclusions from stage I siderite at the Gold Hunter mine exhibit the highest average fluid density (1.01 ± 0.07 g/cm^3) and the lowest molar volume (20 ± 1 cm^3 mole^{-1}) amongst all fluid inclusion populations studied. A decrease in the density and an increase of the molar volume of type 2 inclusions from stage 2 siderite suggests a pressure drop during stage II (Table 5.2).

Stage III

Type 3 fluid inclusions in stage III quartz at the Gold Hunter exhibit average density and molar volume of 0.87 ± 0.03 g/cm^3, and 25 ± 0.1 cm^3 mole^{-1}, respectively, which are very much similar to that of type 3 inclusions at the Lucky Friday main vein (Table 5.2). Calculated X_{CO2} and X_{N2} values are 0.14 ± 0.03 and 0.01 ± 0.005, respectively. The CO_2-rich inclusions exhibit nearly identical average densities (0.87 ± 0.03 g/cm^3) and molar volumes (25 ± 2 cm^3 mole^{-1}) to that of type 4a inclusions from the Sunshine and Lucky Friday main veins and also to type 4 inclusions from the Coleman Au-quartz vein (Table 5.2).

Coleman Au-quartz vein

Calculated average densities and molar volumes of type 3, intermediate-X_{CO2} fluid inclusions from the Coleman Au-quartz vein average 0.87 ± 0.01 g/cm^3 and 25 ± 1 cm^3 mole^{-1}, respectively. The inclusions contain 0.17 mole fraction CO_2 and 0.01 mole fraction CH_4. The CO_2-rich fluid inclusions in the Au-quartz vein contain 0.05 mole fraction N_2, and as mentioned above, exhibit calculated average densities and molar volumes similar to CO_2-rich inclusions at the Sunshine, Lucky Friday, and Gold Hunter mines (Table 5.2).

VI. LIGHT STABLE ISOTOPE STUDY

Introduction

In conjunction with the fluid inclusion study, a light stable isotope study of vein minerals from the Ag-Pb-Zn and Au-quartz veins was carried out. The aims of the stable isotope study were to constrain the isotopic composition and temperature of the hydrothermal fluids associated with the different vein types in the Coeur d'Alene district.

Comprehensive stable isotope studies were conducted on vein quartz from various Ag-Pb-Zn vein types in the district (Constantopoulus and Larson, 1991; Constantopoulus, 1994), and also on siderite and quartz from the SQT veins in the Galena and Sunshine mines (Yates and Ripley 1985; Eaton et al., 1995). The present study includes a considerable number of siderite and sulphide samples from QSG and SQS veins at the Gold Hunter and Lucky Friday mines, and also of quartz from the Au-quartz Coleman vein for which there are little or no published data. Also for the first time stable isotopic data of siderite from the alteration envelopes of individual silver-, lead-, and zinc-rich veins in the district are reported.

Analytical techniques

Standard methods were used to prepare mineral samples for analysis on an isotopic ratio mass spectrometer. All carbonate samples were outgassed for 24 hours on a high vacuum line. Siderite and ankerite were reacted with 100% orthophosphoric acid (H_3PO_4) for one hour at 150° and 100°C respectively following the slightly modified method of Rosenbaum and Sheppard (1986). Acid fractionation factors of 1.00771 and 1.00901 for siderite and ankerite respectively were applied to correct for the difference between the $\delta^{18}O$ of the carbonate mineral and that of the acid-extracted CO_2 (Rosenbaum and Sheppard, 1986). Calcite was reacted with phosphoric acid according to the method of McCrea (1951). Quartz samples were analyzed using the standard

BrF_5 technique of Clayton and Mayeda (1963). All isotopic data are reported in the conventional δ notation, relative to SMOW (Standard Mean Ocean Water) standard for oxygen, and PDB (Pee Dee Belemnite) for carbon isotopes. Uncertainties on $\delta^{18}O$ and $\delta^{13}C$ analyses are ± 0.1 ‰. The sulphur isotopic composition of sulphide minerals was determined in the stable isotope laboratory at the University of Calgary.

Oxygen and carbon isotopic composition of siderite

The results of the stable isotopic analyses of vein and alteration siderite from the Sunshine, Coeur, Lucky Friday, and Gold Hunter mines are presented in Table 6.1 and on Figures 6.1 and 6.2. The oxygen and carbon isotopic composition of siderite analyzed in this study varies from 12.2 to 20.2 ‰ and from –4.6 to –9.5 ‰, respectively. The results presented in Table 6.1 demonstrate that the stable isotopic composition of siderite from individual Ag-Pb-Zn veins does not vary dramatically from vein to vein, despite the suggested age difference of ~1 Ga between the QSG and SQS, and the SQT veins. However, a variance in the isotopic composition of vein siderite and quartz indicates that variable PT conditions and/or fluids of slightly different isotopic compositions have dominated the different paragenetic stages at the individual veins (Fig. 6.1 A, B; Table 6.1).

SQT veins

Stage I

The oxygen and carbon isotopic compositions of stage I siderite from the SQT veins at the Sunshine and Coeur mines vary from 14.5 to 20.2 ‰, and from –8.3 to –4.6 ‰ respectively. It can be seen on Fig. 6.1 A and B that stage I siderite from the Coeur mine exhibits slightly more variable $\delta^{18}O$ and $\delta^{13}C$ than stage I siderite from the Sunshine mine. In addition, stage I siderite from the Coeur mine has average $\delta^{18}O$ and $\delta^{13}C$ of approximately 1.5 and 2.5 ‰ higher than the average $\delta^{18}O$ and $\delta^{13}C$ of stage I siderite from the Sunshine mine (Table 6.1).

Table 6.1. Range and average $\delta^{18}O_{SMOW}$ and $\delta^{13}C_{PDB}$ isotopic composition of vein and alteration siderite from the SQT veins at the Sunshine and Coeur mines, and the QSG and SQS veins at the Lucky Friday and Gold Hunter mines respectively. The errors quoted are ± 1σ.

Vein type/description	Stage	$\delta^{18}O_{Sid}$ (‰) (range)	$\delta^{18}O_{Sid}$ (‰) (average)	$\delta^{13}C_{Sid}$ (‰) (range)	$\delta^{13}C_{Sid}$ (‰) (average)	n
Sunshine Mine						
SQT vein	I	14.7 to 17.3	15.7 ± 1.1	-8.3 to -6.0	-6.9 ± 0.9	8
SQT vein	II	12.8 to 14.4	13.8 ± 0.4	-8.5 to -6.3	-7.2 ± 0.6	10
Alt. envelope	I	13.6 to 14.7	14.1 ± 0.5	-7.5 to -7.2	-7.3 ± 0.1	6
Coeur Mine						
SQT vein	I	14.5 to 20.2	17.4 ± 2.0	-6.4 to -4.6	-4.6 ± 0.7	6
SQT vein	II	13.1 to 14.3		-8.1 to -7.3		2
Qtz - dominant vein	(?)	13.2 to 13.3		-9.3 to - 8.9		2
Lucky Friday Mine						
QSG vein	I	15.2 to 16.5	15.8 ± 0.5	-7.6 to - 6.9	-7.3 ± 0.2	7
QSG vein	II	12.7 to 13.3		-8.9 to -9.5		3
Subhorizontal vein	III	12.9		-7.5		1
Alt. envelope	I	12.2 to 14.4	13.6 ± 0.8	-8.3 to - 7.3	-7.5 ± 0.4	6
Gold Hunter Mine						
SQG vein	I	15.9 to 18.2	16.3 ± 1.0	-6.5 to -5.41	-6.1 ± 0.4	6
SQG vein	II	14.2 to 15.9	15.0 ± 0.9	-8.7 to -6.7	-7.3 ± 1.0	4
Subhorizontal vein	III	13.9		-10.4		1
Alt. envelope	I	14.9 to 15.2	15.0 ± 0.1	-7.7 to-6.7	-7.0 ± 0.4	5

Abbreviations: Alt: alteration; n: number of samples; QSG: quartz-siderite-galena; Qtz; quartz; Sid: siderite; SQT: siderite-quartz-tetrahedrite; SQS: siderite-quartz-sphalerite.

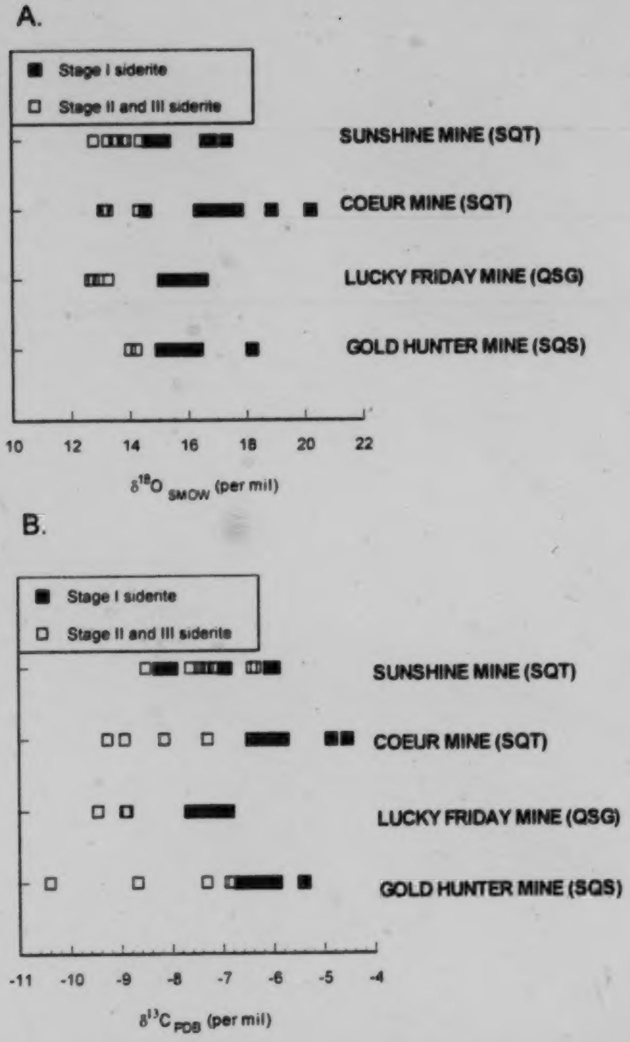

Fig. 6.1. Range of $\delta^{13}C_{PDB}$, (A) and $\delta^{18}O_{SMOW}$ (B) of stage I siderite from SQT veins at the Sunshine and Coeur mines, and QSG and SQS veins at the Lucky Friday and Gold Hunter mines. Two samples of stage III siderite from subhorizontal quartz of stage II siderite veins at the Lucky Friday and Gold Hunter mines have $\delta^{18}O$ and $\delta^{13}C_{PDB}$ similar to that and are thus included in the stage II siderite group.

Stage II

In contrast to stage I siderite, stage II siderite from the SQT veins has lower average $\delta^{18}O$ and $\delta^{13}C$ (e.g., stage I siderite $\delta^{18}O$: 16.5 ± 1.7 ‰; $\delta^{13}C$: -6.4 ± 1.0 ‰, n = 14; stage II siderite $\delta^{18}O$: 13.6 ± 0.5 ‰; $\delta^{13}C$: –7.3 ± 0.6 ‰; n = 12). The stable isotopic composition of stage II siderite is also less variable than that of stage I siderite (Fig. 6.1 A, B). Two samples of vein siderite from subvertical quartz-dominant veins at the Coeur mine (see Chapter IV), also have $\delta^{18}O$ values similar to stage II siderite (e.g., 13.1 and 13.3 ‰; Table 6.1). Their $\delta^{13}C$ (-9.3 and –8.1), however, is lower than the average $\delta^{13}C$ of stage II siderite (–7.3 ± 0.6 ‰; Table 6.1).

Siderite from the alteration envelope

Siderite from the alteration envelope of the SQT veins at the Sunshine mine has lower average $\delta^{18}O$ and $\delta^{13}C$ relative to stage I siderite (e.g., alteration siderite $\delta^{18}O$: 14.1 ± 0.5 ‰, n = 6; -7.3 ± 0.1 ‰, n = 6; stage I siderite: 16.5 ± 1.7, n =14; -6.4 ± 1.0 ‰; n=14; Table 6.1). It can be seen on Fig. 6.2 that alteration siderite from the SQT veins at the Sunshine mine has generally similar $\delta^{18}O$ and $\delta^{13}C$ to alteration siderite from the QSG Lucky Friday main vein.

QSG veins

Stage I

The $\delta^{18}O$ and $\delta^{13}C$ of stage I siderite from the QSG Lucky Friday main vein range from 15.2 to 16.5 ‰ and from –7.6 to –6.9 ‰ respectively. The average $\delta^{18}O$ and $\delta^{13}C$ values of stage I siderite from the Lucky Friday mine are similar to those of stage I siderite from the SQT veins at the Sunshine mine (e.g., Lucky Friday mine - $\delta^{18}O$: 15.8 ± 0.5 ‰, n =7; $\delta^{13}C$: -7.3 ± 0.2 ‰, n = 7; Sunshine mine - $\delta^{18}O$: 15.7 ± 1.1 ‰, n = 6, and $\delta^{13}C$: -6.9 ± 0.9 ‰, n = 6).

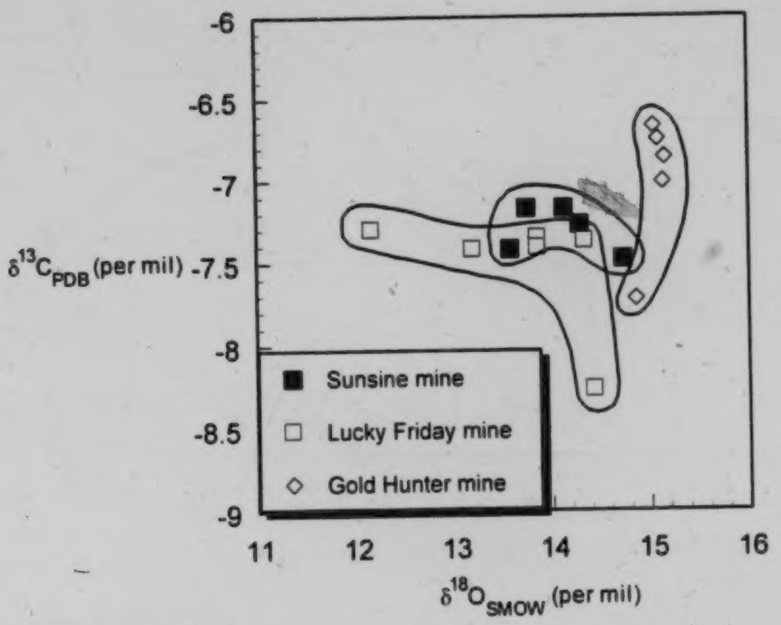

Fig 6.2. Oxygen and carbon isotopic composition of siderite from the alteration envelopes of the SQT, QSG, and SQS veins from the Sunshine, Lucky Friday, and Gold Hunter mines. Note that the veins at the Sunshine and Lucky Friday mines are hosted by the predominantly quartzitic rocks of the Revett and/or St. Regiss Formations, whereas the SQS veins at the Gold Hunter mine are hosted in the carbonate bearing argillites of the Wallace Formation, which may explain the slightly higher $\delta^{13}C$ and $\delta^{18}O$ values of the alteration siderite.

Stage II

Stage II siderite from the QSG Lucky Friday main vein has about 2 to 3 ‰ lower $\delta^{18}O$ and $\delta^{13}C$ than stage I siderite (e.g., stage I siderite $\delta^{18}O$: 15.2 to 16.5 ‰; $\delta^{13}C$: -7.6 to - 6. 9 ‰; stage II siderite $\delta^{18}O$: 12.7 to 13.3 ‰; $\delta^{13}C$: -8.9 to -9.5 ‰; Fig. 6.1 A, B; Table 6.1). A single stage III siderite sample falls within the $\delta^{18}O$ and $\delta^{13}C$ range of stage II siderite (Table 6.1).

Siderite from the alteration envelope

Siderite from the alteration envelope of the QSG Lucky Friday main vein has on average 2 to 3 ‰ lower $\delta^{18}O$ and $\delta^{13}C$ than stage I siderite from the vein (Table 6.1). As mentioned above, the alteration siderite from the Lucky Friday main vein has similar oxygen and carbon isotopic composition to alteration siderite from the Sunshine mine (Fig. 6.2; Table 6.1). The alteration siderite from the Lucky Friday however, exhibits a greater spread of $\delta^{18}O$ and $\delta^{13}C$ (Fig. 6.2; Table 6.1).

SQS veins

Stage I

The $\delta^{18}O$ of stage I siderite from the SQS veins falls within the range of stage I siderite from the SQT and the QSG veins at the Lucky Friday and Sunshine mines (Table 6.1; Fig. 6.1 A, B). The average $\delta^{13}C$ (-6.1 ± 0.4 ‰, n = 6) of stage I siderite from the SQS veins however, is approximately one per mil higher than that of stage I siderite from the QSG and SQT veins (e.g. -7.3 ± 0.2 ‰, n = 7; -6.9 ± 0.9 ‰, n = 8, respectively), although it is not as high as the $\delta^{13}C$ of stage I siderite from the SQT veins at the Coeur mine (e.g., -4.1 ± 0.7, n = 6).

Stage II

Stage II siderite from the SQS veins has $\delta^{18}O$ and $\delta^{13}C$ which vary from 14.2 to 15.9 ‰ and from -8.7 to -6.7 ‰, respectively. These ranges are lower than that of stage I siderite from the SQS veins. An exception from the rule that stage II siderite has always lower $\delta^{18}O$ and $\delta^{13}C$ relative to stage I siderite is observed in a SQS vein at the Gold Hunter mine (i.e., early siderite: 13.4 and 13.6 ‰, late siderite: 14.2 and 15.9 ‰, respectively.

Siderite from the alteration envelope

Siderite from the alteration envelope of the SQS veins has $\delta^{18}O$ and $\delta^{13}C$ values that vary from 14.9 to 15.2 ‰, and -7.7 to -6.7 ‰, respectively. These values are higher compared to the $\delta^{18}O$ and $\delta^{13}C$ of alteration siderite from the SQT and the QSG veins (Fig. 6.3) and define a distinct field on Fig. 6.2.

Oxygen and carbon isotopic variance of stage I siderite

The oxygen and carbon isotopic compositions of stage I siderite from the Ag-Pb-Zn veins at the four mines define a positive trend on a $\delta^{18}O$ against $\delta^{13}C$ plot (Fig 6.3). Such a trend is expected for hydrothermal systems that precipitate carbonates at variable temperature. Similar trends were previously reported from the Sunshine and Galena mines (Yates, 1987; Eaton et al., 1995). The significance and implications of the stable isotopic variance of stage I siderite from the Ag-Pb-Zn veins will be discussed in more detail in Chapter VIII.

Stable isotopic composition of vein ankerite and calcite

Only three ankerite samples were analyzed during this study. The ankerites are from the QSG veins at the Lucky Friday and Gold Hunter mines. The oxygen and carbon isotopic compositions of ankerite range from 12.7 to 14.3 ‰ and from –5.8 to –7.3 ‰ respectively. A single calcite from the QSG Lucky Friday main vein has oxygen and carbon isotopic signature similar to that of ankerite (e.g. 12.9 ‰ and -7.3 ‰, respectively).

Oxygen isotopic composition of vein quartz

Vein quartz from the base- and precious metal-rich veins has uniform $\delta^{18}O$ composition which varies from 13.2 to 16.1 ‰ with an average of 14.4 ± 0.7 ‰ (n=20). These values are similar to previously reported $\delta^{18}O$ data of vein quartz from all over the district (e.g., 9.5 to 18.0 ‰; average: 14.6 ± 1.1 ‰; n = 100; Constantopoulus, 1994). In contrast to stage I siderite, the $\delta^{18}O$ compositional range of quartz within an individual vein does not exceed two per mil, and in two cases is less than one per mil (Fig. 6.4).

Massive quartz from the Au-quartz Coleman vein has $\delta^{18}O$ (13.6 to 15.1 ‰) which is within the range of quartz from the Ag-Pb-Zn veins (Fig 6.4). Six samples taken along two profiles across the Coleman vein, both at the surface and underground, show no statistically significant isotopic variance.

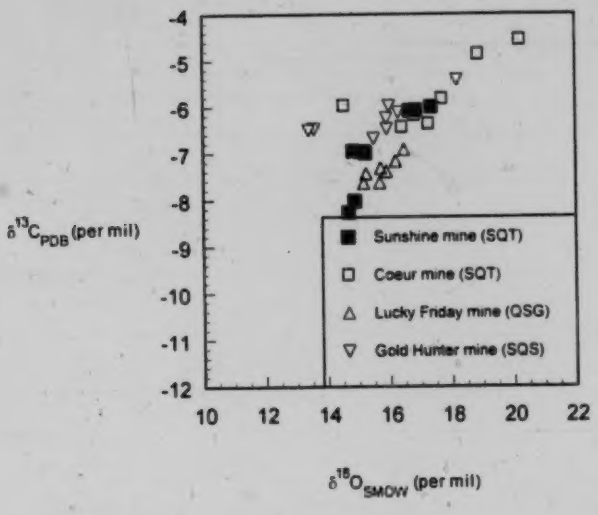

Fig 6.3. Plot of $\delta^{13}C_{PDB}$ vs. $\delta^{18}O_{SMOW}$ of stage I siderite from SQT veins in the Sunshine and Coeur mines, and from QSG and SQS veins in the Lucky Friday and Gold Hunter mines, respectively.

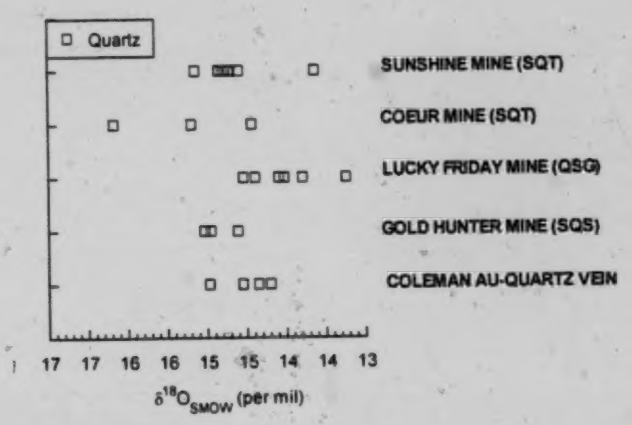

Fig. 6.4. Oxygen isotopic composition of stage II and III quartz from the SQT veins at the Sunshine and Coeur mines, the QSG and SQS veins at the Gold Hunter and Lucky Friday mines, and main stage quartz from Coleman Au-quartz vein.

Mineral pair thermometry

Mineral pair thermometry is based on the assumption that isotopic equilibrium is attained during the simultaneous precipitation of at least two mineral phases that contain the isotope of interest. An important requirement is that the isotopic fractionation between the two minerals has to be temperature sensitive and also sufficiently large so that the effect of the analytical accuracy of the stable isotope determinations is a negligible factor. Previous studies reported oxygen isotopic disequilibrium between vein siderite and quartz from SQT veins at the Sunshine and Galena mines (Yates and Ripley, 1985; Eaton et al., 1995). Petrographic evidence for precipitation of the majority of siderite and quartz in two different paragenetic stages (Chapter IV), however, provides an explanation why the two minerals may not be in isotopic equilibrium. Thus only siderite and quartz from stage II and III which are apparently coexistent were analyzed for the purposes of mineral pair thermometry in this study.

Sample size and heterogeneity are also important requirements. Reported oxygen isotopic gradients of as much as 9 ‰/mm in quartz veins from central Australia (Kirschner et al., 1993), and oxygen and carbon gradients of up to 5 ‰/20 mm in syntectonic carbonate veins from the South Pyrenean thrust belt (Kirby et al., 1997) clearly demonstrate the limitations of bulk sampling techniques in stable isotope thermometry. In addition, a 1.5 ‰ variance in the $\delta^{18}O$ of vein quartz on a distance of 0.64 cm was reported from a SQT vein in Coeur mine by Constantopoulus (1994). Thus, although a considerable effort has been made to select and analyze only coexisting minerals it is possible that some questionable fractionations between quartz and siderite result from small-scale isotopic gradients rather than from secondary alteration or lack of primary isotopic equilibrium.

Choice of equilibrium fractionation expressions

To calculate the $\delta^{18}O$ values of hydrothermal fluid in equilibrium with quartz, the quartz-H_2O fractionation equation of Matsuhisa et al. (1979) was applied. There is fairly good agreement between the theoretical calculations of Becker and Clayton (1976) for $\Delta^{18}O_{SIDERITE-H2O}$ and the experimental equation of Carothers et al. (1988) for the siderite-H_2O fractionation. However, because most siderite in the silver-, lead-, and zinc-rich veins in the district formed at temperatures higher than the upper limit in the experiments of Carothers et al. (1988; e.g. 199°C) the equation of Becker and Clayton (1976) was preferred.

In a previous study at the Sunshine mine, Eaton et al. (1995) applied the $\Delta^{13}C_{CALCITE-CO2}$ fractionation equation of Bottinga et al. (1968) to calculate the carbon isotopic composition of fluids in equilibrium with vein siderite. An extrapolation of the preliminary results of the experimental work of Carothers et al. (1988), however, demonstrated a difference from 2 to 3 ‰ between the $\Delta^{13}C_{CALCITE-CO2}$ and $\Delta^{13}C_{SIDERITE-CO2}$ over the temperature range of interest (e.g. 200 to 300°C; Carothers et al., 1988; see Hoefs, 1997). In addition, the $\Delta^{13}C_{SIDERITE-CO2}$ fractionation equation of Carothers et al. (1988) is in relatively good agreement with the theoretical calculations of Golyshev et al. (1981) for $\Delta^{13}C_{SIDERITE-CO2}$ in the temperature interval of interest, i.e., 200 to 300°C. Thus, the equation of Carothers et al. (1988) was favored in this study. The results of the $\delta^{18}O$ geothermometry are given in Table 6.2.

Quartz-siderite pairs

Three stage II quartz-siderite pairs from the SQT Sunshine vein yielded homogeneous temperatures of 350 ± 50°, 315 ± 50°, and 270 ± 50°C respectively (Table 6.2). One mineral pair, however, returned a lower temperature of 210 ± 50°C (Table 6.2). Similar results yield two pairs at the Coeur mine (355 ± 50°C, and 200 ± 50°C). Three stage II quartz-siderite pairs from the QSG Lucky Friday main vein exhibit isotopic fractionation factors that vary from 0.5 to 1.6 ‰ (Table 6.2). The estimated temperatures are between

390° and 210°C suggesting a certain degree of isotopic disequilibrium or sample heterogeneity. One quartz-siderite pair from a stage III subhorizontal vein at the Gold Hunter mine yielded a temperature of 290 ± 50°C.

Table 6.2. Geothermometry results based on $\Delta^{18}O_{QUARTZ\text{-}SIDERITE}$.

Sample No.	Mineral pair	Stage	$\Delta^{18}O_{QUARTZ\text{-}SIDERITE}$*	T (°C)
SQT veins (Sunshine mine)				
SSM-41	Qtz-Sid	II	0.66	350 ± 50
SSM-92	Qtz-Sid	II	0.80	315 ± 50
SSM-102	Qtz-Sid	II	1.44	210 ± 50
SSM-132	Qtz-Sid	II	1.04	270 ± 50
SQT veins (Coeur mine)				
COM-22	Qtz-Sid	II	0.64	355 ± 50
COM-52f	Qtz-Sid	II	1.51	200 ± 50
QSG veins (Lucky Friday mine)				
LF-14s	Qtz-Sid	II	1.29	230 ± 50
LF-15s	Qtz-Sid	II	0.52	390 ± 50
LF-7cc	Qtz-Cal	III	1.61	210 ± 50
SQS veins (Gold Hunter mine)				
LF-20s	Qtz-Sid	III	0.93	290 ± 50

*Temperatures are calculated by combining the fractionation equations for siderite-H_2O and quartz-H_2O of Becker and Clayton (1976) and Matsuhisa et al. (1978). Given an analytical error of ± 0.1 ‰ the uncertainty in the temperature determination for the quartz-siderite pairs at 300 °C is approximately ± 50 °C

Quartz–ankerite and quartz-calcite pairs

The temperature dependence of the oxygen isotope fractionation between ankerite and water is not known. The ankerite-H_2O empirical calibrations proposed by Fisher and Land (1986) and Mumin et al. (1996) estimate values for water in equilibrium with ankerite at 300°C which are 4.5 ‰ apart. Three quartz-ankerite pairs exhibit oxygen isotopic fractionations of 1.8, 0.9, and -1.0 ‰, and do not yield geologically reasonable temperatures if the above mentioned calibrations are used. A single quartz-calcite pair at the Lucky Friday mine has $\Delta^{18}O_{QUARTZ-CALCITE}$ of 1.61 that yields a temperature of 210 ± 50°C.

Sulphur Isotopes

Chalcopyrite, sphalerite, galena, and tetrahedrite from the silver-, lead-, and zinc-rich veins studied exhibit a narrow range of $\delta^{34}S$ values from 1.1 to 7.2 ‰, average 4.0 ± 1.9 ‰, (n = 20). Although the number of samples is limited there appears to be no statistically significant difference in the $\delta^{34}S$ of sulphides and sulphosalts from the individual veins (Table 6.3). Apart from a 27 per mil range in the $\delta^{34}S$ of sulphides from several mines in the district, including the Lucky Friday mine (Sorenson, 1972), all other studies reported $\delta^{34}S$ for sulphides and sulphosalts which are within the range of values of this study (Fryklund, 1964; Harris et al., 1981; Yates and Ripley; 1985).

The $\delta^{34}S$ of sphalerite from the individual veins varies from 1.7 to 7.2 ‰. Three duplicated sphalerite analyses demonstrate sulphur isotopic inhomogeneity which reaches as much as 4.6 ‰. The $\delta^{34}S$ variance indicates that either sphalerite was internally inhomogeneous due to variable P-T-X conditions during deposition, or that despite careful hand picking different generations of sphalerite with contrasting $\delta^{34}S$ were sampled. Petrographic evidence for the existence of two generations of sphalerite at the QSG and SQS veins (Chapter IV) indicates that the latter is more likely. The sulphur isotopic composition of galena from the Ag-Pb-Zn veins varies in a manner similar to that of sphalerite (1.2 to 5.1 %). Two tetrahedrite samples from SQT and QSG veins at the Coeur and Lucky Friday mines have very similar $\delta^{34}S$ of 5.1 and 5.7 ‰ respectively. In contrast, tetrahedrite from the SQT Sunshine vein has $\delta^{34}S$ of 1.1 ‰. This is an unusually low value, however, because it is nearly 3 ‰ lower than the range of $\delta^{34}S$ values for tetrahedrite (2.9 to 5.9 ‰) reported from the Sunshine mine (Harris et al., 1981).

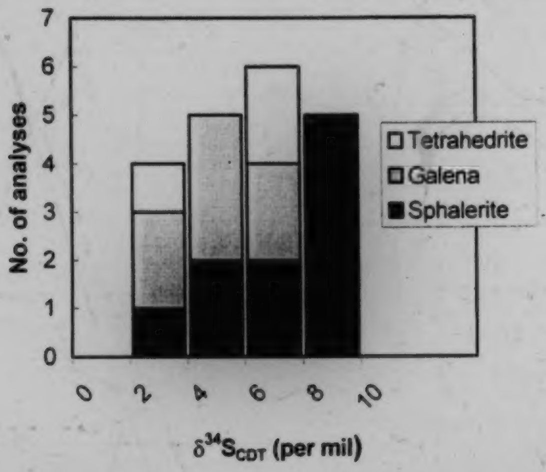

Fig. 6.5. Histogram of the sulphur isotopic composition of sphalerite, galena, and tetrahedrite from the SQT, QSG, and QSQ veins in Coeur d'Alene district.

Mineral Pair Thermometry

Sphalerite-galena mineral pair temperatures were calculated using the equation of Ohmoto and Rye (1979). Although great care was taken to pick coexisting minerals the results of the analyses demonstrate that the majority of the galena-sphalerite pairs are not in isotopic equilibrium (Table 6.3).

Only two sphalerite-galena pairs from moderately deformed parts of SQT and QSG veins in the Sunshine and Lucky Friday mine, respectively, (e.g., SSM-50 and LF-13) yield temperatures in agreement with the microthermometric data and with other independent thermometers. In contrast, all other sphalerite-galena pairs from moderately to strongly deformed portions of the QSG and SQS veins at the Gold Hunter and Lucky Friday mines exhibit highly variable $\Delta^{34}S_{SPHALERITE-GALENA}$ (0.1 to 4.6 ‰) which yield temperatures from 2414° to 123°C (Table 6.3). These temperatures are not in agreement with the microthermometric results and with independent thermometers and are considered to reflect isotopic disequilibrium. The reason for the disequilibrium, as mentioned above, may be internal isotopic inhomogeneity or a mixture of sulphides from different paragenetic stages.

Table 6.3. Sulphur isotopic data for sulphides and sulphosalts from the Coeur d'Alene district.

Sample No.	Vein type/mine	Stage	Tetrahedrite (chalcopyrite) (‰)	Sphalerite (‰)	GalenA (‰)	$\Delta^{34}S$ SPHALERITE-GALENA (‰)	Calculated temperature (°C)
SSM-16	SQT (Sunshine)	II	1.1				
SSM-50	SQT (Sunshine)	II		6.6	4.6	2	327 ± 21
COM-T	SQT (Coeur)	II	5.7				
LF-5t	QSG (L. Friday)	II	5.1				
LF-5c	QSG (L. Friday)	II	(2.3)				
LF-10	QSG (L. Friday)	I (?)		6.3	1.6	0.1	2414 ± 95
LF-10	QSG (L. Friday)	I (?)		1.7	1.6	4.6	123 ± 14
LF-13	QSG (L. Friday)	I (?)		3.4	1.2	2.2	300 ± 20
LF-17	QSG (L. Friday)	I (?)		3.3	3.6	0.3	1278 + 55
LF-31	QSG (L. Friday)	I		6.1	5.1	1.5	420 + 24
LF-21	SQS (G. Hunter)	II		4.2	2.4	1.8	360 + 23
LF-26	SQS (G. Hunter)	II		4.1	2.7	1.4	443 + 24

Abbreviations: QSG = quartz-galena-siderite vein; SQS = siderite-quartz-sphalerite vein; SQT = siderite-quartz-tetrahedrite vein. The errors quoted are ± 1σ and are estimated on the basis of an analytical uncertainty of ± 0.1‰.

VII. SOLUTE THERMOMETRY

In this chapter an attempt was made to determine the temperature of the paleofluids in the Coeur d'Alene district veins by crushing and analyzing the relative concentrations of Na and K in inclusion fluids from various vein minerals. The relative concentration of chlorine was also determined. Although not often used in inclusion fluid analysis chemical thermometry has been widely applied in the exploration and exploitation of geothermal energy (Nicholson, 1993). The most commonly used chemical thermometers are those based on the ratios of sodium, potassium, lithium, calcium, and magnesium in natural waters. Another popular thermometer uses the absolute concentration of silica in natural waters. Generally the temperatures of the subsurface reservoirs obtained by different chemical thermometers match well the temperatures measured by conventional methods such as direct measurement of the temperature of surface discharges (Kharaka and Mariner, 1992).

One of the oldest thermometers which has been successfully applied in the exploration and exploitation of geothermal energy is the Na/K thermometer (Fournier and Truesdel, 1973). The Na/K of natural waters is controlled by ion-exchange reactions between albite and potassium feldspar.

$$\text{Na-feldspar} + K^{+}(aq) = \text{K-feldspar} + Na^{+}(aq)$$

The Na/K thermometer was chosen in this study on the basis of its relative reliability and accuracy. There are, however, limitations that have to be taken into consideration prior to applying the Na/K thermometer. The most important being that both albite and potassium feldspar must be present in the rock hosting the fluid reservoir. Secondly, the application of the Na/K thermometer is limited to fluid temperatures at or above 150ºC (Kharaka and Mariner, 1992). At lower temperatures, the sodium and potassium concentrations are controlled by exchange reactions with clay minerals, and excessively high temperatures may result from the use of the Na/K thermometer. The Na/K thermometer also yields anomalously high temperatures for fluids that contain significant amounts of Ca, and/or other divalent cations (Kharaka and Mariner, 1992), or for waters with a high ammonia content due to reactions with organic-rich sedimentary horizons (Fournier 1989, cited in Nicholson, 1993). In addition, the Na/K thermometer has a slower rate of equilibration compared to other chemical thermometers (e.g., silica content, K-Mg; Nicholson, 1993) and it is possible that the fluid Na/K may not reflect the true temperature at the site of mineral deposition. An inherited problem of the bulk crush-leach procedure is the possibility of analyzing different fluid inclusion populations trapped at different temperatures and/or times.

Efforts were made to minimize the effects of the above mentioned limitations. The Na/K thermometer applied in this study is a modified version developed by Kharaka and Mariner (1992) to be used with waters from sedimentary basins. These waters are similar to the inclusion fluids from the Coeur d'Alene silver-, lead, and zinc-rich veins (Chapter V) in that that they contain high amounts of dissolved salts, including salts of the divalent cations Ca, Mg, and Fe (Chapter V). The relatively high trapping temperature (200° to 350°C) and homogeneous nature of Coeur d'Alene inclusion fluids (Chapter V) also favors the use of the Na/K thermometer. The homogeneity of the results from minerals which belong to different paragenetic stages suggests that primary Na/K signature was most likely preserved.

Analytical methods

The relative concentrations of Na, K, and Cl in inclusion fluids were determined using a technique similar to that described in Botrell et al. (1988). Vein minerals were crushed to a grain size between 0.25 and 1.0 mm, and were handpicked in deionized water and/or ethanol under binocular microscope until all grains with visible impurities were removed. Quartz was washed in boiling HNO_3 for one hour and in cold HNO_3 for 24 hours. Siderite, sulphides, and sulphosalts were repeatedly washed in deionized water only. After washing all samples were soaked in deionized water to remove impurities absorbed on the mineral surfaces. The deionized water was changed once at every 24 hours. The soaking continued from three to five days until no Na and Cl could be detected in the deionized water by ion chromatography. All chemical reagents used were either ultra pure quality or were additionally cleaned in the laboratories of the Geowissenschaften, Montanuniversität, Leoben.

To analyze the relative concentrations of Na, K, and Cl one gram of sample and 5 ml deionized water were transferred to a thoroughly cleaned agate mortar and crushed for one minute. The milky solution was centrifuged to separate the leachate from the ground sample. The leachates were transferred to pre-cleaned HDPE vials and were stored for a limited time (2 to 20 hours) prior to analysis. Both Perkin Elmer AAS and Dionex (DX-500) ion chromatography systems were used for the analysis of cations. Cl was analyzed by ion chromatography. Accuracy of 5% for the element ratios was estimated by running standards. An average error of ± 25°C was determined on the basis of 12 duplicated bulk crush-leach analyses of various vein minerals from the district.

Results of the Na/K thermometry

SQT veins (Sunshine and Coeur mines)

Stage I

Seven stage I siderite samples from the Sunshine mine have Na/K from 11.51 to 15.26. These results indicate that the fluid that precipitated stage I siderite was relatively homogeneous with respect to Na/K (Table 7.1). The samples yield an average temperature of 270 ± 25 °C ([n= 8]; Table 7.1).

Stage II

Two stage II sphalerite and tetrahedrite samples from the Sunshine mine have Na/K of 7.1 to 10.8 which corresponds to temperatures of 340 ± 25°C and 285 ± 25°C respectively (Table 7.1). In contrast, all stage II quartz samples

Table 7.1. Summary of the important element ratios and temperatures obtained from bulk crush-leach analysis of vein quartz, siderite, sphalerite, and tetrahedrite from different precious and base-metal veins at the Coeur d'Alene district.

Sample No.	**Mineral**	**Stage**	**Na/K**	**T (°C)**
SQT veins (Sunshine mine)				
SSM-4	Sid.	I	13.51	260± 25
SSM-7	Sid.	I	12.41	270± 25
SSM-9	Sid.	I	11.61	275± 25
SSM-10	Sid.	I	11.75	275± 25
SSM-11	Sid.	I	12.93	265± 25
SSM-13	Sid.	I	12.65	267± 25
SSM-15	Sid.	I	13.07	265± 25
SSM-50	Sph.	II	7.09	340± 25
SSM-16	Tetr.	II	10.75	285± 25
SSM-4Q	Qtz.	II	2.11	565± 25
SSM-9Q	Qtz.	II	1.61	645± 25
SSM-13Q	Qtz.	II	1.70	630± 25
SSM-41	Qtz.	II	1.78	615± 25
QSG veins (Lucky Friday mine)				
LF-7	Qtz.	II	7.65	325± 25
LF-14	Qtz.	II	9.25	305± 25
LF-19	Qtz.	II	7.60	330± 25
LF-10'q	Qtz.	III	7.59	330± 25
LF-6	Qtz.	III	4.00	430± 25
SQS veins (Gold Hunter mine)				
LF-22	Sid.	I	13.83	260± 25
LF-21	Sid.	I	20.47	220± 25
LF-22q	Qtz.	II	5.04	390± 25
LF 20	Qtz.	III	4.83	395± 25
LF-28	Qtz.	III	2.83	500± 25
Coleman Au-quartz vein				
CV-1	Qtz.	Main stage	9.30	305± 25
CV-3	Qtz.	Main stage	21.26	220± 25
CV-5	Qtz.	Main stage	11.39	280± 25
CVU-1	Qtz.	Main stage	7.12	340± 25
CVU-4	Qtz.	Main stage	2.18	560± 25
CVU-5	Qtz.	Main stage	17.25	235± 25
CVU-6	Qtz.	Main stage	9.82	295± 25

Abbreviations: Qtz: quartz; Sid: siderite; Sph: sphalerite; Tetr: tetrahedrite.

exhibit very low Na/K (e.g. 2.1 to 1.2; Table 7.1). The calculated temperatures of these samples vary between 565 ± 35° and 750 ± 25°C. Those temperatures are not in agreement with the results from the stable isotope thermometery (Chapter VI), or with previously estimated temperatures of vein deposition from the district (Leach et al., 1988). Although it is not clear what causes the anomalously low Na/K ratio of stage II quartz in the SQT veins it is possible that it is an analytical artifact. As mentioned above, quartz samples have been repeatedly treated with HNO_3 as a part of the cleaning procedure. During the treatment microscopic flakes of vein muscovite could have been hydrated and altered to illite. The subsequent crushing could than have released potassium, thus altering the Na/K ratio of the leaching solution (cf. Christie et al, 1989). Although great care was taken to remove all visible impurities it is possible that muscovite remained undetected in the samples. As mentioned in Chapter IV vein muscovite is a common stage II mineral at the SQT and SQS veins but it is absent from the QSG and the Au-quartz vein samples collected during this study. The low Na/K of all stage II and III quartz from the SQS veins, where muscovite is a common stage II mineral, supports this hypothesis. In contrast, most quartz samples at the QSG veins, where no muscovite is seen, have K/Na which yield temperatures in agreement with the microthermometry and the stable isotopic thermometry (Chapters V and VI). Only one quartz sample at the Lucky Friday main vein (i.e. LF-6; Table 7.1), which was collected proximal to the sericitic wall rock has low Na/K, which may have resulted from muscovite/illite related potassium contamination.

QSG veins (Lucky Friday mine)

Stage II

Three stage II quartz samples from the QSG Lucky Friday main vein yield temperatures of 305 ± 25°, 325 ± 25°, and 330 ± 25°C (Table 7.1).

Stage III

One stage III quartz sample yields a temperature of 330 ± 25°C which is in good agreement with the Th_{total} of the fluid inclusions from stage III quartz (e.g. 305 ± 24°C [n=21]; Chapter V), and indicates that Th_{total} is close to $T_{trapping}$.

SQS veins (Gold Hunter mine)

Stage I

Two siderite samples from a SQS vein at the Gold Hunter mine have Na/K of 20.5 and 13.8 which correspond to temperatures of 220 ± 25°C and 260 ± 25°C, respectively.

Stages II and III

As mentioned above, all stage II and III quartz samples from the SQS veins at the Gold Hunter mine yield anomalously high temperatures (e.g. from 390 ± 25° to 500 ± 25°C; Table 7.1) possibly due to potassium contamination.

Au-quartz vein (Coleman vein)

Quartz samples from the Coleman Au-quartz vein exhibit Na/K from 21.3 to 2.2 which yield temperatures from 220 to 560°C. A correlation between the Na/K of the inclusion fluid and sample position with respect to the vein walls, was observed (Fig. 7.1). Quartz samples from the central parts of the vein have higher Na/K, and yield temperatures from 220 to 250°C which are close to, or slightly bellow the Th_{total} of type 3 fluid inclusions (269 ± 8.0°C). In contrast, samples close to the vein walls yield temperatures of up to 560°C (Table 7.1). The lack of corresponding change in the $\delta^{18}O$ of vein quartz indicates that the high Na/K along the vein walls are not temperature dependent.

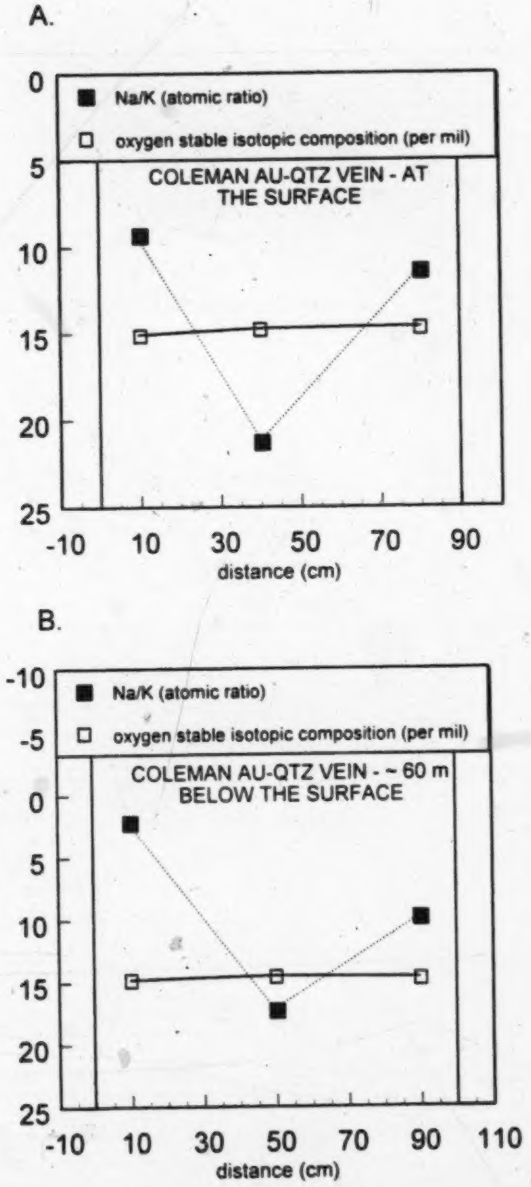

Figure 7.1. A. Graph of δ^{18}O and Na/K (atomic) against distance across Coleman Au-quartz vein at the surface and approximately 60 m underground (B). Note the V–shaped Na/K trends in vein quartz with the lowest values near the vein walls. The lack of correlation between the Na/K and δ^{18}O values indicates that the variance in the Na/K ratios is not temperature dependent (see text for details).

VIII. DISCUSSION

Estimation of fluid trapping P-T conditions.

Type 2, low-X_{CO2} fluid inclusions

Microthermometric data indicate that low-X_{CO2} fluid inclusions from stages I and II siderite, quartz, and sphalerite at the silver and base metal veins trapped single-phase homogeneous fluids. To determine the P-T conditions at which these fluids were trapped independent estimates of the fluid trapping temperatures are needed (Roedder, 1984; Shepherd et al., 1985). Trapping temperature estimates for type 2 inclusions were derived from independent stable isotopic and Na/K thermometry (Chapters VI and VII). Fluid isochores and trapping pressures were calculated using MacFlincor 0.93 (Brown and Hagemann, 1994) with the equation of state of Zhang and Frantz (1987). The pressure calculations, however, do not account for the presence of CO_2 and/or other volatiles dissolved in the inclusion fluids. As mentioned in chapter V, clathrate formation indicates that type 2 fluid inclusions contain between 1.6 and 4.0 mol % CO_2 which will affect trapping pressure estimates. For example, if the moderately saline (2 to 3 molal NaCl) type 2 inclusions, are assumed to contain 1 molal CO_2, which is close to the minimum amount necessary to nucleate clathrate (i.e. 0.85 molal, Hedenquist and Henley, 1995), then CO_2 vapor pressures from 180 to 270 bars are to be expected between 200 and 300°C (Drummond, 1981). Because such small amounts of CO_2 are assumed to have little effect on the slope of isochores calculated assuming a H_2O-NaCl-KCl±$CaCl_2$ system (e.g. Richards and Kerrich, 1993), trapping pressures will be at least 180 to 270 bars higher than that calculated in the absence of gas (Drummond, 1981). This is a conservative estimate, however, because the CO_2 content of type 2 inclusions may be as high as 2.2 molal (~4 mol %), and in this case pressure correction would reach 600 bars. Even higher pressures are possible if due to the poor optics of siderite the presence of liquid CO_2 in some type 2 inclusions was overlooked during the microthermometric study.

To provide a reasonable trapping pressure estimate for type 2 inclusions all type 2 inclusions were assumed to contain 2.5 molal NaCl and 1.5 molal CO_2. Thus, at temperatures between 250 and 300°C the partial pressure of CO_2 will contribute ~390 bars to the fluid pressure calculated for a gas free system (Drummond, 1981). Both corrected and uncorrected trapping pressure values are presented in Table 8.1.

Type 3, intermediate-X_{CO2} and type 4, CO_2-rich fluid inclusions: Evidence for fluid immiscibility?

Fluid compositions and trapping pressures for stage III intermediate-X_{CO2}, and CO_2-rich inclusions were calculated using MacFlincor 0.93 with the equation of state of Holloway (1977). Although no aqueous phase was detected in type 4 inclusions thermodynamic calculations predict that certain amounts of water must be present in natural CO_2-rich inclusions unless they were subjected to post-entrapment changes (Hollister, 1990). The generally unstrained nature of stage III quartz and the relative homogeneity of the microthermometric properties of type 3 and 4 inclusions argue against such changes. Thus, it seems reasonable to assume that some water is present in the CO_2-rich inclusions. Although the presence of <10 vol. % water in type 4 inclusions will have little impact on the pressure calculations, estimated pressures from individual populations must be regarded as minimum values. The results of the pressure calculations are presented in Table 8.1.

Fluid immiscibility was previously reported in individual veins from the Coeur d'Alene district (Bijak and Norman, 1982; Leach et al., 1988; Thieriault 1989). Some authors, however, argue that immiscibility was rare (Leach et al., 1988), whereas others find no evidence for immiscibility at all (Yates and Ripley, 1985). The presence of coexisting intermediate-X_{CO2} and high-X_{CO2} inclusions in stage III quartz from the Ag-Pb-Zn veins, and in the Au-quartz Coleman vein (see Chapter V) satisfies an important criterion for fluid immiscibility (Ramboz et al.,1982). However, the lack of visible aqueous phase in the CO_2-rich inclusions

Table 8.1. Calculated trapping temperatures and pressures of individual fluid inclusion populations from SQS, QSG, and SQT veins and also from Au-quartz Coleman vein, Coeur d'Alene district.

Vein type deposit	Stage	Incl. type	Temperature of trapping (°C)(1)	Pressure at trapping (bars)(2)	Corrected fluid pressure for type 2 inclusions (kb)(3)	EOS(4)
SQT vein - Sunshine vein, Sunshine mine						
	I	2	270	520 ± 200(2)	0.9 ± 0.4	Zhang and Frantz (1987)
	II	2	325	620 ± 420(2)	1.0 ± 0.6	Zhang and Frantz (1987)
	III	3	290	1560 ± 570		Holloway (1977)
		4	290	1875 ± 550		Holloway (1977)
QSG veins - Lucky Friday Main vein, Lucky Friday mine						
	II		320	730 ± 500(2)	1.3 ± 0.6	Zhang and Frantz (1987)
	III	3a	305	2340 ± 230		Holloway (1977)
	III	3s	305	2430 ± 270		Holloway (1977)
		4a	305	1607 ± 100		Holloway (1977)
		4b	305	2410 ± 200		Holloway (1977)
SQS veins - Gold Hunter mine						
	I	2	240	1500 ± 450(2)	1.8 ± 0.6	Zhang and Frantz (1987)
	II	2	280	980 ± 520(2)	1.4 ± 0.6	Zhang and Frantz (1987)
	III	3	280	1550 ± 350		Holloway (1977)
		4	280	1240 ± 130		Holloway (1977)
Au-quartz veins - Coleman vein						
	NA	3	270	1680 ± 250		Holloway (1977)
	NA	4	270	1301 ± 170		Holloway (1977)

(1)See text for details.
(2)Pressure calculated assuming no CO_2 dissolved in inclusion fluids.
(3)Pressure correction calculated assuming an average NaCl content of 2.5 molal and CO_2 from 1 to 2 molal (see text for details).
(4)Equation of state applied by using MacFlincor 0.93 (Brown and Hagemann, 1993).

precludes the observation of Th_{total} and renders it difficult to determine whether type 3 and 4 fluid inclusions are truly coeval.

There is also indirect evidence in support of phase separation during stage III at the Ag-Pb-Zn veins and at the Coelman Au-quartz vein. For example, the relatively good agreement between Th_{total} of the intermediate-X_{CO2} fluid inclusions and the results of the independent thermometers (Chapters VI and VII) indicates that hydrothermal fluids were trapped close to the solvus. Due to lack of experimental data the PT coordinates of the solvi in the $NaCl-CO_2-CH_4-N_2$ system are not known. However, the low solubility of methane and/or N_2 in aqueous brines would expand the two-phase field of the $CH_4(N_2)-H_2O$ system(s) well beyond the pressure and temperature limits of CO_2-H_2O and/or $CO_2-H_2O-NaCl$ systems (Naden and Shepherd, 1989; Duan, 1992). Richards et al. (1997) also argued that non-ideal mixing in the system $H_2O-CO_2-CH_4$ results in lower gas solubilities. Thus, fluid immiscibility over the 250 to 350°C and 1 to 3 kb ranges will be more common in the $CH_4(N_2)-H_2O(NaCl)$ system than in the CO_2-H_2O and/or $CO_2-H_2O-NaCl$ systems. In addition, similarities in the calculated trapping pressures of type 3 and type 4 inclusions from stage III quartz at the individual silver and base metal veins, and also at the Coleman Au-quartz vein indicate that these fluid inclusions were trapped at or very close to the two phase boundary. (cf. Ramboz et al., 1982; Diamond, 1990).

Preferential partitioning of individual gases into the vapor phase during phase separation (e.g., $N_2>CH_4>CO_2$; Giggenbach, 1980) renders the CO_2/N_2 and CO_2/CH_4 ratios of inclusion fluids useful in identifying fluid unmixing (Channer and Spooner, 1994). A notable decrease of CO_2/N_2 and/or CO_2/CH_4 from type 3 to type 4 inclusions from stage III quartz in all individual veins studied is also consistent with phase separation.

Unmixing of homogeneous miscible fluid can be caused by temperature and/or pressure reduction. However, there is no microthermometric evidence for a temperature decrease during the stage III in the Ag-Pb-Zn veins and also during main stage mineralization at the Coleman Au-quartz vein. Therefore, fluid immiscibility most likely resulted from pressure fluctuations.

The small number of type 4 inclusions in stage III quartz and in quartz from the Coleman vein indicates that fluid immiscibility in the Coeur d'Alene district was limited. In addition, lack of NaCl enrichment in the aqueous phase of type 3 inclusions indicates that immiscibility never reached the stage of true boiling with the separation of vapour H_2O phase. Therefore, it is possible that the CO_2-rich fluids were homogeneous and became immiscible only when pressure drops occurred.

Petrographic evidence for very limited sulphide deposition in stage III at the silver and base metal veins also indicates that phase separation was not an important depositional mechanism. However, phase separation possibly played a major role for gold deposition at the Coleman Au-quartz vein.

Trapping P-T conditions in the SQT veins (Sunshine Vein)

Stage I

On the basis of fluid inclusion data from SQT veins at the Galena mine (Yates and Ripley, 1986), and SQS veins at the Star-Morning mine (Constantopoulus, 1989), Eaton et al. (1995) suggested that vein siderite at the Sunshine mine precipitated at about 325°C. The fluid inclusion data in both studies, however, were obtained primarily from quartz. Although it is not clear from what paragenetic stage the quartz data of Constantopoulus (1989) were derived from, the data of Yates and Ripley (1985) were obtained from liquid-rich H_2O-CO_2-bearing inclusions in late quartz which, as demonstrated in this study, are not representative of conditions during stage I. In contrast to the suggested 325°C of Eaton et al. (1995) Na/K thermometry on siderite yielded an average temperature of ~270°C for stage I (Chapter VII). A trapping pressure of 520 ± 200 bars was calculated for stage I considering an H_2O-$NaCl$-KCl-$CaCl_2$ system (Chapter V). However, as mentioned above, the partial pressure of CO_2 dissolved in the inclusion fluid will contribute ~390 bars to the latter value. Thus, stage I siderite in the Sunshine vein was deposited at a temperature of ~270°C and a pressure of approximately 0.9 kb.

Stage II

The reasonably good agreement between stable isotopic and Na/K inclusion fluid thermometry (Chapters VI and VII) suggests a trapping temperature of ~325°C for stage II. Calculated trapping pressure assuming an H_2O-NaCl-KCl-$CaCl_2$ system is approximately 620 bars. Considering the impact of dissolved CO_2 the trapping pressure during stage II reaches ~ 1.0 kb (Drummond, 1981).

Stage III

Petrographic evidence for fluid immiscibility in stage III quartz suggests that trapping temperature may have been close to the average Th_{total} of type 3 fluid inclusions (289 ± 42°C). Thus, by assuming a trapping temperature of ~290°C, calculated pressure for type 3 fluid inclusions averages 1560 ± 570 bars. Type 4, CO_2-rich inclusions yield trapping pressures which fall within the same range (e.g., 1875 ± 550 bars).

Trapping P-T conditions in the QSG veins (Lucky Friday main vein)

Stage I

Due to lack of suitable minerals no microthermometric data are available for stage I at the QSG Lucky Friday main vein. In addition, galena-sphalerite pairs taken from stage I sulphide ore are out of isotopic equilibrium, as discussed in Chapter VI, and also do not provide information about the P-T conditions during the deposition of stage I minerals at the QSG veins. Only one galena-sphalerite mineral pair yields a temperature of 300 ± 20°C, which is higher than the fluid temperatures of 270°C and 240°C determined at the SQT Sunshine vein and at SQS veins in the Gold Hunter mine, respectively. Therefore, in the absence of reliable independent thermometry and on the basis of close similarities in the stable isotopic compositions of stage I siderite from the silver and base metal veins, a fluid temperature of 270°C is suggested for stage I at the Lucky Friday main vein.

Stage II

A trapping temperature of ~320°C was determined for stage II at the Lucky Friday main vein on the basis of Na/K thermometry of three quartz samples and one sphalerite-galena pair. Calculated trapping pressure for type 2 inclusions from quartz, siderite, and sphalerite at this temperature averages 730 ± 500 bars, or ~1.3 kb if the effect of CO_2 dissolved in the inclusion fluid is considered (Drummond, 1981).

Stage III

Coexisting type 3 and 4 fluid inclusions are common in stage III quartz at the Lucky Friday Main vein. Type 3, intermediate X_{CO2} inclusions exhibit Th_{total} of 305 ± 24°C which agrees with a Na/K temperature of 330 ± 25°C yielded by a single quartz III sample from the Lucky Friday Main vein. Another quartz sample taken proximal to vein walls yields anomalously high K/Na temperature of 430 ± 25°C. As discussed in Chapter VII the latter value most likely reflects contamination during sample preparation. Thus, a fluid temperature of 320°C is suggested for stage II at the Lucky Friday main vein. Calculated trapping pressure for type 3 fluid inclusions averages 2340 ± 230 bars.

As in stage III quartz at the Sunshine mine there are two types of CO_2-rich inclusions in stage III quartz at the Lucky Friday Main vein. By assuming trapping temperature of ~305°C type 4b inclusions yield fluid trapping pressure of approximately 2400 bars which is nearly identical to the pressure obtained by type 3 inclusions (2340 ± 230 bars). Type 4a inclusions, however, yield average trapping pressure of 1610 ± 100 bars which suggests that these inclusions were trapped separately, possibly during significant pressure decrease associated with vein dilation.

Trapping P-T conditions in the SQS veins (Gold Hunter mine)

Stage I

As discussed in Chapter VII the discordant, high temperatures yielded from several stage I sphalerite-galena mineral pairs indicate that the sulphides are most likely out of isotopic equilibrium. However, two stage I siderite samples yielded Na/K temperatures of 220 ± 25°C and 260 ± 25°C, respectively. Calculated trapping pressure assuming an average temperature of 240°C is ~1500 bars. If the effect of the dissolved CO_2 is taken into consideration fluid trapping pressure during stage I reaches 1.7 kb (cf. Drummond, 1981).

Stage II

Type 2 fluid inclusions from stage II siderite exhibit average Th_{total} of 229 ± 17°C (n = 11). There is no independent thermometery available for stage II. However, stage II and III siderite from SQS veins at the Gold Hunter mine have similar oxygen isotopic compositions (Chapter VI). Thus, if stage II and III fluids had similar oxygen isotopic signature maximum fluid temperature during stage II was ~280° C (see below). Calculated average trapping pressure for stage II is slightly lower than that for stage I (e.g., ~980 bars, or ~1.4 kb if the CO_2 effect is considered).

Stage III

On the basis of coexisting liquid- and CO_2-rich fluid inclusions in quartz, Leach et al. (1988) suggested that fluid immiscibility at the Gold Hunter mine occurred at approximately 290°C and 0.9 kb. The authors argued, however, that the pressure may have been higher because the CO_2-rich inclusions had an average of 1 mol % CO_2 more than the fluid composition for the experimental solvus determined by Franck (1977).

Coexisting type 3 and 4 inclusions are observed in stage III quartz at the Gold Hunter mine. Type 3 inclusions have Th_{total} of 280 ± 15°C which agrees with a temperature of 290 ± 50°C yielded by a single quartz-siderite mineral pair from a stage III subhorizontal quartz vein (Chapter VI). Calculated trapping pressures from type 3 and type 4 inclusions at this temperature, however, are higher (e.g., 1810 ± 350 and 1340 ± 130 bars respectively) than the pressure suggested by Leach (1988).

Trapping conditions in the Coleman Au-quartz vein

The fluid temperatures yielded by Na/K thermometery from samples in the central parts of the Coleman Au-quartz vein are 220 ± 25°C and 250 ± 25°C, respectively, which are slightly lower or overlap within error with the average Th_{total} of 269 ± 8°C (n = 11) for the dominant type 3 inclusions. Evidence for phase separation suggests that the latter value reflects better the fluid temperature during quartz precipitation. Assuming a trapping temperature of 270°C estimated trapping pressures of coexisting type 3 and 4 fluid inclusions (e.g., 1680 ± 250 kb, and 1300 ± 170, respectively) fall within the same range.

Summary of P-T-X data

QSG, SQS, and SQT veins

The results of the fluid inclusion study demonstrate that the Ag-Pb-Zn veins in Coeur d'Alene trapped up to three different fluids including: (1) moderately saline CO_2-poor fluids; (2) immiscible CO_2-rich fluids of low salinity; and (3) aqueous moderate salinity fluids of secondary origin.

Microthermometric data and independent thermometry indicate that CO_2-poor fluids trapped in paragenetic stage I at the SQS veins at the Gold Hunter mine are on average slightly more saline and cooler (~17 eq. wt. % NaCl; 240°C) than stage I fluids at the Sunshine mine (~13 eq. wt. % NaCl; 270°C; Chapter V). Estimated average densities and fluid pressures are also higher at the Gold Hunter mine. Despite these differences, however, both fluids exhibit similar trends which suggest progressive mixing between more saline colder solutions and less saline warmer fluids (Chapter V, Fig. 5.2, 5.6).

The P-V-T-X properties of stage II fluids from all Ag-Pb-Zn veins studied are comparable. The fluids have average apparent salinity of 11.0 ± 1.5 wt. %

NaCl and the results of the independent thermometry indicate that they were trapped at about 300 ± 20°C. Calculated average fluid trapping pressure decreases slightly from ~1.4 kb at the Gold Hunter mine to ~1.0 kb at the Sunshine mine.

The average Th_{total} of the type 3 inclusions ranges from 305 ± 24°C at the Lucky Friday mine to 280 ± 15°C at the Gold Hunter mine. Primary stage III fluids exhibit salinities from 0.2 to 11 eq. wt. % NaCl with an average value of approximately 4.0 eq. wt. % NaCl. Estimated densities and trapping pressures range from 0.8 to 0.9 g/cm^3 and from of 1.3 to 2.6 kb, respectively. The microthermometric study (Chapter V) did not find evidence for large variance in the gas composition of stage III fluid inclusions from the individual veins such as the variance reported by Hofstra et al. (1985) and Leach et al. (1988). None of the individual fluid inclusions studied contains more than 20 mol % N_2, CH_4, and/or C_nH_n, in its carbonic phase and the calculated values are usually much less (Chapter V). Similarities in the P-V-T-X properties and gas compositions of type I, II, and III fluids indicate that these fluids are most likely of common origin and entered the vein fractures in the district simultaneously.

In contrast with previous studies (Leach et al., 1983; 1988) the microthermometric results demonstrate that stage I and II fluids associated with Pb, Zn, and Ag mineralization at the individual veins contain less than 4 mol % CO_2 (i.e. the mineralizing fluids were CO_2-poor).

Coleman Au-quartz vein

Main stage quartz at the Coleman Au-quartz vein trapped CO_2(CH_4, N_2)-rich fluids with P-T-X characteristics statistically indistinguishable from those of stage III fluids at the silver and base metal veins. Type 3 inclusions homogenize at ~270°C and contain ~ 17 mol % CO_2 with minor CH_4 and N_2. Average fluid salinities are ~2.0 eq. wt. % (Chapter V).

Stable isotope systematics

Prior to drawing conclusions about the significance of the stable isotopic composition of the minerals the analytical results need to be evaluated to ensure that the $\delta^{18}O$ and $\delta^{13}C$ signature is not affected by secondary processes such as post depositional isotopic exchange. O'Neil (1987) demonstrated that quartz resists oxygen isotopic exchange at temperatures at or below 250°C. Given the very low metamorphic grade in the district (White, 1989) it appears unlikely that the $\delta^{18}O$ of vein quartz was modified by post-depositional processes. Carbonate minerals, however, continue to exchange oxygen at temperatures as low as 25°C (O'Neil, 1987), and their present day $\delta^{18}O$ may not reflect their original oxygen isotopic compositions. Vein dolomites and ankerites from Archean mesothermal Au-quartz deposits which are out of oxygen isotopic equilibrium with coexisting quartz indicate that post-depositional alteration of the stable isotopic composition of carbonate minerals is a common process (Kerrich, 1990).

Experimental studies demonstrate that oxygen and carbon diffusion in calcite proceeds at different rates (Kronnenberg et al., 1984). Oxygen diffusion in calcite is enhanced by higher P_{CO2}, P_{H2O}, and is affected by the presence of small amounts of divalent cations other than Ca^{2+}. In contrast, carbon diffusion is generally independent of P_{CO2}, P_{H2O}, and mineral composition, and is several times slower than oxygen diffusion (Kronnenberg et al., 1984). The slower rate of carbon diffusion indicates that solution-precipitation reactions are necessary to alter the primary $\delta^{13}C$ signature of carbonate minerals (O'Neil, 1987). Given the lack of petrographic evidence for solution-precipitation in the siderite samples studied, their $\delta^{13}C$ and signature is expected to be preserved relatively unchanged. However, post-depositional alteration of the $\delta^{18}O$ of vein siderite cannot be precluded.

It is generally accepted that the primary $\delta^{34}S$ signature of sulphide minerals is preserved during moderate to high-degrees of metamorphism (Lyons et al., 2000, and the references therein). Thus, the $\delta^{34}S$ values of vein sulphides and sulphosalts from the Coeur d'Alene district most likely reflect their original sulphur isotopic composition.

δ^{18}O and δ^{13}C variation

Previous studies demonstrated systematic variations in the stable isotopic composition of vein minerals in the Coeur d'Alene Ag-Pb-Zn veins (Yates and Ripley, 1985; Constantopoulus and Larson, 1991; Constantopoulus, 1994; Eaton et al., 1995). Constantopoulus and Larson (1991) reported a negative correlation between depth and δ^{18}O of quartz in the large SQS Star-Morning vein. This trend was initially interpreted to be due to cooling related to boiling (Constantopoulus and Larson, 1991). In a later study however, Constantopoulus (1994) attributed the trend to fluid mixing. Yates and Ripley (1985) observed that the carbon and oxygen stable isotopic composition of vein siderite from SQT veins at the Galena mine define a positive linear correlation (Fig. 8.1). Yates and Ripley (1985) attributed the trend to siderite deposition from a constant carbon and oxygen reservoir at variable temperatures. Eaton et al. (1995) did not find systematic variations in the stable isotopic composition of vein minerals as a function of depth, but reported that vein siderite at the Sunshine mine which has δ^{18}O higher than 16 per mil plots along a temperature dependent trend similar to that of Yates and Ripley (1985). Thus, coupled δ^{18}O and δ^{13}C trends are common in the SQT veins. This study, however demonstrates that stage I siderite at the SQS and QSG veins also plots along the same trend as stage I siderite from the SQT veins (Chapter VI; Fig. 8.1). This is a significant discovery, because it implies that a common process controlled the oxygen and carbon stable isotopic composition of stage I siderite at the individual veins.

Coupled δ^{18}O and δ^{13}C trends with a shallow positive slope have been documented at a large number of carbonate-bearing hydrothermal deposits (Rye, 1966; Rye and Williams, 1981; Matsuhisa et al., 1985; Zheng, 1990; Hein, 1993; Zheng and Hoefs, 1993).

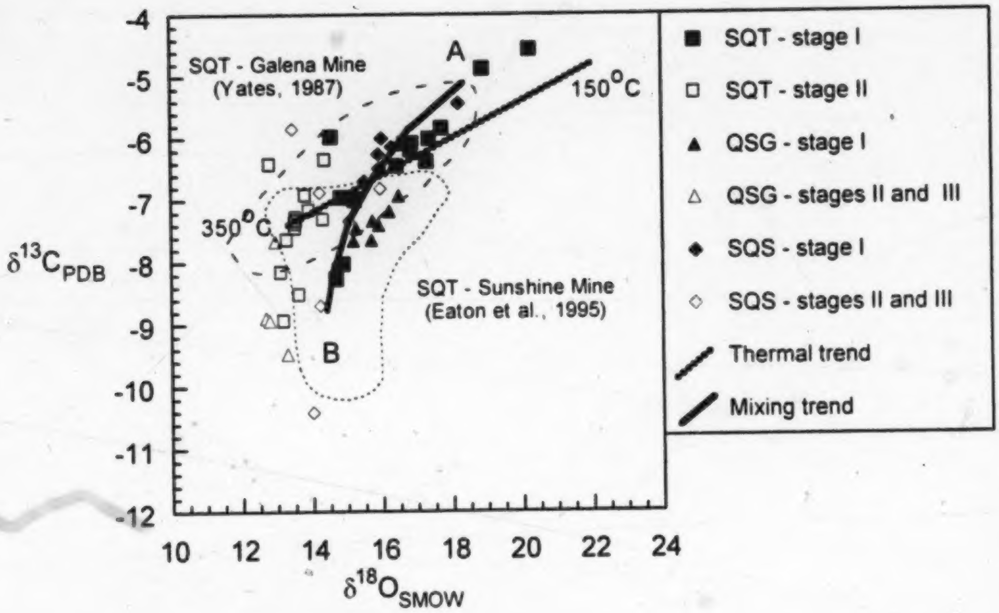

Figure 8.1. Plot of $\delta^{13}C$ against $\delta^{18}O$ for vein siderite from stages I, II, and III at the SQT, QSG, and SQS veins. The fields of vein siderite from SQT veins at the Sunshine and Galena mines are from Eaton et al. (1995) and Yates (1987), respectively. The temperature dependent trend is calculated for siderite precipitated from a fluid having an average $\delta^{18}O$ and $\delta^{13}C$ of +8.5 ‰ and –10.7 ‰, respectively. The mixing trend is calculated assuming $\delta^{18}O$ and $\delta^{13}C$ of fluid A = +5 and –2; and +9 and –12 per mil for fluid B. The temperatures of the two fluids are assumed to be 150 and 325°C, respectively, and the fluid A is assumed to be dominated by HCO_2^-, whereas fluid B contains $H_2CO_{3\,(aq.)}$.

As mentioned above there is a general agreement that such trends result from precipitation of carbonates at variable temperature from a hydrothermal fluid with a constant oxygen and carbon isotopic signature. Calculations based on isotopic fractionation between carbonate minerals such as calcite, dolomite, and the two major oxidized carbon species in hydrothermal fluids (e.g., H_2CO_3 and HCO_3^-) demonstrated that carbonate stable isotopic composition would exhibit positive correlation if dominant carbon species in the fluid is H_2CO_3. In contrast, precipitation of calcite and dolomite from HCO_3^- dominated fluid would produce trends with a negative slope (see Zheng, 1989 and the references therein). However, if the preliminary results of the experimental work on carbon isotopic fractionation of Carothers et al. (1988) were considered trends with positive slope would result even if the fluid is HCO_3^--dominant. Because of a difference of almost 8 ‰ between $\Delta_{SIDERITE\text{-}CO2}$ and $\Delta_{SIDERITE\text{-}HCO3}$ at 250°C (Carothers et al., 1988) it is important to determine the carbon speciation of the hydrothermal fluids which precipitated vein siderite. Otherwise large errors may result in the interpretation of the fluid isotopic signature and origin.

The carbon speciation of hydrothermal fluids is temperature and pH dependent (Ohmoto and Rye, 1979). From 250° to 300°C the transition from HCO_3^- to H_2CO_3 takes place at pH of approximately 8 (Patterson et al., 1982). Lynch (1989) and Bowers (1991) demonstrated that at 250°C a hydrothermal fluid with similar a Fe^{2+} and Ca^{2+} content will precipitate siderite instead of calcite at or below pH of 5.5. Therefore, hydrothermal fluids with tempertaure of 250°C (or higher), which precipitated stage I siderite in the individual silver and base metal veins at the in Coeur d'Alene district were most likely H_2CO_3 -bearing and had a pH of 5.5 or less. At lower temperatures, however, (e.g. ~100°) the HCO_3^- to H_2CO_3 transition is shifted to pH of 5.5 (Patterson et al. 1982).Thus, low temperature fluids in the district (e.g., 100° to 150°C) were most likely HCO_3^--dominant.

An alternative explanation for the coupled $\delta^{18}O$ and $\delta^{13}C$ trends is mixing of two fluids with contrasting temperature, metal chloride content, and stable isotopic signature. For example, mixing of higher salinity, $FeCl_2$ bearing fluid with rich in CO_2 less saline, warmer fluid would result in siderite precipitation. The mixing trend plotted on Fig. 8.1 reflects the stable isotopic composition of siderite which would precipitate as a result of mixing of two fluids with different temperatures and stable isotopic compositions. The first fluid (A) is assumed to have $\delta^{18}O$ and $\delta^{13}C$ of +5.0 and -2.0 ‰, respectively, and a temperature of 150°C. The low temperature of fluid A is inferred on the basis of microthermometric data from stage I siderite at the SQS and SQT veins (Chapter V). As mentioned above, low fluid temperature will favor HCO_3^- instead of H_2CO_3 as a major dissolved carbon species. Therefore, fluid A will precipitate siderite with high $\delta^{18}O$ and $\delta^{13}C$ values, similar to those of some siderite I from the SQT and SQS veins (Table 8.2, Fig. 8.1).

The second fluid (B) has $\delta^{18}O$ and $\delta^{13}C$ of +9 and –12 ‰, respectively, and a temperature of 325°C. The stable isotopic systematics of fluid B are estimated from the $\delta^{18}O$ and $\delta^{13}C$ of stage II and III siderite at the SQT veins (Table 8.2), whereas the fluid temperature is assumed to be equal to the temperature of stage II and III fluids determined from the independent thermometry (Chapter VII). The high $\delta^{18}O$ and $\delta^{13}C$ signature of some stage I siderite is compatible with deposition from fluid of such temeperature and stable isotopic composition.

The temperature and stable isotopic composition of fluid A are consistent with those of isotopically modified formation water or basinal brine (Kerrich, 1987; Welhan, 1987). Such fluids often have salinities that exceed NaCl saturation, low pH, and may be oxidized (e.g. $SO_4^{2-} > H_2S$; Hanor, 1994; Cooke et al., 2000). In contrast fluid B has stable isotopic characteristics indicative of possible metamorphic origin.

The mixing trend is calculated using the equations of Zheng and Hoefs, (1993). In contrast to the temperature dependent trend the mixing trend has a slightly steeper slope than and is concave towards the $\delta^{18}O$ axis (Fig. 8.1). As mentioned in Chapter V, fluid inclusion data from stage I siderite at both the SQT and the SQS veins exhibit a possible fluid mixing trend (Fig. 8.2). However, the microthermometric record does not provide evidence for large temperature variations which would be expected if the two fluids with the above mentioned temperatures (e.g., 150 and 325°C) were mixing. In fact, the difference in Th_{total} between the more saline and less saline fluid inclusions in stage I siderite at the Gold Hunter mine is 75°C, and it is even less at the Sunshine mine (Chapter V). In addition, Eaton et al., (1995) described U-shaped profiles for both $\delta^{18}O$ and $\delta^{13}C$ of siderite taken across two SQT veins in the Sunshine mine, which the authors considered to be inconsistent with fluid mixing. Lower $\delta^{18}O$ and $\delta^{13}C$ in siderite from the central parts of the veins were interpreted to be due to siderite deposition with increasing temperature during vein filling (Eaton et al., 1995). Siderite from the central parts of the veins, however, exhibits unusually low $\delta^{13}C$. The samples deviate from the temperature dependent trend and plot along a steep curve concave toward the ^{13}C axis (Fig. 8.1). This deviation could not be accounted for by a thermal gradient alone. Instead, Eaton et al. (1995) attributed the low $\delta^{13}C$ values to sudden CO_2 releases triggered by brecciation during the sealing of the veins. Loss of CO_2 would preferentially remove ^{13}C from the fluid without significantly affecting the $\delta^{18}O$ values. The authors also suggested that a continuous precipitation of siderite from a finite carbon reservoir could also deplete the fluid in ^{13}C (Eaton et al., 1995).

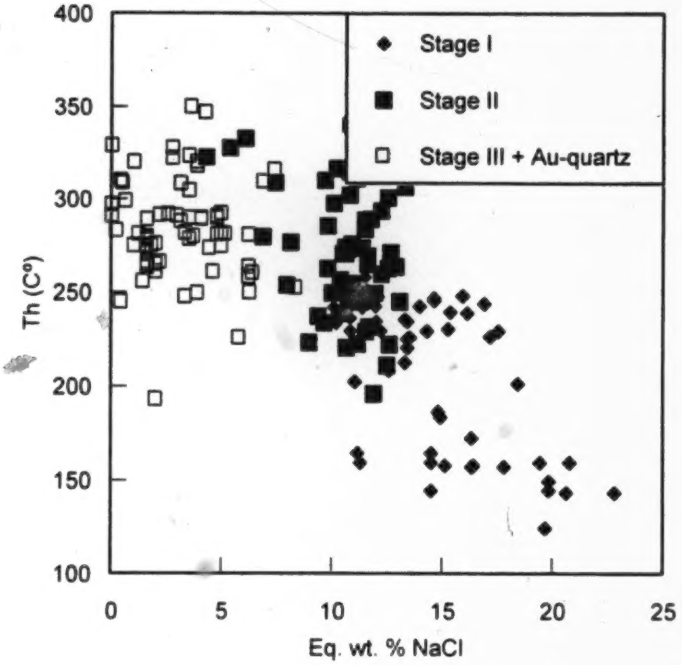

Fig. 8.2. Total homogenization temperature (Th_{total}) against salinity (eq. wt. % NaCl) for fluid inclusions from different paragenetic stages at the QST, SQS, and QSG veins.

In contrast to the observations of Eaton et al. (1995), a sample profile taken across the Sunshine vein at level 3100 demonstrates a notable increase of $\delta^{18}O$ and $\delta^{13}C$ of stage I siderite towards the center of the vein (Fig. 8.3. A, B). The Π-shaped profile defined by stage I siderite is exactly the opposite of the trends reported by Eaton et al. (1995). Careful examination of the vein in the stope provided no evidence for faulting that could have juxtaposed parts of the vein formed at different P-T conditions and/or times. Although post-depositional alteration can not be ruled out as a possible reason for the modification of $\delta^{18}O$ of stage I siderite it is difficult to attribute a simultaneous shift toward more negative

$\delta^{13}C$ values to alteration. As mentioned in Chapter V, secondary fluids at the Coeur d'Alene district are CO_2-poor and would not alter the primary carbon signature of vein carbonates (cf. Kerrich, 1989). Zheng and Hoefs (1993) described trends similar to that of Eaton et al. (1995) in calcite veins from the Bad Grund Pb-Zn deposit in the western Hartz Mts. The authors argued that the trends cannot be produced by fluid mixing, because mixing would be expected to take place along the vein strike rather than perpendicular to it. Nevertheless, the trends would be consistent with a systematic change of the fluid temperature and/or chemical composition caused by a gradual influx of fluids derived from different sources (Fig. 8.3 A, B). Mixing of fluids from different sources and/or gradual fluid evolution is also consistent with the highly variable $^{87}Sr/^{86}Sr$ of vein siderite at the Sunshine mine (Eaton et al., 1995).

The low CO_2 content of type 2 fluid inclusions and lack of microthermometric evidence for phase separation during stage II rules out CO_2 loss as a reason for the variable low $\delta^{13}C$ of stage II siderite. Instead, it is more likely that lower $\delta^{13}C$ of stage II siderite resulted from siderite deposition from a finite carbon reservoir. This mechanism is compatible with the random $\delta^{13}C$ variance of stage II siderite (Chapter VI). If stage II hydrothermal fluids were separated from a steady CO_2 supply in small isolated fractures siderite would be depleted of ^{13}C due to a continuous precipitation from a finite reservoir. In contrast, fluids in interconnected fractures will precipitate stage II siderite with higher $\delta^{13}C$.

Evidence for phase separation in stage III suggests that CO_2 loss could have caused the ^{13}C depletion of the two stage III siderite samples. In addition, due to large carbon isotopic fractionation between CO_2 and CH_4 (e.g., $\Delta_{CO2-CH4}$ = 28.7‰ at 250°C; Ohmoto, 1986) a preferential CH_4 loss during fluid unmixing could have induced shifts towards even more negative $\delta^{13}C$ values of stage III siderite.

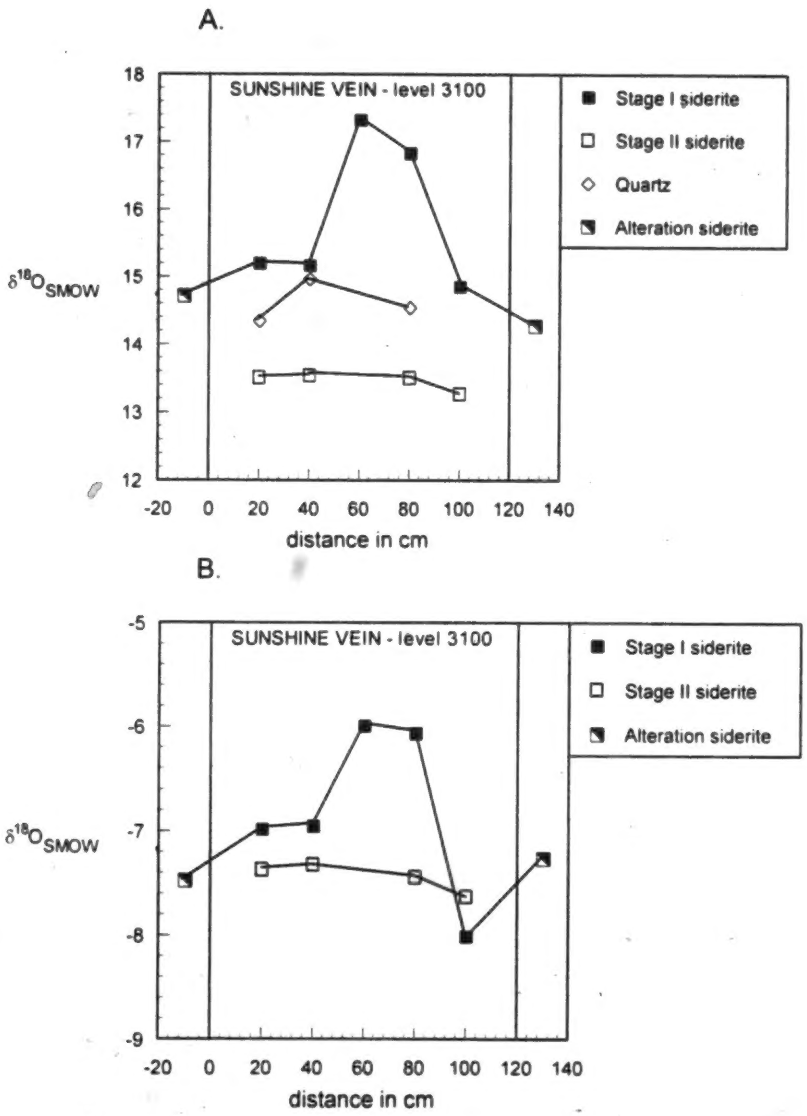

Figure 8.3. A. Graph of δ^{18}O against distance across Sunshine vein, level 3100, Sunshine mine. Note the Π–shaped isotopic trend in stage I siderite with the highest values at the vein centre. This trend is exactly the opposite of what was observed by Eaton et al. (1995) in SQT veins at the Sunshine mine. No evidence for faulting that could have juxtaposed parts of the vein formed at different places and or times were seen in the stope. B. Graph of δ^{13}C against distance. The δ^{13}C values of siderite I show a trend similar to that of the δ^{18}O values in (a). The only exception is a single stage I siderite near the hanging wall which exhibits an unusually low δ^{13}C.

An alternative explanation for the non-systematic behaviour of $\delta^{13}C$ during stages II and III may be local carbon buffering from a varied host rock and vein carbon reservoir (e.g. carbonate minerals and/or organic carbon). This alternative is in agreement with the small amounts of siderite deposited in stages II and III, which implies that local carbon sources could have affected $\delta^{13}C$ of siderite.

Fluid Isotopic Signature

If the temperature of the hydrothermal fluid is known or can be inferred with sufficient certainty, the isotopic signature of the fluid can be calculated from oxygen and/or carbon isotopic analyses of minerals precipitated from the fluid. Such data, although not necessarily a source of information about the ultimate source of the fluid, may provide information about the degree of interaction with the country rock, and may also shed light on the mechanisms of vein formation. The calculated fluid stable isotopic signature is presented on Table 8.2. The oxygen and carbon stable isotopic fluid values are also plotted on Fig 8.4. Using the results from the fluid inclusion study and independent thermometry $\delta^{18}O_{fluid}$ values which range from 6.8 to 12.5 ‰ and average 8.9 ± 1.2 ‰ (n = 24) were estimated for hydrothermal fluids in equilibrium with stage I siderite from individual veins at the Sunshine, Coeur, Lucky Friday and Gold Hunter mines. Calculated $\delta^{18}O_{fluid}$ values for stage II and III siderite range from 7.1 to 9.3 ‰ with an average of 8.2 ± 0.6 ‰ (n = 21) and the $\delta^{18}O_{fluid}$ for stage II and III quartz ranges from 7.1 to 9.0 ‰ with an average of 8.2 ± 0.6 ‰ (n = 16). The calculated fluid composition for the Coleman Au-quartz vein ranges from 7.1 to 6.6 per mil and is generally similar to the composition of stage III quartz from the silver- and lead-zinc-rich veins.

Table. 8.2. Calculated stable isotope compositions of hydrothermal fluids in equilibrium with stage I and stage II siderite from SQT, QSG, and SQS veins.

Vein type/description	Stage	$\delta^{18}O_{fluid}$ ‰ (range)	$\delta^{18}O_{fluid}$ ‰ (average)	$\delta^{13}C_{fluid}$ ‰ (range)	$\delta^{13}C_{fluid}$ ‰ (average)	T (°C)	n
Sunshine Mine							
SQT vein	I	7.7 to 10.3	8.7 ± 1.1	-12.0 to -9.7	-10.6 ± 0.9	270	8
SQT vein	II	7.5 to 9.1	8.3 ± 0.4	-11.7 to -9.6	-10.5 ± 0.6	325	10
Alteration siderite	I	6.6 to 7.7	7.1 ± 0.5	-11.2 to -10.9	-11.0 ± 0.1	270	6
Coeur Mine							
SQT vein	I	6.8 to 12.5	9.7 ± 2.0	-10.4 to -8.5	-9.6 ± 0.7	250	6
SQT vein	II	7.8 to 9.0		-11.3 to -10.5		325	2
Lucky Friday Mine							
QSG vein	I	8.2 to 9.5	8.8 ± 0.5	-11.4 to -10.6	-11.1 ± 0.2	270	7
QSG vein	II	7.4 to 8.0		-12.1 to -12.7		320	3
flat vein	III		7.7		-10.9	320	1
Alteration siderite	I	5.2 to 7.4	6.8 ± 0.8		-11.2 ± 0.4	270	6
Gold Hunter Mine							
SQS vein	I	7.7 to 10.0	8.3 ± 1.0	-10.5 to -9.5	-10.1 ± 0.4	240	6
SQS vein	II	7.6 to 9.3	8.3 ± 0.8	-12.3 to -10.3	-10.9 ± 0.8	280	4
flat vein	III		7.4		-14.0	280	1
Alteration siderite	I	6.7 to 7.0	6.9 + 0.1	-11.8 to -10.7	-11.1 ± 0.4		

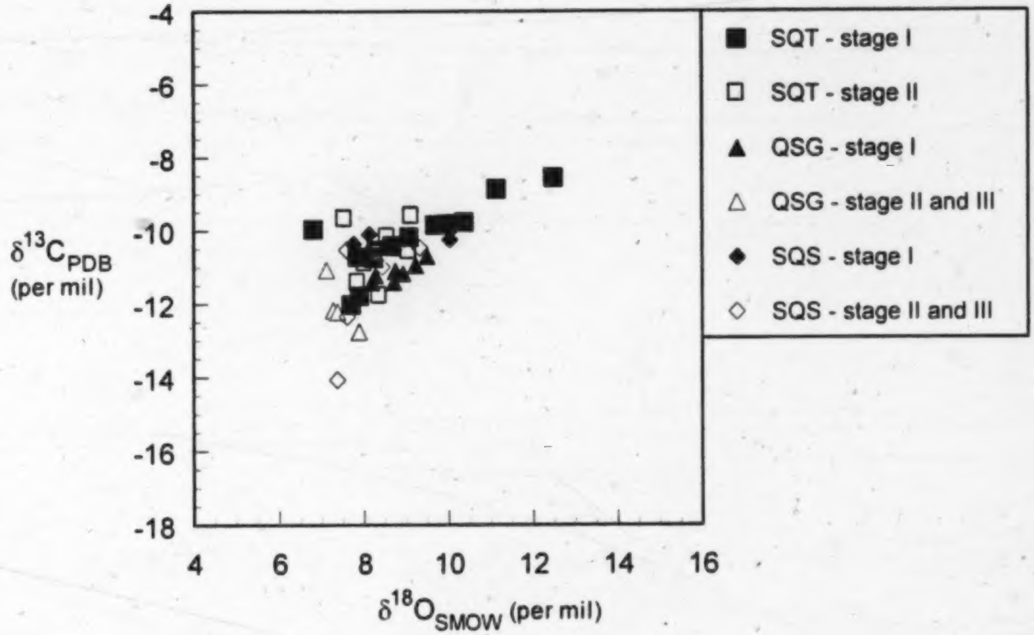

Figure 8.4. Calculated oxygen and carbon isotopic composition of hydrothermal fluids in equilibrium with vein siderite from stages I, II, and III at the SQS, QSG, and SQT veins.

These fluid isotopic values fall within the broader range of previously calculated $\delta^{18}O_{fluid}$, which range from 6.4 to 13.7 ‰ for siderite and from 3.8 to 11.9 ‰ for quartz (Yates and Ripley, 1985; Constantopoulus, 1994; Fleck et al., 1991; Eaton et al., 1995). Estimated average $\delta^{18}O_{fluid}$ of approximately 8.5 and 9.5 ‰ for hydrothermal fluids in SQT veins at the Galena and Sunshine mine (Yates and Ripley, 1985; Fleck et al., 1991; Eaton et al.,1995) are statistically indistinguishable from the average $\delta^{18}O_{fluid}$ of 8.5 ± 1.1‰ determined by Constantopoulus (1994) for quartz samples collected from various Ag-Pb-Zn veins in the district.

Yates and Ripley (1985) and Eaton et al. (1995) calculated average $\delta^{13}C_{fluid}$ values of approximately -5 and -6 ‰ for hydrothermal fluids in equilibrium with vein siderite from SQT veins at the Galena and Sunshine mines using the fractionation equation for $\Delta_{CALCITE\text{-}CO2}$ of Bottinga et al. (1968). This equation, however, may not be accurate when used for siderite. For this reason the experimentally derived equation for $\Delta_{SIDERITE\text{-}CO2}$ of Carothers at al. (1988) was favored in this study. Calculated $\delta^{13}C_{fluid}$ values for fluids in equilibrium with stage I, II, and III siderite at the different veins are significantly lower to those determined by Yates and Ripley (1985) and Eaton et al. (1995), and vary from -8.5 to -14.0 ‰ , average -10.7 ± 2.1 ‰.

The calculated oxygen and carbon fluid stable isotopic compositions are plotted on Fig. 8.4. Although the dispersion on the plot is less than that exhibited by the original siderite values the distribution of $\delta^{18}O_{fluid}$ and $\delta^{13}C_{fluid}$ values still outline trends similar to those discussed above.

The estimated average $\delta^{18}O_{fluid}$ for siderite from the alteration envelope at the Sunshine, Lucky Friday, and Gold hunter mines is 1.5 ‰ lower to that of stage I siderite at the respective mines (Table 8.2). The negative $\delta^{18}O_{fluid}$ values were expected, however, because Eaton et al. (1995) reported 1 to 3 ‰ ^{18}O enrichment in the silicate rocks close to the vein walls at the Sunshine mine, which resulted from fluid/rock interaction during the emplacement of the SQT veins. Although the stable isotopic composition of the metasedimenary hosts at the Lucky Friday and Gold Hunter mines is not known, the isotopic composition of alteration siderite indicates that similar oxygen isotopic exchange also took place at the QSG and SQS veins.

Using the equations in Ohmoto and Rye (1979), calculated $\delta^{34}S_{\Sigma S}$ of hydrothermal fluids from the Coeur d'Alene district varies from 1.4 to 7.4 ‰ (average 4.4 ± 1.6 ‰; n = 15). The sulphur isotopic composition of fluids in equilibrium with tetrahedrite could not be calculated due to the lack of data on the tetrahedrite - H_2S sulphur isotopic fractionation. Field and Moore (1971), however, demonstrated that tetrahedrite from Pb-Zn-Ag veins at Bingham is depleted in ^{34}S relative to coexisting sphalerite and enriched relative to coexisting galena. Therefore, the sulphur isotopic composition of hydrothermal fluids in equilibrium with tetrahedrite will be similar to that calculated for fluids in equilibrium with galena and sphalerite.

Origin of Coeur d'Alene Ag-Pb-Zn hydrothermal fluids

Source of water

The average oxygen fluid composition of 8.3 ± 2.4 ‰ determined in this study is consistent with a fluid in isotopic equilibrium with magmatic and metamorphic rocks at 250° to 350°C (Sheppard, 1986). The uniformity of the calculated $\delta^{18}O_{fluid}$ for Coeur d'Alene Ag-Pb-Zn veins is similar to mesothermal Au-quartz vein deposits which often exhibit regional oxygen isotopic homogeneity (Kerrich 1989). This homogeneity is attributed to fluid derivation from metamorphic devolatilization reactions (Kerrich and Fyfe, 1981; Jia and Kerrich, 1999). However, crustal fluids that undergo extensive isotopic evolution at high temperatures (300 to 350°C) and low fluid to rock ratios may also acquire similar homogeneous high $\delta^{18}O$ values (Sheppard, 1986; Nesbitt and Muehlenbachs, 1989; Wickham et al., 1993).

Constantopoulus and Larson (1991) reported a wide range of δD values (–18 to –108 per mil) from inclusion fluids in vein quartz from SQS veins at the Star Morning mine. Yates and Ripley (1985) determined an average δD value of -

144% from vein quartz in SQT veins at the Galena mine. In addition, Fluet et al. (1987) demonstrated that inclusion fluids from quartz at the similar Zn-Pb-Ag veins of the Deer Trail mine in northeastern Washington, some 150 km to the west of Coeur d'Alene district, contain with δD values which range from -89 to -143 per mil. Constantopoulus and Larson (1991) attributed the δD range at the Star Morning to mixing of fluids of metamorphic and meteoric origin. Eaton et al. (1995) argued that the δD range is also consistent with contributions of fluid of formation water origin. Yates and Ripley (1985) and Fluet et al. (1987) however, argued that hydrothermal fluids at the Galena and Deer Trail mines, respectively, were entirely of ground water origin.

Although involvement of fluids of magmatic origin in the silver and base metal veins at the district was not entirely ruled out (Constantopoulus, 1994), Leach et al. (1988) and Constantopoulus and Larson (1991) argued that the lack of apparent vertical and lateral zoning in the fluid inclusion and stable isotope systematics of the Ag-Pb-Zn veins over an area of several thousands square kilometers can not be consistent with magmatic fluid origin. The lack of typical hypersaline fluid inclusions also does not support magmatic fluid involvement. In addition, Eaton et al. (1995) argued that the ^{87}Sr/^{86}Sr ratios of vein siderite from SQT veins at the Sunshine mine are highly radiogenic (e.g. ^{87}Sr/^{86}Sr = 0.9 to 1.01) and are not compatible with a magmatic source. In a later study Criss and Eaton (1999) argued that 9 more mines in the district contain vein siderite with ^{87}Sr/^{86}Sr higher than 0.8. In contrast, the ^{87}Sr/^{86}Sr of various igneous rocks in the area varies from 0.703 to 0.720 (Criss and Fleck, 1987), and the ^{87}Sr/^{86}Sr of all fluids of suggested magmatic origin are supposed to lie within this range.

Another evidence against the involvement of magmatic fluids in the Coeur d'Alene veins is the discordant age of the SQT veins and the magmatic rocks. According to Leach et al. (1998) the SQT veins formed between 86 and 64 Ma, whereas monzonite is ~134 m. y. old. Geochronological constraints, e.g., the lack of intrusive rocks of Late Proterozoic age, also appear to rule out a magmatic contribution to the mineralizing fluids at the QSG and SQS veins.

Thus, on the basis of the available $\delta^{18}O$ and δD data hydrothermal fluids at Coeur d'Alene most likely comprise a mixture of predominantly metamorphic and highly evolved crustal fluids of ultimate meteoric and/or formation water origin.

Source of carbon

Calculated $\delta^{13}C_{fluid}$ values for the hydrothermal fluids in the district (–8.5 to –14.0 ‰) lie outside the composition range of fluids derived from dissolution of marine carbonates (–8 to +4 ‰; Ohmoto and Rye, 1979), and require a significant contribution of carbon from an organic source. According to the fractionation equation of Bottinga (1968) a hydrothermal fluid with an average $\delta^{13}C$ of –11 ‰ is in equilibrium with organic matter with carbon isotopic composition of approximately -24 ‰ over the temperature range 250° to 300°C. This value lies between the average values of terrestrial and marine organic carbon, respectively (e.g., -26 and -22 ‰; Ohmoto, 1986). Carbonaceous matter is a common constituent of the unaltered metasedimentary rocks in the district, but is conspicuously missing from the altered zones near the vein walls (Fryklund, 1964), which indicates that carbon was mobilized by the hydrothermal fluids. In a recent study Lyons et al. (2000) demonstrated that the unmetamorphosed equivalent of Prichard argillite in the eastern and north-eastern parts of the Belt basin contains up to 4 wt. % organic carbon. Therefore, the low $\delta^{13}C$ of hydrothermal fluids in the Coeur d'Alene district is largely derived from a ^{13}C-depleted organic carbon reservoir in the host metasediments. The range of calculated $\delta^{13}C_{fluid}$ values (–8.5 to –14.0 ‰) may indicate that part of the carbon was derived from carbonate-rich horizons in the Belt metasediments.

Source of Sulphur

Previous studies suggested sulphur sources ranging from magmatic contribution (Fryklund, 1964) to leaching of syngenetic sulphides from the lower Belt strata (Yates and Ripley, 1985; White, 1998). The calculated average $\delta^{34}S_{\Sigma S}$ value of ~ 4.4 per mil of this study, however, is not diagnostic as the sulphur may be of magmatic, metamorphic, or sedimentary origin (Ohmoto, 1986; Hoefs, 1997).

Due to the insignificant sulphur isotopic fractionation during solution-precipitation sulphides which form as the result of mobilization of preexisting sulphides will have nearly identical $\delta^{34}S$ to that of their precursors (Ohmoto, 1986). The sulphur isotopic composition of disseminated sulphides in the Coeur d'Alene district is not known. However, disseminated framboidal pyrite from the unmetamorphosed equivalets of the Prichard Formation in the eastern and north-eastern parts of the Belt basin exhibits a significantly broader range of $\delta^{34}S$ values (-8.7 to +36.3 ‰; Lyons et al., 2000) than that of vein sulphides in the district (1.1 to 7.2 %). A similar wide range of $\delta^{34}S$ values (-12.1 to +19.7 ‰) exhibits also massive bedded pyrite from the syngenetic Cu-Co Sheep Creek deposit hosted in the lower Belt strata in Montana (Lyons et al., 2000). In contrast, the sulphur isotopic composition of massive pyrrhotite at the large SEDEX Sullivan deposit in British Columbia varies from -5 to +4 per mil and averages near 0 per mil (Campbell et al., 1980). The higher-temperature chalcopyrite mineralization at the Sheep Creek deposit also exhibit $\delta^{34}S$ values which cluster close to 0 per mil (Lyons et al., 2000).

The broad range of isotopic values of disseminated and massive pyrite from the lower Belt strata (-12.1 to 36.3 ‰) is consistent with a dominant seawater source for the sulphur, and with kinetic fractionation effects related to low temperature bacteriogenic origin. The narrower $\delta^{34}S$ range of pyrrhotite at the Sullivan and chalcopyrite at the Sheep Creek could be due to magmatic contributions, although influx of magmatic fluid in these deposits has not been proven (cf. Lyons et al, 2000). In fact, abiotic reduction of marine sulphate would also produce sulphur with similar "magmatic" values (Ohmoto, 1986; Machel et al., 1995). Campbell et al. (1980) also argued that the sulphur isotopic composition of sulphides from the Sullivan deposit reflects high temperature sulphate reduction in an environment similar to that of the sulphide-producing plumes in the Red sea and the Galapagos ridge.

Considering the narrow $\delta^{34}S$ range of sulphides and sulphosalts in the Coeur d'Alene district leaching of disseminated pyrite from the Belt strata can be rejected as a possible sulphur source. Therefore, Coeur d' Alene fluids either acquired their $\delta^{34}S_{\Sigma S}$ by dissolving preexisting sulphides of abiotic or magmatic origin, or gained sulphur directly from a magmatic source. In the absence of definitive evidence for the involvement of magmatic fluids in Coeur d'Alene district, the former hypothesis seems more likely.

Coleman Au-quartz vein fluid source

The calculated average oxygen fluid compositions for the Coleman Au-quartz vein samples ($\delta^{18}O_{fluid}$ 6.8 ± 0.2 ‰) is within the range of that of the silver and base metal veins. There are no δD data available for the Au-quartz veins in the district, and as mentioned above, the oxygen isotopic composition alone is not sufficient to establish fluid origin.

The P-V-T-X properties of the fluids from the Coleman Au-quartz vein are also very similar to that of stage III at the Ag-Pb-Zn veins. Thus, it may be possible that the Au-quartz veins and stage III quartz at the Ag-Pb-Zn veins formed concurrently and had a common fluid source. However, the lack of absolute age dating for the Au-quartz veins precludes speculations about a common fluid origin at this stage.

Synthesis

Conditions of mineral deposition during stage I at the QSG, SQS, and SQT veins

The microthermometric studies demonstrate that stage I inclusion fluids at the SQS and SQT veins exhibit broadly similar P-V-T-X properties. However, lack of fluid inclusion data from stage I at the Lucky Friday main vein does not allow comparison of the fluid properties of the QSG veins. General similarities in the stable isotopic composition of stage I siderite from the three vein types suggests that the P-T conditions of mineral deposition during stage I at the Lucky Friday main vein were not different than those at the SQS and SQT veins.

Despite similarities in the P-V-T-X of inclusion fluids from the SQS and SQT veins petrographic observations, demonstrate important mineralogical and textural differences between the veins (Chapter IV). In contrast to the SQT veins where sulphide deposition in stage I is restricted to minor pyrite and arsenopyrite (i.e. largely uneconomic), the bulk of the Pb-Zn mineralization at the SQS and QSG veins is in fact deposited in stage I.

Petrographic observations also demonstrate that mineral deposition during stage I at the SQS and to a lesser extent QSG veins at the Gold Hunter and Lucky Friday mines is characterized by open space filling textures such as crustification banding and mineral growth zoning (Chapter IV). The open space filling textures at the SQS and QSG veins are consistent with previously reported occurrences of colloform pyrite in several mines in the district including SQS veins in the Star mine where colloform pyrite is partially replaced by sphalerite (Fryklund, 1964). Fryklund (1964) also wrote that colloform pyrite "…was once widespread…and has been mostly obliterated by recrystallization".

Open space filling textures such as crustification banding and mineral growth zoning indicate that vein minerals in the SQS and QSG veins precipitated from hydrothermal solutions with fluctuating chemical composition or at variable P and/or T. Mineral deposition most likely proceeded undisturbed, with little movement along the vein fractures. The open space filling textures also indicate moderate to slow rates of mineral growth (Wiltschko, 1998). In contrast, the dominantly anhedral "bull" or "buck" texture of stage I siderite at the QST veins indicates rapid fracture opening and competitive mineral growth (Wiltschko, 1998). Local siderite banding, similar to the "banded spar" textures in synkinematic siderite veins at the Rhenohercynian thrust belt of Central Europe (Hein, 1993) indicates repetitive shearing during vein filling. Conditions of rapid fracture opening and repetitive shearing are consistent with QST vein formation in a transpressive environment during dip slip with dominant reverse component as suggested by Bond et al. (1991) and Wavra et al. (1994).

In contrast to the SQT veins, most large SQS and QSG vein deposits in the district lie within a wide zone of ductile faulting - the Terror fault zone (Fig. 1.3; Chapter I). The structural geometry and slip line orientation of the veins within the zone are unstudied (Reid, 1995). Therefore, it is possible that differences in the depositional environments during stage I at the SQS, QSG, and SQS veins resulted largely from their different structural orientation with respect to the far-field stress during a single tectonic event. However, it is also possible that the structural position of the SQS and QSG veins within the Terror fault zone reflects the geometry of a different stress field associated with an earlier tectonic event.

The contrasting mineralogy of stage I at the SQS-QSG, and the SQT veins suggests different metal content of the hydrothermal fluids. The moderate to high salinity of stage I fluids at the SQS veins (up to 20 eq. wt. % NaCl) indicate that the base metals were most likely carried by the hydrothermal fluids as $MeCl^o$ or $MeCl_2^-$ complexes. Solubility data indicate that Pb and Zn concentrations of as little as 1 ppm are sufficient for precipitation of economic quantities of galena and sphalerite (Seward and Barnes, 1997). Analyses of inclusion fluids from Pb- and Zn-bearing veins reveal Pb and Zn concentrations of up to 2200 ppm (Roedder, 1979). Thus, stage I fluids at the SQS and QSG veins may have contained from 1 to ~2000 ppm Pb and Zn.

There is no microthermometric evidence for boiling or cooling during stage I at the SQS veins. Mineral deposition due to wall rock reactions is also unlikely because of the relatively nonreactive nature of the Belt metasediments. Microthermometric data from stage I siderite at the SQS veins, however, exhibit a negative correlation between fluid temperature and salinity indicative of fluid mixing (Fig. 5.6; Chapter V). Henley (1985) demonstrated that a 5 wt. % decrease in the NaCl content of a hydrothermal fluid (which is similar to that observed at the SQS veins) would decrease the Pb and Zn solubilities by ~4 log units. Thus, the deposition of base metal sulphides in the SQS and possibly the QSG veins most likely resulted from mixing of a cool and relatively oxidized (?) metalliferous brine with a warmer reduced (?) H_2S-rich fluid. Galena and sphalerite deposition most likely proceeded according to the reaction:

$$MeCl_n^{2-n} + H_2S_{(aq.)} = MeS_{(s)} + 2H^+ + nCl^- \quad \text{(Seward and Barnes, 1997)}$$

Fluid mixing has previously been invoked to explain ore deposition in Coeur d'Alene district. For example Leach et al. (1988) suggested that mixing of metamorphic fluid with local formation waters was the mechanism for precipitation of vein sulphides in the district. Thiereault (1989) also suggested mixing of reduced CH_4 bearing fluids of local origin with more oxidized external (?) fluids at the Pb-Ag Atlas mine. In addition, Constantopoulus (1994) concluded that only fluid mixing could have created the observed small scale oxygen stable isotope variance of vein quartz at the SQS Morning-Star vein.

The lack of base metal sulphides in stage I at the SQT veins indicates that in contrast to stage I fluids at the SQS and QSG veins, stage I hydrothermal fluids at the SQT veins contained very little or no Pb and/or Zn, or the P-T conditions were not favorable for galena and sphalerite deposition. Therefore, stage I hydrothermal fluids at the SQS, QSG, and SQT veins either followed different flow paths which resulted in selective metal enrichment or had different origin despite the general P-V-T-X similarities.

Silver mineralization

Stage II at the SQT veins has a very important economic significance. During this stage silver-rich tetrahedrite, which is the main source of silver in the Coeur d'Alene district, was deposited in the SQT veins. Petrographic evidence indicates that some tetrahedrite was also deposited at the SQS and QSG veins in stage II.

Most studies agree that tetrahedrite precipitation at the SQT mines follows that of siderite (Harris et al., 1981; Bond et al., 1991; Reid, 1995). Petrographic observations indicate that stage I siderite, pyrite, and arsenopyrite at the SQT veins were sheared and brecciated prior to the deposition of silver-rich tetrahedrite (Bond et al., 1991; Chapter IV). Harris et al. (1981) reported isotopic evidence in support of a late tetrahedrite deposition from hydrothermal fluids with district metal and sulphur isotopic composition at the Sunshine mine. Eaton et al. (1995), however, argued that tetrahedrite deposition at the Sunshine mine was intimately associated with that of massive siderite.

This study demonstrates subtle but systematic differences in the P-V-T-X properties and the stable isotopic compositions of stage I and II fluids at the SQS Sunshine vein. Although fluid pressure during stages I and II falls within the same range (~1 kb), stage II fluids exhibit slightly lower average salinities (e.g., stage I: 12.6 ± 2.1 eq. wt. % NaCl; stage II: ~10.6 ± 2.3 eq. wt. % NaCl). Microthermometric data and independent thermometry also indicate that stage II fluids were warmer (~325ºC) than stage I fluids (~270ºC). In addition, stage I pyrite at the Sunshine mine is systematically depleted of ^{34}S relative to tetrahedrite, although empirical observations indicate that if the two minerals were deposited from the same fluid tetrahedrite must be depleted of ^{34}S relative to pyrite (cf. Harris et al., 1981). Thermodynamic calculations predict that, a sulphur fugacity (fS_2) of at least -10 log units is necessary to stabilize tetrahedrite (Craig and Barton, 1979). Therefore, absence of tetrahedrite from stage I at the Sunshine mine indicates that either stage I fluids had a low sulphur content, or that the they simply did not contain sufficient amounts of silver, copper, and antimony.

The low total volatile content (e.g. $X_{CO2} < 0.04$) and moderate salinities of stage II fluids at the SQT veins suggests that Ag, Cu, and Sb were transported as chloride complexes (Seward and Barnes, 1997; Obolenskiy et al., 1999). The lack of fluid inclusion evidence for boiling during stage II suggests that tetrahedrite precipitation was not related to this process. The nearly vertical spread of microthermometric data from stage II siderite and quartz at the Sunshine vein (Chapter V, Fig. 5.2) could be attributed to temperature and/or pressure fluctuation, or to mixing of fluids with different temperature and similar or only slightly different salinities. Alternatively the trend may be produced by post-depositional stretching of the fluid inclusions. The lack of similar trend for stage I inclusions however, suggests that stretching was not important.

Pressure fluctuations would have no significant effect on sulphide solubilities (Seward and Barnes, 1997). In contrast, a decrease of the fluid temperature or fluid mixing would destabilize metal-chloride complexes and would cause tetrahedrite precipitation. However. the relatively uniform oxygen stable isotopic compositions of stage II siderite and quartz from the SQT veins, are not in favor of either of the two processes. Thus, on the basis of the available fluid inclusion and stable isotopic data it is hard to determine what caused tetrahedrite precipitation at the SQT veins.

As mentioned above the similar P-V-T-X properties and stable isotopic composition of stage II fluids from the different veins suggest a common origin. Thus, it is possible that the elevated silver content of the QSG and/or SQS veins at the Lucky Friday and Gold Hunter mines is related to the introduction of silver, copper, and antimony-rich fluids in stage II.

Petrographic observations demonstrate that common ore and gangue minerals were deposited in stage II at the SQT, SQS, and QSG veins (Chapter . Those include quartz, siderite ± ankerite, sphalerite, galena, pyrite, chalcopyrite, tetrahedrite ± arsenopyrite ± meneghinite ± boulangerite. Textural evidence suggests that brecciation of stage I vein minerals precedes the deposition of stages II minerals in all silver and base metal veins studied. However, petrographic observations also indicate that the amount of stage II minerals at the individual veins varies significantly. For example, tetrahedrite deposited during stage II at the QST veins may locally reach 30 vol. % whereas the amount of all stage II minerals at the SQS veins is only 5 to 10 vol.%. Due to intense shearing it is impossible to determine the relative amount of stage II minerals at the QSG veins.

It is possible that differences in the distribution of stage II vein minerals was controlled by the structural orientation of the veins in the district. Structural studies demonstrate that the SQT veins were formed during dip slip along a line defined by slickenfiber and grooving in the host metasedimentary rocks (Bond et al., 1991; Wavra et al., 1994). The long axes of the tetrahedrite ore shoots parallel the direction of the same slip line (Bond et al., 1991). Therefore, both the siderite veins and the tetrahedrite ore shoots were formed in a stress field of a similar orientation. However, the SQS and QSG veins have different structural geometry (Reid, 1995). The unfavorable orientation of these veins relative to the stress field during stage II could have prevented significant vein dilation and resulted in the absence of appreciable stage II mineralization.

Petrographic data also show that remobilization of stage I sulphides at the SQS and QSG veins was a common process. Evidence for remobilization is the deposition of light colored presumably Fe-poor sphalerite along with siderite II in fractures within stage I minerals at the SQS veins (Chapter IV). Cook and Spry (1999) argued that late Fe-poor sphalerite in metamorphosed ore deposits often forms as a result of dissolution and reprecipitation from Fe-poor hydrothermal fluids. The sharp sinuous contacts between sections of coarse grained and fine grained galena at the QSG Lucky Friday main vein, which are not consistent with shearing and deformation, also indicate that significant amounts of galena may have been remobilized during stage II at the QSG veins (Plate 6a; Chapter IV). Therefore, it is possible that some stage II silver-rich tetrahedrite at the QSG was formed as a result of local redistribution of Ag, Cu, and Sb.

Late stage CO_2-rich fluids and subhorizontal quartz veins

Leach and Hofstra (1983), Hofstra et al. (1985), and Leach et al. (1988) suggested that intermediate-CO_2 fluid inclusions with gas contents from 10 to 15 mol % and salinities from 5 to 10 eq. wt. % NaCl reflect the composition of the hydrothermal fluids responsible for the Ag-Pb-Zn mineralization in the Coeur d'Alene district. However, petrographic and microthermometric data of this study demonstrate that intermediate-CO_2 and CO_2-rich fluid inclusions are confined mostly to unmineralized late stage (stage III) quartz at the silver- and base metal-rich veins (Chapter IV). The ductile behavior of galena possibly precluded opening of brittle fractures, which explains why flat veins are absent at the QSG veins. Instead, stage III quartz at the Lucky Friday main vein fills irregular voids within stage I and II quartz and siderite

In contrast to the well studied subhorizontal quartz veins at the mesothermal Au-quartz deposit Sigma mine, Quebec (Robert et al., 1983; Matthai and Garofalo, 1999), the flat veins at the Coeur d' Alene district lack mutual crosscutting relationships with the mineralized subvertical veins. In addition, Coeur d'Alene flat veins are generally barren, whereas subhorizontal veins at the Sigma mine often contain economic Au-mineralization (Robert et al., 1983). This indicates that the subhorizontal veins in the Coeur d' Alene formed after the main mineralization stages at the silver- and lead-zinc-rich veins.

Microthermometric data demonstrate that the sub-horizontal quartz veins were deposited from relatively hot, dilute $CO_2(CH_4\text{-}N_2)$-rich fluid under higher pressure (1.3 to 2.4 kb) than the saline, CO_2-undersaturated stage I and II fluids (1.0 to 1.4 kb). According to Sibson et al. (1988) higher fluid pressures are expected to be associated with the formation of flat veins because the veins comprise hydraulic fractures created by fluid pressures in excess of the lithostatic load. However, Matthai and Garofalo (1999) argued that the development of subhorizontal fractures is not controlled by the fluid pressure but by the magnitude of the displacement gradients along the associated subvertical shears. Therefore, a mechanical control as opposed to high fluid pressure could have also played a major role in the formation of the subhorizontal veins in the

Coeur d'Alene district. Matthai and Garofalo (1999) agree, however, that for permeability reasons supralithostatic fluid pressures will be common in those subhorizontal veins located near the tips of the subvertical vein fracures. Therefore, it is possible that the formation of flat veins in Coeur d'Alene reflects episodes of movement along the vein fractures associated with supralithostatic fluid pressures which occurred after the end of the main mineralization stages at the individual silver- and lead-zinc- rich veins. Such high pressure episodes could be related to suhorizontal shortening and trusting which according to White (1978) and Harrison and Cressman (1993) continued in the Belt basin until early to mid Tertiary. The observation that mineralized veins in Coeur d'Alene district are locally cut by thrust faults may also support this suggestion (White, 1999).

Coleman Au-quartz vein

The high volatile content and low salinity of the hydrothermal fluids at the Coleman Au-quartz vein favor gold transportation in the form of a bisulphide complex (Wood, 1987; Seward and Barnes, 1997). The narrow range of fluid temperatures, and lack of sulphides along the vein walls indicate that fluid mixing, cooling, or sulphidation reactions were not associated with the precipitation of sulphides and gold at the Coleman Au-quartz vein. The presence of coexisting type 3 intermediate-X_{CO2} and type 4 high-X_{CO2} fluid inclusions with overlapping pressure ranges in main stage quartz indicates that gold deposition was triggered by fluid unmixing.

The most widely accepted model for fluid generation in the Au-quartz mesothermal vein genesis is metamorphic devolatilization (Kerrich and Fyfe, 1981; Goldfarb et al., 1989). Recent precise age dating and radiogenic isotope studies demonstrated that mesothermal gold veins in Brusson, Western Alps were formed during tectonic unroofing, from fluids generated by devolatilization reactions in rocks of calcsilicate composition (Pettke et Frei, 1996; Pettke et al., 1999). Nitrogen isotopic signature of phylosilicates from Archean mesothermal Au-quartz vein deposits also supports a metamorphic origin of the mineralization fluid (Jia and Kerrich , 1999). Thus, it is nevertheless possible that the fluids associated with the Coleman Au-quartz vein were generated as a result of metamorphic devolatilization of the Belt metasedimentary rocks.

On the basis of field observations and Pb isotopic data Fryklund (1964) and Leach et al. (1998) suggested that the Au-quartz veins in the district were formed at a later stage than the QSG, SQS, and SQT veins. The contrasting P-V-T-X properties of main stage fluids at the Ag-Pb-Zn veins and the Coleman Au-quartz vein also indicate that the veins were not related. However, as mentioned above the P-V-T-X properties of the stage III fluid inclusions at the Ag-Pb-Zn veins are very similar to those of main stage inclusions at the Coleman Au-quartz vein. Although these similarities may be fortuitous, it may also be possible that the two hydrothermal fluids are related.

Gold mining in Coeur d'Alene historically preceded the silver and base metal production but it has never been an important source of revenue in the district (Hobbs and Fryklund, 1968). Gold has been a common by-product of the Ag-Pb-Zn mining, although mining companies do not publicize gold grades and/or modes of occurrence. However, although it is possible that stage III fluids and main stage fluids at the Coleman Au-vein are related it would be speculative to suggest a common origin in the absence of precise age dating and more field and isotopic evidence.

A model for Ag-Pb-Zn vein formation

This study demonstrates that the SQG, SQS, and SQT veins in the Coeur d'Alene district share more common features than differences. Although there is a significant mineralogical and textural variance between the QSG-SQS, and SQT veins, there are also striking similarities in the P-V-T-X properties and stable isotopic compositions of the vein minerals. Therefore, if the arguments of Leach et al. (1998, 1999) for Late Proterozoic and Late Cretaceous-early Tertiary mineralization events are accepted, an extraordinary sequence of events is required to explain the formation of three different vein types at the same stratigraphic level and at broadly similar P and T conditions. Late Proterozoic mineralization is also inconsistent with the lack of data for a major tectonic event at this time (Harisson and Cressman, 1993). Instead, the similar P-V-T-X and stable isotopic characteristics determined in this study are more consistent with vein formation as a result of a compression and deformation associated with collision between the Walowa Seven Devils island arc terrane and the North American craton which continued from ca. 130 to 50 Ma (Snee et al., 1995). In this scenario the QSG and SQS veins were formed shortly prior to ~134 Ma, which is consistent with the evidence of contact metamorphism associated with the emplacement of the monzonite stocks. The Proterozoic Pb-isotopic signature of the veins could be explained if the source of Pb were not disseminated sulphides within the Belt metasediments but a preexisting massive sulphide deposit similar to the Sullivan deposit. Such a possibility was not dismissed by Silverman et al. (1960) and Zartman and Stacey (1971) who agreed that Phanerozoic mobilization of Pb from a "protore with an anomalously high lead content" would not lead to significant alteration of the primary Pb-isotopic signature. A contamination with more radiogenic lead during the fluid flow through the Belt strata would also be consistent with the observed array of Pb-isotopic data from samples with "Proterozoic" Pb-signature (Zartman and Stacey, 1971).

Field and ^{39}Ar^{40}/Ar data constrained the timing of formation of the SQT veins between ca. 136 and 64 Ma (Zartman and Smith, 1995; Leach et al., 1998). The veins possibly formed from Pb- and Zn-poor metamorphic fluids which acquired Ag and Cu from stratabound copper-silver deposits in the Middle Belt (Bennet and Venkatakrishnan, 1982; Leach, 1998). Hydrothermal fluids associated with the formation of the SQT veins penetrated QSG and SQS veins along fractures and precipitated silver-rich tetrahedrite, which resulted in elevated silver contents in the lead- and zinc-rich veins at the Lucky Friday and Gold Hunter mines. Higher fluid pressures related to the formation of late subhorizontal quartz veins resulted from continuous compression and thrusting prior to the Eocene extension.

The hydrothermal fluids associated with the lead-zinc and silver mineralizations in the district were supplied mainly by protracted metamorphism in the deeper stratigraphic levels in the Belt metasediments. Mineral precipitation resulted from mixing of warmer less saline metamorphic fluids with isotopically evolved colder and more saline metalliferous fluids of probable formation or ground water origin (Fig. 8.5). Fluid mixing is consistent with the microthermometric and stable isotopic results of this study (Chapters V and IV) and also with the highly variable $^{87}Sr/^{86}Sr$ signature of vein siderite at the SQT veins (Eaton et al., 1995; Leach et al., 1999) and with the variable δD values (Constantopoulus and Larson, 1991, and Yates and Ripley, 1985).

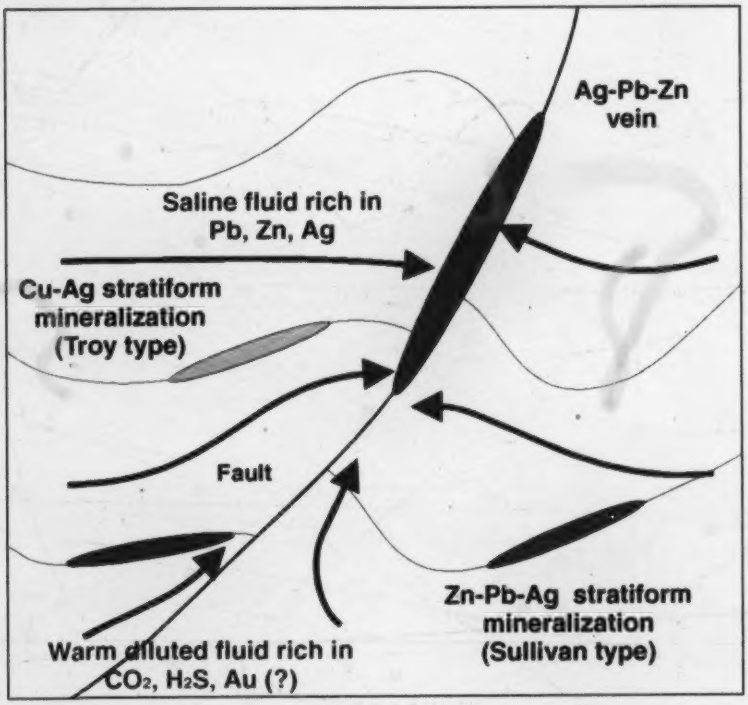
Ag-Pb-Zn vein
Saline fluid rich in Pb, Zn, Ag
Cu-Ag stratiform mineralization (Troy type)
Fault
Zn-Pb-Ag stratiform mineralization (Sullivan type)
Warm diluted fluid rich in CO_2, H_2S, Au (?)

Figure 8.5. A schematic section through a Ag-Pb-Zn vein in the Coeur d'Alene district. Mineral deposition took place in steeply dipping fractures with minor tectonic displacement. Mineralization was triggered by mixing of cooler saline metalliferous fluids of probable formation water origin and warmer CO_2 bearing fluids generated by metamorphic devolatilization. Source of silver and base metals are suggested to be preexisting stratabound Cu-Ag and Pb-Zn-Ag deposits hosted in the Middle and Lower Belt strata, respectively.

Coeur d'Alene and other Ag-Pb-Zn vein deposits

Large Ag-Pb-Zn vein systems are common along the western border of the North American craton (Lynch, 1989). The veins lie along the Omineca Crystalline Belt which formed during the collision between the North American craton and composite allochtonous terranes in Mid Jurassic-Late Cretaceous times. The vein systems are often 25 to 40 km long and the veins contain mostly galena, sphalerite, pyrite, and tetrahedrite in a siderite and quartz gangue (Lynch, 1989). Similar vein systems are also found in the Variscan and Alpine orogens in Europe (Beaudoin and Sangster, 1992; Hein, 1993; Pohl and Belocky, 1999; Seifert, 1999).

Based largely on the Eocene vein and replacement deposits at the Kokanee Range, B. C., and on data from 5 other major Ag-Pb-Zn vein districts including the Coeur d'Alene district, Beaudoin and Sangster (1992) concluded that the silver-lead-zinc veins form a distinct class of mineral deposits. Beaudoin and Sangster (1992) also proposed a general descriptive model for Ag-Pb-Zn vein deposits in metasedimentary terranes and outlined the most important characteristics of the deposits: (1) The Ag-Pb-Zn veins have distinct mineralogy, metal ratios and local phyllitic alteration; (2) the veins are in faults that are commonly associated with deep crustal breaks at terrane boundaries; (3) the veins are hosted by monotonous sequences of clastic rocks deposited in basins within various tectonic settings and which have been intruded by granitic to gabbroic plutonic rocks; (4) the veins occur late in the tectonic evolution of the orogen and in some cases are associated with the extensional collapse of the orogen. (5) The vein minerals were precipitated by mixing and local boiling of different hydrothermal fluids, which may include a deep seated fluid of ultimate metamorphic or magmatic origin, hydrothermal fluid of ultimate meteoric origin that has chemically and isotopically equilibrated with the upper crust, and a fluid dominated by meteoric water; (6) mineralization occurred at temperatures around 250°C to 300°C; (7) sulphur is derived from the local country rocks, whereas carbon is produced by mantle CO_2 degassing, and Pb is mainly derived from local upper crustal rocks, but significant lower crustal or mantle contributions are identified in some groups of deposits. In a later paper, Beaudoin et al. (1999) also suggested that the tectonic setting may be playing a more important role in the origin of Ag-Pb-Zn veins than previously thought. Beaudoin et al. (1999) argued that Ag-Pb-Zn veins would preferably form in extensional settings, whereas compressional environments would favor mesothermal Au-quartz veining.

The results of the present and previous studies indicate that the Ag-Pb-Zn veins in the Coeur d'Alene fit the Beaudoin and Sangster's (1992) descriptive model. However, complicated relationships between individual veins and vein stages including the suggested different ages and origin of the silver and base metal veins in the district (Leach et al., 1998) make it difficult to compare Coeur d'Alene veins to similar deposits worldwide. In addition, although lack of structural data precludes the interpretation of the tectonic regime associated with the formation of the SQS and QSG veins, the siderite-quartz-tetrahedrite veins are clearly of synkinematic origin. The veins occupy steep fractures with mainly reverse slip component which were formed in a transpressional environment (Bond et al., 1991; Wavra et al., 1994; Reid, 1995). Therefore, the SQT veins can not be related to extensional collapse of an orogen as suggested by Beaudoin and Sangster (1992), and Beaudoin (1999). In that sense the SQT veins are more similar to the synkinematic siderite veins in the Rheinische thrust belt (Hein, 1993) and to the Austroalpine syn-orogenic siderite vein and replacement deposits of the Eastern Alps (Pohl and Belocky, 1999). Although these siderite veins and replacement deposits do not contain significant sulphide mineralization they share many common features with the SQT veins at Coeur d'Alene. Fluid inclusion compositions of vein siderite and/or quartz indicate that the veins were deposited from CO_2-undersaturated fluids (X_{CO2} is usually less than 0.04) of variable salinity (5 to 30 eq. wt. % NaCl), at temperatures of 220° to 350°C and pressures from 0.7 to 3.5 kb similar to stages I and II fluids at Coeur d' Alene. Also CO_2-rich (X_{CO2} > 0.04) fluids are associated either with late paragenetic stage minerals (Reinische Massif), or with the formation of distinct veins which clearly postdate main stage metamorphism and deformation (Eastern Alps; Hein, 1993; Pohl and Belocky, 1999). The carbon isotopic signature of vein siderite from these deposits indicates crustal origin with contributions from organic carbon and marine carbonate reservoirs. The main stage fluids are of suggested metamorphic origin (Hein , 1993; Pohl and Belocky, 1999).

Recently Seifert (1999) suggested that late Variscan Zn-Cu-Sn-Pb-Ag veins similar to the Ag-Pb-Zn veins at the Coeur d'Alene (Beaudoin et al., 1999) were formed as a result of the emplacement of HFSE and LILE enriched lamprophyres in the high grade metamorphic rocks in the area of Ertzgebirge. On the basis of Pb and carbon isotopic evidence, Seifert (1999) proposed a genetic model for mantle-induced base metal-bearing hydrothermal deposition associated with lamprophyric magmatism. Although dikes of lamprophyric composition are also found in the Coeur d' Alene district they cut across all major vein types and clearly postdate the Pb-Zn and Ag mineralization (Fryklund, 1964). In addition, undeformed lamprophyric dikes are intruded along the Osburn fault, which indicates that they were formed during or after the Eocene extension which started at ca. 50 Ma.

Conclusions

Three different types of Ag-Pb-Zn veins and a quartz-gold vein in the Coeur d'Alene district were studied by microthermometry, stable isotopes and bulk crush-leach methods. The results of the study are in general agreement with previous studies, but provide new detail for the nature of the hydrothermal fluids at the SQT, SQS, and QSG veins in the district.

Petrographic evidence demonstrates that the SQT, SQS, and QSG veins consist of minerals deposited during at least three separate paragenetic stages. Although stage I at the QSG and SQS veins is characterized by different mineralogy and textural features relative to stage I at the SQT veins the next two paragenetic stages (stage II and III) are associated with the deposition of similar ore and gangue minerals common to all silver and base metal veins studied.

A simultaneous precipitation of siderite, sphalerite, and galena in an open space associated with minor tectonic disturbance is characteristic for the SQS and QSG veins. Microthermometric data and results of the independent thermometry indicate that stage I vein minerals at the SQS veins precipitated from CO_2-undersaturated ($X_{CO2}<0.04$) fluids of moderate to high salinity (11 to 23 eq. wt. % NaCl) at a temperature of ~240°C and pressure of ~1.4 kb. Mineral deposition was triggered by mixing of metal-rich saline cool brines with warmer and less saline fluids.

In contrast, stage I at the SQT veins is largely barren of sulphides and is marked by the precipitation of massive siderite in an environment of rapid fracture opening and synkinematic mineral growth. Stage I siderite, pyrite, and arsenopyrite at the SQT veins were deposited from low-CO_2 fluids of variable apparent salinities (10 to18 eq. wt. %) at approximately 270°C and ~1.0 kb. Mineral deposition probably resulted from mixing of fluids with contrasting salinity and or temperature. Despite similar P-V-T-X properties and stable isotopic compositions stage I fluids at the SQT veins contain very little Pb and/or Zn.

Silver rich tetrahedrite was deposited in the SQT veins soon after the precipitation of stage I minerals from warmer and moderately saline fluids (~325°C; 10.6 ± 1.3 eq. wt. % NaCl). Microthermometric data from the QSG and the SQS veins demonstrate that stage II minerals including tetrahedrite were also deposited from fluids with similar P-V-T-X properties to those of stage II fluids at the SQT veins. In addition, stage II tetrahedrite deposition at the SQS and QSG veins was also preceded by brecciation of early vein minerals. Thus, the unusually high silver content of the SQS and QSG veins at the Gold Hunter and Lucky Friday mines may be due to secondary enrichment with Ag, Cu, and Sb during the formation of the SQT veins in the district. The relatively small volume of stage II minerals deposited in the SQS and QSG veins possibly reflects unfavorable vein orientation relative to the dominant stress field during the silver mineralization. Tetrahedrite precipitation was most likely caused by mixing of fluids with different temperature and similar salinities.

The last stage in all Ag-Pb-Zn veins is marked by the influx of warm (280 to 320°C), $CO_2(N_2, CH_4)$-rich fluids. The stage III fluids precipitated barren subhorizontal quartz veins which crosscut the SQT and SQS veins, and fill small voids in the more ductile QSG veins. The presence of coeval type 3 intermediate-X_{CO2}, and type 4 high-XCO_2 inclusions in stage III quartz in the Ag-Pb-Zn veins and in the main stage quartz at the Au-quartz veins indicates fluid effervescence.

The lack of mutual crosscutting relationships between the stage III subhorizontal quartz veins and the Ag-Pb-Zn veins, and the high fluid pressures calculated for stage III inclusion fluids indicate formation in a transpressional regime after the main mineralization stage at the Pb-Zn- and Ag-rich veins. Crosscutting of the veins by thrust faults suggests that the compression was associated with thrusting which continued in the district until ca. 50 Ma.

The similarities in the fluid inclusion compositions of the Au-quartz Coleman vein and late stage quartz in the Ag-Pb-Zn veins suggest that the fluids may be related, which is supported by the presence of minor amounts of gold in the Ag-Pb-Zn veins. However, more data are needed to prove or to refute such a connection.

In contrast to previous studies (e.g. Leach et al., 1983, 1988) this study demonstrates that Pb-Zn and Ag mineralization at the individual veins in the Coeur d'Alene district is associated with CO_2-poor fluids of moderate to high salinities. It also demonstrates that CO_2-rich fluids were late and most likely unrelated to silver and base metal mineralization.

The oxygen and carbon stable isotopic composition of stage I siderite from the QSG and SQS veins is not only similar to that of the SQT veins, but also plots along a similar positive correlation trend. This trend is best explained by siderite precipitation from a uniform reservoir at variable temperature or more likely by a systematic variance in the temperature and chemical/isotopic composition of the fluids along the vein fractures.

A Π-shaped trend defined by the oxygen and carbon stable isotopic composition of stage I siderite samples collected across the QST Sunshine vein is exactly the opposite to other such trends previously described in the literature (e.g. Eaton et al., 1995). The observed variation could be attributed either to fluid cooling or to gradual fluid evolution/fluid mixing.

Stage II and III siderite and quartz exhibit uniform oxygen isotopic signatures. The carbon isotopic composition of stage II and III siderite is generally lower than that of stage I siderite. Variations in the carbon isotopic composition of stage II and III siderite are most likely associated with siderite precipitation from a finite reservoir and phase separation, respectively, although buffering from different host rock carbon reservoirs is also possible.

The results of the stable isotopic studies reveal a broadly similar oxygen isotopic signature of the hydrothermal fluids at the different Ag-Pb-Zn veins and the Coleman Au-quartz vein which suggests an origin from a common source or more likely a protracted interaction between the fluids and the Belt metasedimentary rocks prior to vein formation. Therefore, a major fluid source for the different Ag-Pb-Zn veins in the district was possibly metamorphic devolatilization related to a regional metamorphic events in Late Cretaceous-early Tertiary. However, published δD data indicate that isotopically evolved fluids of ultimate ground water origin were also involved in the mineralization (Yates and Ripley, 1985; Constantopoulus and Larson, 1991).

The calculated low average carbon isotopic content of hydrothermal fluids from the different Ag-Pb-Zn veins is consistent with carbon derivation from the oxidation of organic matter abundant in the unaltered Belt metasedimentary rocks in the district. The uniform calculated sulphur isotopic content of the fluids indicate that sulphur was most likely derived from leaching of sulphides of abiogenic or magmatic origin, or less likely directly from a magmatic source.

On the basis of similarities in the P-V-T-X properties and stable isotopic compositions of the hydrothermal fluids and published geological and geochronological data an attempt was made to place the formation of the different vein types into a coherent geological model. According to this model the SQS, QSG, and SQT veins in the district were formed as a result of a protracted regional metamorphism of the Belt strata during the Mesozoic. Saline hydrothermal fluids associated with the base metal veins acquired S, Pb, Zn, and/or Ag from preexisting stratabound deposit(s) of Sullivan type. Similar hydrothermal fluids associated with the silver-rich veins mobilized Ag and Cu from stratabound silver copper deposits in the Middle Belt. Microthermometric evidence suggests that late stage (III) fluids in the Ag-Pb-Zn veins and main stage fluids in the Au-quartz veins in the district may be of common metamorphic origin. Mixing of these warm CO_2-rich fluids with colder metalliferous brines most likely triggered vein siderite and Ag-Pb-Zn ore deposition in the vein fractures at Coeur d'Alene. A combination of existing field and geochronologic data suggests that the SQT vein deposition may have postdated the formation of the SQS and QSG veins. Nevertheless, the conditions of mineral deposition at the individual veins did not differ significantly. This model, however, is speculative at best in the absence of precise age dating of the different vein types in the Coeur d'Alene district.

REFERENCES

Aitiken, J.D., and McMechan, M.E., 1992, Middle Proterozoic Assemblages, in Geology of the Cordilleran orogen in Canada: (ed.) Geological Survey of Canada No. 4, 99-124

Anderson, H.E. and Davis D.W., 1995, U-Pb geochronology of the Moyie sills, Purcell Supergroup, SE British Columbia,: Implications for the Mesoproterozoic history of Purcell (Belt) basin: Can. J. of Earth Sci. V.32, p 1180-1193

Audetat, A., and Gunter, D., 1999, Mobility and H_2O loss from fluid inclusions in natural quartz crystals: Contr. Min. Petrology 137, 1-14

Beaudoin, G., and Sangster, D. F., 1992, A descriptive model for silver-lead-zink veins in clastic metasedimentary terranes.: Econ. Geol. 87; 1005-1021

Beaudoin, G., Leach d.,, Hofstra A., Seifert T, and Zak K., 1999, Silver-lead-zinc vein: A descriptive model. In Mineral deposits: Processes to Processing, Proc. V. SGA meeting, London; 923-926

Beaudoin, G., 1997, Proterozoic Pb isotope evolution of the Belt-Purcell basin: Constraints from syngenetic and syndiagenetic suphide deposits: Econ. Geol., 92: 343-350

Becker, R., and Clayton R.N., 1976, Oxygen isotope study of a Precambrian banded iron formation, Hamersley Range, Western Australia: Geochimica Cosmochimica Acta 40, 1153-1165

Bennet, H.E., and Venkatakrishnan R., 1982, A palinspastic reconstruction of the Coeur d'Alene mining district based on ore deposits and structural data: Econ. Geol., vol. 77, 1851-1866

Bijak, M.K, and Norman D,I., 1982, Mineralization of the Bunker Hill mine Coeur d'Alene mining district, Idaho, in the light of fluid inclusion studies: Geol. Soc. of Am. Abstracts with Programs v.14, 443

Bodnar, R.J., and Vityk M.O., 1994, Interpretation of microthermometric data for H2O-NaCl fluid inclusions: in Fluid Inclusions in minerals: Methods and Applications, (ed.) De Vivo and Frezotti, Virginia Tech, Blacksburg, VA, 117-130

Böhlke, J.K., and Kistler, 1986, Rb-Sr, K-Ar, and stable isotope evidence for the ages and sources of fluid components of gold bearing quartz veins in the northern Sierra Nevada foothils metamorphic belt, California: Econ. Geol. 81, 269-322

Boiron, M.C., and Dubessy J., 1994, Determination of fluid inclusion compositions: Microanalytical techniques. In: Fluid Inclusions in minerals: Methods and Applications, (ed.) DeVivo and Frezotti, Virginia Tech, Blacksburg, VA, 45-72

Bond, W.D., Wavra C.S., Cleland, R.W., and Reid R.R., 1992, Nature and genesis of ore shoots at the Sunshine mine, Coeur d'Alene district (abs.): Geological Society of America Abstracts with Programs 24, 4

Botrell, S.H., Yardley B.W.D., and Buckley, F., 1988, A modified crush-leach method for the analysis of fluid inclusion electrolytes: Bull. Mineral. 111, 279-290

Bottinga, Y., 1968, Calculation of fractionation factors for carbon and oxygen exchange in the system calcite-carbon dioxide-water: Journal of Physical Chemistry 72, 4338-4340

Bowers, T.S., 1991, The deposition of gold and other metals: Pressure induced fluid immiscibility and associated stable isotopic signatures: Geochimica et Cosmochimica Acta 55, 2417-2334

Brown, P. and Hagemann S.G., 1994, MacFlinCor: A computer program for fluid inclusion data reduction and manipulation: in: Fluid inclusions in minerals: methods and applications, Virginia Tech, Blackbburg. 231-250

Brown, P. and Lamb W., 1989, P-V-T properties of fluids in the system H_2O-CO_2-NaCl: new graphical presentation and implications for fluid inclusion studies. Geochimica et Cosmochimica Acta 53, 1209-1221

Burwash, R.A., 1993, Overwiew of Belt geochronology and problems dating the Belt/Purcell Supergroup (abs.): Montana Bureau of Mines Special Publication 111.

Caddey, S.W., 1975, Deformational ore structures in the "J" vein at the Bunker Hill mine, Coeur d'Alene mining district, Idaho, and their exploration significance: Geological Society of America Abstracts with Programs, 591

Campbell, F.A., Ethier V.G., and Krouse H.R., 1980, The massive sulphide zone: Sullivan ore Body, British Columbia: Econ. Geol. 75, 916-926

Carothers, W.W., Adami, L.H. and Rosenbauer R.J., 1988, Experimental oxygen isotope fractionation between siderite-water and phosphoric acid liberated CO_2-siderite: Geochimica et Cosmochimica Acta 52, p. 2445-2450

Chistie, A.B., Goguel, R.L., and Robinson, B.W., 1989, Problems of crush-leach analyses of low-salinity inclusion-poor material: Chem. Geol. 78, 35-49

Clayton R.N. and Mayeda T.K., 1963, The use of bromine pentafluoride in the extraction of oxygen from oxides and silicates for isotopic analysis: Geochimica et Cosmochimica Acta 27, 43-52

Collins, P.L.F., 1979, Gas Hydrates in CO2-bearinf fluid inclusions and the use of freezing data for estimation of salinity. Econ. Geol. 74, 1435-1444

Constantopoulus, J.T., 1989, Oxygen and Hydrogen isotopic geochemistry of the Coeur d'Alene Mining district, Idaho (Ph.D. thesis): Moscow, Univerity of Idaho, ID.

Constantopoulus, J.T., and Larson P., 1991, Oxygen and Hydrogen geochemistry of the Star-Morning mine, Coeur d'Alene mining district, Idaho, Geology, 19, 131-134

Constantopoulus J.T., 1994, Oxygen isotopic geochemistry of the Coeur d'Alene mining district, Idaho, Econ. Geol. 89, 944-951

Cook, N.J., and Spry, P.G., 1999, Sulphur isotope characteristics of remobilized ores from Bleikvassli Zn-Pb-(Cu) deposit, Nordland, Norway. in: Mineral deposits: Processes to Processing, Stanley et al. (eds.), Balkema, Roterdam.

Craig, J.R., and Barton, P.B., 1979, Thermochemical approximations for sulphosalts: Econ. Geol. 68, 493-506

Criss, R.E., and Eaton, G., 1999, Evidence for Proterozoic and Late Cretaceous-early Tertiary ore-forming events in the Coeur d'Alene district, Idaho and Montana – a discussion: Econ. Geol., vol. 93, 345-359

Criss, R. E, and Fleck R.J, 1987, Petrogenesis geochronology and hydrothermal systems of the northern Idaho Batholith and adjacent areas based on $^{18}O/^{16}O$; D/H; $^{87}Sr/^{86}Sr$ and $^{40}Ar/^{39}Ar$ studies, USGS Professional Paper 1436, 95-137

Criss, R. E., and Fleck, R.J., 1990, Oxygen isotopic map of the giant metamorphic-hydrothermal system around the Northern part of the Idaho batholith, USA: Applied Geochemistry, Vol. 3, No. 5-6; 641-655

Crosby G., 1959. The Gem stocks and adjacent ore bodies, Coeur d'Alene distrct, Idaho: Mining Engineering, 697-700

Darling, R.S., 1991, An extended equation to calculate NaCl contents from clathrate melting temperatures in H_2O-CO_2-NaCl fluid inclusions: Implications for P-T isochore location: Geochimica et Cosmochimica Acta 55, 3869-3871

De Paoli, G.R., and Pattison D.R., 1995, Constraints on pressure and temperature conditions and fluid compositions during metamorphism of the Sullivan orebody, Kimberly, B.C., from silicate-carbonate equilibria: Can. J. of Earth Sci. 32, 1037-1052

Diamond, L.W., 1990, Fluid inclusion evidence for the P-V-T-X evolution of hydrothermal solutions in late-Alpine gold quartz veins at Brusson, NE Italian Alps: American Journal of Science, v. 209, 912-958.

Doughty, P.T., and Chamberlain K.R., 1996, Salmon River arch revisited: New evidence for 1370 Ma rifting near the end of the deposition of the Middle Proterozoic Belt basin: Can. J. of Earth Sci, 33, 1037-1052

Doughty, P.T., Price R.A., and Parrish R.R., 1998, Geology and U-Pb geochronology of Archean basement and Proterozoic cover in the Priest Riever complex, NW USA, and their implications for Cordilleran structure and Precambrian continental reconstruction: Can. J. Earth Sci. 35, 39-54

Drummond, S.E., 1981, Boiling and mixing of hydrothermal fluids: Chemical effects on mineral precipitation: Unpublished Ph.D. thesis, Pennsilvania State University, 380 p.

Duan, Z., Moller N., and Weare J.H., 1992, An equation of state for the CH_4-CO_2-H_2O system: Mixtures from 50 to 1000°C and O to 1000 bar. Geochimica et Cosmochimica Acta 56, 2619-2631

Eaton, G., Criss, R., Fleck, R., Bond W., Cleland, R. and Wavra, C., 1995, Oxygen, carbon and strontium isotope geochemistry of the Sunshine mine, Coeur d'Alene mining district, Idaho: Econ. Geol., 90, 2274-2286

Eckelman, W.R. and Kulp J.L., 1957, Uranium-lead method for age determination: Geological Society of America Bulletin 68, 1117-1140

Fisher, R.S., and Land, L.S., 1986, Diagenetic history of Eocene Wicox sandstones, south-central Texas: Geochimica et Cosmochimica Acta 50, 551-561

Fleck, R., Criss, R., Eaton G., Wavra, C., and Bond W., 1991, Strontium and oxygen isotopic characteristics and the age of siderite-tetrahedrite veins in the Sunshine mine, Coeur d'Alene district, Idaho (abs.): Geological Society of America Abstracts with Programs 23, No. 5, A137

Fluet, D.W., 1986, Genesis of the Deer Trail Zn-Pb-Ag Vein deposit, Washington, USA, Unpublished MsC thesis, University of Alberta, Edmonton, Alberta, 129 pages.

Fournier, R.O., and Truesdel, A.H., 1973, An empirical Na-K-Ca geothermometer for natural waters: Geochimica et Cosmochimica Acta 37, 1255-1275

Franck, E.U., 1977, Equilibria in aqueous electrolite systems at high temperatures and pressure, in Phase equilibria and fluid properties in the chemical industry: Washington, D.C., Am. Chem. Soc., Symp. Series 60.

Fryklund, V.C. Jr., 1964, Ore deposits of the Coeur d'Alene district, Shoshone county, Idaho. USGS Prof. Paper 445.

Ghosh, A., 1986, Geochemistry of the Nelson-Rosland area: Unpublished Ph.D. thesis, University of Alberta, AB

Giggenbach, W., 1980, Geothermal gas equilibria: Geochimica et Cosmochimica Acta 44, 2021-2032

Goldfarb, R.J., Snee L.W., Miller, L.D., and Newberry, R.J., 1989, Rapid dewatering of the crust deduced from ages of mesothermal gold deposits: Nature 354, 296-298

Golyshev, S.I.,Padalko N.L., and Pechenekin, S.S., 1981, Fractionation of stable oxygen and carbon isotopes in carbonate systems: Geochemistry International 18, 85-99

Harris, R.H., Lange I., and Krouse R., 1981, Major element and sulphur isotopic variation in the lower Chester vein, Sunshine mine Idaho: Econ. Geol. 76, 706-715

Harrison, J.E. and Cressman E.R., 1993, Geology of the Libby thrust belt of northwestern Montana and its implications to regional tectonics: USGS Prof. Paper 1524

Harrison, J.E., 1972, Precambrian Belt bassin of northwestern United States: Its Geometry and copper occurrences: Geol. Soc. of America Bulletin 83, 1215-1240

Harrison, J.E. 1993, Preliminary geologic section to basement from Chewlah, Washington, to Glacier National Park, Montana, Belt Symposium III, Abstracts, Montana Bureau of Mines and Geology, 26-27

Haynes, T.S. and Einaudi M.T., 1986, Genesis of Spar Lake Stratabound copper-silver deposit, Montana Part I: Econ. Geol. 81, 1899-1931

Hedenquist, J.W. and Henley, 1985a, The importance of CO_2 on freezing point measurements of fluid inclusion: Evidence from active geothermal systems and implications for epithermal ore deposition, Econ. Geol. 80, 1379-1406

Hein, U., 1993, Synmetamorphic Variscan siderite mineralization of the Reinische massif, Central Europe: Mineral. Magazin 57, 457-465

Henley, R.W., 1985, The geothermal framework of epithermal deposits: In: Geology and geochemistry of epithermal systems. Berger, B.R., (editor); Bethke, P.M., (editor) Reviews in Economic Geology. 2, 1-24.

Hershey, O.H., 1916, Origin and distribution of ore in Coeur d'Alene: Mining and scientific press, San Francisco, CA.

Hobbs, S.W., and Fryklund V.C., 1968, The Coeur d'Alene district, Idaho: In ore deposits of the United States, vol. 2, American Institute of Mining Engineers, NY, 1417-1435

Hobbs, S.W., 1965, Geology of the Coeur d'Alene district, Shoshone county, Idaho: USGS Prof. Paper 478

Hoefs, J., 1997, Stable isotope geochemistry - 4th edition, Springer

Hoffman, P.F., 1989, Precambrian geology and tectonic history of North America: in The geology of the North America – an overview, vol. A, Geological Society of America, 447-513

Hofstra A.H., Landis G.P. and Leach D.L., 1985, Volatile evolution of ore fluids in Coeur d'Alene veins during metamorphism of the Belt basin: Geol. Soc. of Am. Abstracts with Programs, v.17., 612

Hollister, L.S., 1990, Enrichment of CO_2 in fluid inclusions in quartz by removal of H_2O during crystal-plastic deformation: J. Struct. Geol. 12, 895-901

Holloway, J.R., 1977, Fugacity and activity of molecular species in supercritical fluids. In: Fraser D.G. (ed.) Thermodynamics in Geolog, Dreidel publ. Co., Boston, 161-181.

Hoy, T., 1989, The age, geochemistry and tectonic setting of the Middle Proterozoic Moyie sills, Purcell Supergroup, SE British.Columbia: Can. J. of Earth Sci. 26, 2305-2317

Jia, Y. and Kerrich, R., 1999, Nitrogen isotope systematics of mesothermal lode gold deposits: Metamorphic, granitic, meteoric water, or mantle origin?: Geology 27, 1051-1054

Juras, D.S., 1982, Structure of the Bunker Hill mine, Kellogg, Idaho, in Society of Economic Geologists Annual Field Conference, Wallace, ID, Idaho Bureau of Mines and Geology Bulletin 24, 31-34

Kell, R.E., and Childs, J.F., 1993, Mesozoic-Cenozoic structural events affecting the Belt basin between the Idaho batholith and the Lewis and Clark line-implications on identifying syndepositional Belt-age structures; Belt Symposium III, Abstracts, Montana Bureau of Mineas and Geology, Berg, R, 32-34.

Kerr, P. and Kulp, J., 1952, Precambrian uraninite, Sunshine mine, Idaho: Science 115, 86-88

Kerrich, R., 1989, Geodynamic settings and hydraulic regimes: Shear zone hosted mesothermal gold deposits, in Bursnall, J.T., (ed.), Mineralization and shear zones: Geol. Assoc. of Canada Short Course notes 6, 89-128.

Kerrich, R. and Fyfe. W.S., 1981. The gold-carbomate association: Source of CO_2 and CO_2 fixation reactions in Archaean lode deposits: Chem. Geol., 33, 265-295

Kerrich, R., 1987, The stable isotope geochemistry of Au-Ag deposits in metamorphic rocks. In Stable isotopic Geochemistry of Low temperature Fluids (ed. T. Kyser): Mineral Association of Canada Short Course 13, 287-336

Kerrich, R., 1990, Carbon-isotope systematics of Archean Au-Ag vein deposits in the Superior Province: Can J. Earth Sci. 27, 40-50

Kharaka, Y.K., and Mariner, R.H., 1992,Chemical geothermometers and their application to formation waters from sedimentary basins: In Thermal history of sedimentary basisns (ed. N.D. Naeser and T. McCulloch), Springer-Verlag, 99-117

Kirschner, D.L., Sharp, Z.D., Teysierr, C., 1993, Vein growth mechenisms and fluid sources revealed by oxygen isotope laser microprobe: Geology 21, 85-88

Kirby, J., McCaig, A., and Sharp, Z., 1997, Fluctuating fluid compositions in syntectonic carbonate veins from the Pyrinees: SEM and in situ laser isotope studies: (abs.) in Geofluids II, Belfast, N. Ireland, 327-330

Kronnenberg, A.K., 1984, Carbon and oxygen diffusion in calcite: effects on Mn content and pH_2O: Phys. Chem. Minerals 11, 101-112

Landis, G., and Hofstra, A.H., 1991, Fluid chemistry as a potential mineral exploration tool, case studies from Creede,CO, Jerrit Canyon, NV, Coeur d'Alene, ID and MT, southern Alasca mesothermal veins, and continental MTV's: Journal of Geochemical Exploration, 42 1, 25-59

Lange, I.M., 1992, Coeur d'Alene Mineral Belt, silver-base metal and greenstone-hosted gold deposits: formation by a similar process?: Geological Society of America Abstracts with programs 23, No.10983

Leach, D.L., and Hofstra, A.H., 1983, Fluid inclusion studies in the Coeur d'Alene district, Idaho: Geol. Soc. Am. Abstracts with Programs, v. 15, 327

Leach, D.L., Landis G.P., and Hofstra A.H., 1988, Metamorphic origin of the Coeur d'Alene base- and precious-metal veins in the Belt basin, Idaho and Montana: Geology, vol. 16, 122-125

Leach, D.L ., Hofstra A.H., Church S.E; Snee. L.W., Vaughn R.B. and Zartman R.E., 1998, Evidence for Proterozoic and Late Cretaceous-early Tertiary ore-forming events in the Coeur d'Alene district, Idaho and Montana, Economic Geology, vol. 93, 345-359

Long, A. Silverman, A., and Kulp, J.L., 1959, Precambrina mineralization of the Coeur d'Alene District, Idaho: (abs.): Journal of Geophysical Research 64, No.8, 1114-

Lynch, J.V.G, 1989, Large scale hydrothermal zoning reflected in the tetrahedrite-freibergite solid solution, Keno Hill Ag-Pb-Zn district, Yukon: Canadian Mineralogist 27 383-400

Lyons, T.W., Luepke J.J., Schreiber M.E., Zieg G.A., 2000, Sulphur geochemical constraints on Mesoproterozoic restricted marine deposition: lower Belt Supergroup, northern United States; Geochimica and Cosmochimica Acta 64, 427-437

Machel, H., Krouse H., and Sassen R., 1995, Products and distinguishing criteria of bacterial and thermochemical sulfate reduction. Applied. Geochemistry, 10, 373-389

Matsuhisa, Y., Goldsmith J., and Clayton, R.N., 1979, Oxygen isotope fractionation in the system quartz-albite-anorthite-water: Geochimica et Cosmochimica Acta, v.43, p. 1131-1140

Matthai S.K., and Garofalo P., 1999, Three-dimensional shear zone and joint geometry and permeability in the Sigma Gold Mine, Canada. In Mineral deposits: (abs.) in Processes to Processing, Proc. V. S.G.A. meeting, London; vol.1, 1411-1414

Matsuhisa, Y., Morishita, Y., and Sato, T., 1985, Oxygen and Carbon isotope variation in gold-bearing hydrothermal veins in the Kushikino mining area, southern Kyushu, Japan, Econ. Geol. 80, 283-293

McCrea J.M., 1951, On the isotope chemistry of carbonates and a paleomagnetic scale: J. Chem. Phys. 18, 849-857

McDowel F.W., 1971, K-Ar ages of igneous rocks from the western United states: Isochron West 2, 1-16

McKinstry, H.E., and Swendsen, 1942, Control of the ore by structure in a Coeur d'Alene mine: Econ. Geol. 37, 215-230

McMechan, M.E., and Price, R.A., 1982, Superimposed low-grade metamorphism in the Mount Fisher area, SE British Columbia-implications of the East Kootenay orogeny: Can. J. of Earth Sci., 476-489

Metz, M., Brookings, D., Rosenberg, P., and Zartman, R., 1985, Geology and Geochemistry of the Snowbird deposit, Mineral county, Montana: Econ. Geol.: vol. 80. 349-409

Mora, C.I., and Valley, J., 1991, Prograde and retrorgade fluid-rock interaction in calc silicates northwest of the Idaho batholith: stable isotopic evidence: Contr. Min. Pet. 108, 162-174

Mora, C.I., and Valley, J., 1989, Halogen-rich scapolite and biotite: Implications for metamorphic fluid-rock interaction, American Mineralogist 74, 721-737

Mumin, A.H, Fleet, M.E., and Longstafe, F.L., 1996, Evolution of HT fluids in the Ashanti Gold belt, Ghana: Stable isotope geochemistry of carbonates, graphite, and quartz: Econ. Geol., 135-148

Naden, J., and Shepherd, T.J., 1989, Role of methane and carbon dioxide in gold deposition: Nature 342, 135-165

Nesbitt B.E., and Muehlenbachs K., 1989, Geology, geochemistry and genesis of mesothermal lode gold deposits of the Canadian Cordillera: Evidence for ore formation from evolved meteoric water: Econ. Geol. Mon. 6, 553-563

Nicholson K., 1993, Geothermal fluids, Springer-Verlag, Berlin, Heidelberg

O'Neil, J.R,, 1987, Preservation of H, C, and O isotopic ratios in the low temperature environment: Min. Assoc. of Canada Short Course 13, 85-128

Obolenskiy, A.A., Guschina, L.V., and Belogutsev, V.I., 1999, Antimony in HT solutions: Forms of transfer, metal content, and conditions of stibnite depositions: (abs.) In Mineral deposits: (abs.) in Processes to Processing, Proc. V. S.G.A. meeting, London; vol.1, 129-132

Ohmoto, H., and Rye, R.O., 1979, Isotopes of sulphur and carbon, in Barnes, H.L., (ed.), Geochemistry of hydrothermal ore deposits: New York, Willey Interscsi., 509-576

Ohmoto, H., 1986, Stable isotope geochemistry of ore deposits: Reviews Mineralogy 16, 491-599

Pettke, T., Diamond., L., Villa I.M., 1999, Mesothermal gold veins and metamorphic devolatilization in the northwestern Alps: The temporal link: Geology 27, 641-644

Pettke, T., and Frei, R., 1996, Isotope systematics in vein gold from Bruisson, Val d'Ayas (NW Italy). 1. Pb evidence for a Piemonte metaophiolite Au-source: Chem. Geol., v. 135, 173-187

Pohl, W., and Belocky, R., 1999, Metamorphism and metalogeny in the Eastern Alps: Mineralium Deposita 34, 614-629

Ramalingaswamy, V.M, 1976, Stratiform Pb-Zn-Ag deposits and the origin of vein ores, Bunker

Hill mine, Idaho (abs.) Geol. Assoc. of America Abstracts with Programs

Ramboz, C., Pichavant, M., and Weisbrod, A., 1982, Fluid immiscibility in natural processes: useand misuse of fluid inclusion data. II Interpretation of fluid inclusion data in terms of immiscibility: Chem. Geol. 37, 29-48

Ransome, F.L., and Calkins, F.C., 1908, The geology of the ore deposits of the Coeur d'Alene District, Idaho: USGS Professional Paper 62

Reid, R.R., Caddey S.W., and Rankin J.W., 1975, Primary Refraction control of ore shoots with examples from the Coeur d'Alene district, Idaho: Economic Geology 70, 1050-1061

Reid, R.R., 1995, Constriction fracture flow: a mechanism for fault and vein formation in the Coeur d' Alene district, Idaho: Econ. Geol. 90, 81-87

Richards, J.P., and Kerrich, R., 1993, The Porgera Gold mine, Papua New Guinea: magmatic-hydrothermal to epithermal evolution of an alkalic-type precious metal deposit: Econ. Geol. 88, 1017-1052

Richards, J.P., Bray, C.J., Channer, D.M.DeR., and Spooner, E.T.C., 1997, Fluid Chemistry and processes at the Porgera gold deposit, Papua New Guinea: Mineral. Deposita 32, 119-132

Robert, F.A., and Brown., A.C, 1985, Archean gold bearing quartz veins at the Sigma mine, Abitibi Greenstone belt: Part 1. Geological relations and formation of the vein system. Econ. Geol. 81, 578-592

Roedder, E., 1984, Fluid inclusions. Reviews in Mineralogy 12, 644, Mineral Society of America

Rosenbaum, J. and Sheppard S.M.F, 1986, An isotopic study of siderites, dolomites, and ankerites at high temperatures: Geochimica et Cosmochimica Acta 50, 1147-1150.

Rosenberg, P.E., and Larson, P.B., 1996, The age of quartz-carbonate veins associated with the Coeur d'Alene mineralization (abs.): Geol. Soc. of America Abstracts with Programs 26, No.7, A475

Ross, G.M, Parish R., Winston, D., 1992, Provenance and U-Pb geochronology of the Mesoprotherozoic Belt Supergroup (NE United States): Implication for age of deposition and Pre-Panthalassa plate reconstructions: Earth and Planetary Sciences Letters 113, 57-76

Rushton, R.W., Nesbitt, B.E, Muehlenbachs, K., and Mortensen, J.K., 1996, A fluid inclusion and stable isotope study of Au-quartz veins in the Klondike district, Yukon Territory, Canada: A section through a mesothermal vein system: Econ. Geol. 88, 647-678

Rye, D.M., and Williams, N., 1981, Studies of the base metal sulphide deposits at McArthur river, Northern teritory, Australia: III The stable isotope geochemistry of the HYC, Ridge, and Cooley deposits: Econ. Geol. 76, 1-30

Rye, 1966, The carbon, hydrogen, and oxygen signatures of the hydrothermal fluids responsible for the lead-zinc deposits at Providencia, Zacatecas, Mexico: Econ. Geol. 66, 1399-1427

Sears, J.W., 1997, A mechanical map of the North American Cordillera, Mexico to Alaska. Abstracts with Programs - Geological Society of America. 29; 6, 203.

Seifert, T., 1999, Relationship between late Variscan lamprophyres and hydrothermal vein mineralization in the Ertzgebirge: In Mineral deposits: (abs.) in Processes to Processing, Proc. V.S.G.A. meeting, London; vol.1, 429-432

Seward, T., and Barnes H.L, 1997, Metal transport by hydrothermal ore fluids: in Barnes, H.L., (ed.), Geochemistry of hydrothermal ore deposits - third edition: New York, John Willey and sons.

Shenon, P., 1938, Geology and ore deposits near Murray, Idaho: In Idaho Bureau of Mining and Geology Pamphlet, 47, 44p.

Shepherd, T.J., Rankin A.H., and Alderton D.H., 1985, A practical guide to inclusion fluid studies: Glasgow, Blackie Sons. Ltd.

Sheppard, S.M.F., 1986, Characterisation and isotopic variations in natural waters: in Valley J.W, Taylor H., and O'Neil, J.R, (ed.): Stable isotopes in high temperature geological processes. Reviews in Mineralogy, v.16 165-183.

Sibson, R.H., Rober F, and Poulse H., 1988, High angle faults, fluid pressure cycling, and mesothermal gold-quartz deposits: Geology, 16 551-555

Silverman, A., Long, A., and Kulp, J.L., 1960, Age of Coeur d'Alene mineralization: An isotopic study: (Discussion of The Gem stocks and adjacent orebodies, Coeur d'Alene district, Idaho by Crosby, G.M.,): Mining Engineering, 470 – 471

Snee, L.W., Lund K., Sutter J.F., Balcer, D.E. and Evans K.V., 1995, An $^{40}Ar/^{39}Ar$ chronicle of the tectonic development of the Salmon River suture zone, western Idaho: USGS Professional Paper 1438 p. 359-414

Sorenson, A.H., 1972, Age and mode of origin of the Coeur d'Alene ore deposits, Idaho: New York Carleton Press, Inc. 85 p.

Theriault, B.D., 1989, Geology, alteration, and mineralization at the Atlas mine, Coeur d'Alene mining District, Shoshone County, Idaho. Unpublished M.Sc. Thesis, Washington State University, Pullman, WA. p.174

Tibbs, N, 1972, Wall rock geochemistry of the Chester vein, Sunshine mine, Idaho. Unpublished Ph.D. dissertation, University of Missouri 278 p.

Touret, J., 1982, An empirical phase diagram for a part of the N_2-CO_2 system at low temperature: Chemical Geology, 37, 49-58

Umpleby, J.B. and Jones E.L., 1923, Geology and Ore deposits of Shoshone county, Idaho, USGS Bulletin 723, 156

van den Kerkhof A.M., and Thiery R., 1994, Phase transitions and density calculations in the CO_2-CH_4-N_2 system: in Fluid Inclusions in minerals: Methods and Applications, (ed.) De Vivo and Frezotti, Virginia Tech, Blacksburg, VA, 171-190

van den Kerkhof A.M, Touret J.R.L., Maijer C., and Jansen J.B.H., 1991, Retrograde methane dominated fluid inclusions from high-temperature granulites of Rogaland, southwestern Norway. Geochimica et Cosmochimica Acta 55, 2533-2544

van den Kerkhof A.M, 1990, Isochoric phase diagrams in the system CO2-CH_4 and CO2-N_2. Application to fluid inclusions. Geochimica and Cosmochimica Acta 54, 895-901

Vityk, M.O., and Bodnar, R.J., 1998, Statistical microthermometry of synthetic fluid inclusions in quartz during decompression reequilibration: Contr. Min. Petr. 132, 149-162

Wallace, C.A., Lidtke, D.J., and Schmidt, R.G., 1990; Faults of the central part of the Lewis and Clark line, and fragmentation of the Late Cretaceous foreland basin in western Montana, Geol. Soc. Am. Bull. 102, 1021-1037

Wavra, C., Bond W., Reid R., 1994, Evidence from the Sunshine mine for dip slim movement during Coeur d'Alene mineralization, Economic Geology 89, 515- 527

Weiss, P.L., 1961, Bleaching in the Coeur d'Alene district, Idaho: Idaho Bureau of Mines and Geology Bulletin 16, 11

White, B, 1989, Superimposed map-scale folds and subsequent veins unrelated to the Osburn fault strike-sli fault, Coeur d'Alene mining district, Shoshone county, Idaho (abs) Geological Society of America Abstracts with programs 21, 158

White, B, 1998, New tricks for an old elephant: Revising concepts of Coeur d'Alene geology: Mining Engineering, 29-35

Wickham, M.S., Peters M.T., Fricke, H.C., O,Neil, J. R., 1993, Identification of magmatic and meteoric fluid sources and upward- and downward-moving infiltration fronts in a metamorphic core complex., Geology 21, 81-84

Wiltschko, D., 1998, Descriptions of veins bearing on filling mechanisms: in Analysis of veins in low temperature environment - introduction for structural geologists, GSA, Short course, Toronto

Wood, S., 1987, Applications of Multiphase ore mineral solubility experiment to the separation of base metal and gold mineralization in Archean greenstone terrains: Econ. Geol. 82, 1044-1048

Yardley, B.W., Banks, D.A., Botrell., S.H., and Diamond., L.W., 1993, Post-metamorphic gold-quartz veins from NW Italy -the composition and origin of the ore fluid: Mineralogical Magazine 57, p. 407-422.

Yates, M. G. 1987, Geology and geochemistry of the Pb-Ag-Cu deposits in the Galena mine, Coeur d'Alene mining district, Idaho: Unpublished Ph.D. thesis, Bloomington, Indiana, Indiana University

Yates, M.G. and Ripley E.M., 1985, Fluid inclusion and isotopic studies of the Galena Mine, Coeur d'Alene district, Idaho: Geological society of America Abstracts with Programs. V.17, 756

Zartman, R.E., and Smith E., 1995, Mineralogy and U-Th_Pb ages of a uranium bearing jasperoid vein from Sunshine mine, Coeur d'Alene district, Idaho, Leon T. Silver symposium, California Institute of Technology, Pasadena, CA, April 10-11, 37-41

Zartman, R.E., and Stacey, J.S., 1971, Lead isotopes and mineralization ages in Belt Supergroup rocks, northwestern Montana and northern Idaho: Economic Geology, vol. 66, 849-860

Zhang, Y., and Frantz, J.D., 1987, Determination of the homogenization temperatures and densities of supercritical fluids in the system NaCl-KCl-$CaCl_2$-H_2O using syntetic fluid inclusions, Chemical Geology, 64: 335-350

Zheng, Y.F., and Hoefs J., 1993, Carbon and Oxygen Isotopic composition of hydrothermal

Calcites.Theoretical modeling on mixing processes and application to Pb-Zn deposits in the Hartz Mountains, Germany: Mineralium Deposita.28, 79-89

Zheng, Y.F., 1989, Carbon and oxygen isotopic composition of hydrothermal calcite during degassing of CO_2: a quantitative evaluation and application to the Kushikino mining area in Japan, Mineral. Deposita 25, 246-250

APPENDIX I

Fluid inclusion data for the principal occurrences studied.

Vein Type	Host Min.	Stage	Incl. type	Volume % vapour	Tm_{CO2} (C°)	Tm_{ice} (C°)	$Tm_{clath.}$ (C°)	Th_{CO2} (C°) (to liquid)	Th_{total} (C°)	Eq. wt. % NaCl
SQT veins (Sunshine Vein)										
SQT	Sid.	I	2	10		-11			240	15.3
SQT	Sid.	I	2	15		-7			241	10.7
SQT	Sid.	I	2	10		-8			235	12.0
SQT	Sid.	I	2	19		-9.7			243	13.9
SQT	Sid.	I	2	5		-9.1			213.2	13.3
SQT	Sid.	I	2	10		-9.2			235	13.4
SQT	Sid.	I	2	10		-7			237.6	10.7
SQT	Sid.	I	2	10		-9.2			225.6	13.4
SQT	Sid.	I	2	10		-9.2			221	13.4
SQT	Sid.	I	2	15		-6.5			242.3	10.1
SQT	Sid.	I	2	10		-7.5			242.3	11.3
SQT	Sid.	I	2	10		-7.5			244.8	11.3
SQT	Sid.	I	2	10		-7.6			244.8	11.5
SQT	Sid.	I	2	5		-7.7			244.6	11.6
SQT	Sid.	I	2	5		-7.8			247.2	11.8
SQT	Sid.	I	2	5		-7.8			247.2	11.7
SQT	Sid.	I	2	10		-10			229.9	14.3
SQT	Sid.	I	2	5		-7.1			243	10.8
SQT	Sid.	I	2	10		-10.3			246	14.6
SQT	Sid.	I	2	15		-9.1			236	13.3
SQT	Sid.	I	2	10		-10.3			247.2	14.6
SQT	Sid.	I	2	10		-9.3			226.6	13.5
SQT	Sid.	I	2	10		-10.9			230.9	15.2
SQT	Sid.	I	2	20		-8.1			248.1	12.1
SQT	Sid.	I	2	15		-8.5			209	12.5
SQT	Sid.	I	2	10		-7.1			236.9	10.8
SQT	Sid.	I	2	5		-7.5			-	11.3
SQT	Sid.	I	2	10		-8.2			230	12.2
SQT	Sid.	I	2	10		-8			243.1	11.9
SQT	Sid.	I	2	5		-6.7			236.8	10.3
SQT	Sid.	I	2	5		-7.1			230	10.8
SQT	Sid.	I	2	-		-6.6			234.2	10.2
SQT	Sid.	I	2	20		-12.9			226.9	17.1
SQT	Sid.	I	2	5		-12.6			244.5	16.9
SQT	Sid.	I	2	20		-			220.6	-
SQT	Sid.	I	2	5		-11.8			239.4	16.1
SQT	Sid.	I	2	15		-13.3			229.8	17.5
SQT	Sid.	I	2	20		-11.6			248.6	15.9
SQT	Sid.	I	2	10		-7.6			258.6	11.5
SQT	Sid.	I	2	10		-7.6			251.4	11.5
SQT	Sid.	I	2	10		-7.6			253.5	11.5
SQT	Sid.	I	2	-		-7.6			-	11.5
SQT	Sid.	II	2	10		-7.5			-	11.3
SQT	Sid.	II	2	10		-7.5			-	11.3

Appendix I (Continued)

Vein Type	Host Min.	Stage	Incl. type	Volume % vapour	Tm$_{CO_2}$ (C°)	Tm$_{ice}$ (C°)	Tm$_{clath.}$ (C°)	Th$_{CO_2}$ (C°) (to liquid)	*Th$_{total}$* (C°)	Eq. wt. % NaCl
SQT	Sid.	II	2	10		-4.8			-	7.7
SQT	Sid.	II	2	10		-6.6			317	10.2
SQT	Sid.	II	2	30		-6.5			-	10.1
SQT	Sid.	II	2	15		-7.6			285.9	11.5
SQT	Sid.	II	2	10		-8.2			294	12.2
SQT	Sid.	II	2	-		-7.7			269.6	11.6
SQT	Sid.	II	2	10		-6.3			285.9	9.8
SQT	Sid.	II	2	20		-7.5			-	11.3
SQT	Sid.	II	2	10		-7.3			311	11.1
SQT	Sid.	II	2	20		-7.5			-	11.3
SQT	Sid.	II	2	20		-4.6			309	7.4
SQT	Sid.	II	2	10		-6.2			310	9.7
SQT	Qtz.	II	2	20		-7.5			274	11.3
SQT	Qtz.	II	2	-		-6.9			274	10.6
SQT	Qtz.	II	2	-		-7			273	10.7
SQT	Qtz.	II	2	10		-7.7			265	11.6
SQT	Qtz.	II	2	10		-6.5			298	10.1
SQT	Qtz.	II	2	10		-7.8			289	11.7
SQT	Qtz.	II	2	15		-4.1			280	6.8
SQT	Qtz.	II	2	10		-7.7			250	11.9
SQT	Qtz.	II	2	10		-6.9			252	10.9
SQT	Qtz.	II	2	10		-7.1			255	11.1
SQT	Qtz.	II	2	10		-6.7			250	10.6
SQT	Qtz.	II	2	20		-6.5			253	10.3
SQT	Qtz.	II	2	20		-6.1			263	9.8
SQT	Qtz.	II	2	10		-5.2			277	8.1
SQT	Qtz.	II	2	10		-7.9			260	12.2
SQT	Qtz.	II	2	-		-7.8			284	11.5
SQT	Qtz.	II	2	10		-6.8			245	10.8
SQT	Qtz.	II	2	10		-6.8			302	10.8
SQT	Qtz.	II	2	10		-6.8			315	10.8
SQT	Qtz.	II	2	10		-7			313	11.0
SQT	Qtz.	III	3	10	-57.6		10	13.3	-	0.02
SQT	Qtz.	III	3	25	-57.9		10	18.2	329	0.02
SQT	Qtz.	III	3	35	-56.9		9.8	20.8	310	0.42
SQT	Qtz.	III	3	25	-57.2		9.8	21.7	-	0.42
SQT	Qtz.	III	3	40	-56.6		10	16.6	-	0.02
SQT	Qtz.	III	3	25	-56.6		10	17.6	-	0.02
SQT	Qtz.	III	3	30	-57.0		10	17.6	291	0.02
SQT	Qtz.	III	3	25	-57.8		9.8	19.4	245	0.42
SQT	Qtz.	III	3	50	-57.3		10	19	297	0.02
SQT	Qtz.	III	3	25	-57.7		10	20	-	0.02
SQT	Qtz.	III	3	25	-57.5		10	21.1	-	0.02
SQT	Qtz.	III	3	50	-56.6		9.4	22.1	281	1.22
SQT	Qtz.	III	3	45	-56.6		9.9	20.2	283	0.22
SQT	Qtz.	III	3	40	-57.9		9.7	20.9	299	0.63
SQT	Qtz.	III	3	50	-57.3		8.9	25.3	266	2.20
SQT	Qtz.	III	3	20	-58.1		8.9	25	-	2.20
QSG veins (Lucky Friday Main Vein)										
QSG	Sph.	II	2	5		-6.9			276	10.9
QSG	Sph.	II	2	20		-6.6			271	10.5
QSG	Sph.	II	2	10		-6.7			271	10.6

Appendix I (Continued)

Vein Type	Host Min.	Stage	Incl. type	Volume % vapour	Tm_{CO2} (C°)	Tm_{ice} (C°)	$Tm_{clath.}$ (C°)	Th_{CO2} (C°) (to liquid)	Th_{total} (C°)	Eq. wt. % NaCl
QSG	Sph.	II	2	10		-8.8			307	13.3
QSG	Sph.	II	2	15		-8.4			301	12.5
QSG	Sph.	II	2	10		-8.4			263	12.5
QSG	Sph.	II	2	10		-8.5			271	12.6
QSG	Qtz	II	2	10		-8.7			264	12.9
QSG	Qtz	II	2	10		-6.8			250	10.5
QSG	Qtz	II	2	10		-7.4			247	11.3
QSG	Qtz	II	2	10		-7			250	10.8
QSG	Qtz	II	2	10		-5.9			237	9.4
QSG	Qtz	II	2	10		-5.6			223	8.9
QSG	Qtz	II	2	10		-4.9			254	7.9
QSG	Qtz	II	2	10		-6.6			239	10.3
QSG	Qtz	II	2	10		-6.9			245	10.7
QSG	Qtz	II	2	10		-6.8			270	10.6
QSG	Qtz	II	2	5		-9.6			145	14.0
QSG	Qtz	II	2	5		-10			-	14.4
QSG	Qtz	II	2	30		-6.1			234	9.6
QSG	Qtz	II	2	5		-17.6			248	21.4
QSG	Qtz	II	2	25		-4.7			316	7.4
QSG	Qtz	II	2	20		-3.9			263	6.2
QSG	Qtz	II	2	10		-3.8			250	6.3
QSG	Qtz.sec	II	2	10		-3.9			260	6.4
QSG	Qtz.sec	II	2	5		-3.5			226	5.8
QSG	Qtz.sec	II	2	5		-3.8			258	6.2
QSG	Qtz.sec	II	2	5		-3.8			280	6.2
QSG	Sph.sec	II	2	10		-3.9			183	6.4
QSG	Sph.sec	II	2	10		-3.9			252	6.4
QSG	Sph.sec	II	2	10		-3.9			181	6.4
QSG	Sph.sec	II	2	10		-3.9			249	6.4
QSG	Sph.sec	II	2	10		-3.9			184	6.4
QSG	Sph.sec	II	2	10		-3.8			183	6.3
QSG	Sph.sec	II	2	10		-3.8			182	6.3
QSG	Sph.sec	II	2	10		-3.9			183	6.4
QSG	Sph.sec	II	2	10		-3.1			266	5.2
QSG	Qtz.	III	3	25	-58.9		7.4	12.6	274	5.0
QSG	Qtz.	III	3	20	-59.2		7.4	12	281	5.0
QSG	Qtz.	III	3	20	-59.2		7.3	11.5	281	5.2
QSG	Qtz.	III	3	25	-58.6		8.9	11.3	291	2.2
QSG	Qtz.	III	3	30	-58.5		8.9	11.3	291	2.2
QSG	Qtz.	III	3	20	-58.6		8.2	11.3	304	3.5
QSG	Qtz.	III	3	20	-58.5		8.4	11.5	308	3.1
QSG	Qtz.	III	3	20	-58.7		8.7	12.2	291	2.6
QSG	Qtz.	III	3	30	-58.6		8.7	12.2	291	2.6
QSG	Qtz.	III	3	30	-60.9		7.8	-	261	4.6
QSG	Qtz.	III	3	30	-59.5		8.5	12.3	291	3.0
QSG	Qtz.	III	3	30	-59.1		7.5	16.6	281	4.8
QSG	Qtz.	III	3	25	-59.3		6.6	-	-	7.6
QSG	Qtz.	III	3	20	-59.1		6.7	-	-	7.5
QSG	Qtz.	III	3	55	-58.8		6.9	-	-	7.2
QSG	Qtz.	III	3	30	-58.6		8.4	-	320	3.9
QSG	Qtz.	III	3	30	-58.4		6.3	8.7	310	6.9
QSG	Qtz.	III	3	60	-57.5		9.5	16	320	1.0
QSG	Qtz.	III	3	30	-58.4		7.2	12.7	327	5.3

Appendix I (Continued)

Vein Type	Host Min.	Stage	Incl. type	Volume % vapour	Tm$_{CO_2}$ (C°)	Tm$_{ice}$ (C°)	Tm$_{clath.}$ (C°)	Th$_{CO_2}$ (C°) (to liquid)	*Th$_{total}$* (C°)	Eq. wt. % NaCl
QSG	Qtz.	III	3	70	-58.1		8.6	11.9	328	2.8
QSG	Qtz.	III	3	20	-57.8		3.8	15	340	10.8
QSG	Qtz.	III	3	60	-58.9		7.8	12	347	4.3
QSG	Qtz.	III	3	40	-59.4		10	-	309	0.5
QSG	Qtz.	III	3	50	-58.7		8.4	-	350	3.6
QSG	Qtz.	III	3	30	-58.7		8	11.8	318	3.9
QSG	Qtz.	III	3	25	-58.2		8.2	13.5	323	3.5
QSG	Qtz.	III	3	20	-58.1		8.6	13.5	322	2.8
QSG	Qtz.	III	3	40	-59		7.8	10.7	323	4.3
QSG	Qtz.	III	3	30	-57.8		6.8	12.8	333	6.0
QSG	Qtz.	III	3	40	-58.1		7.2	13.2	328	5.3
QSG	Sid.sec	III	3	30	-59.4		9.2	17	275	1.6
QSG	Sid.sec	III	3	20	-58.4		9.5	11.3	275	1.0
QSG	Sid.sec	III	3	35	-57.9		9.2	18.4	289	1.6
QSG	Sid.sec	III	3	20	-57.9		9.2	17.7	274	1.6
QSG	Sid.sec	III	3	15	-58.4		9	17.6	276	2.0
QSG	Sid.sec	III	3	40	-58		9.2	14.4	278	1.6
QSG	Qtz.	III	4	>90	-57.5			9.2		
QSG	Qtz.	III	4	>90	-58.2			4.7		
QSG	Qtz.	III	4	>90	-56.9			12.1		
QSG	Qtz.	III	4	>90	-57.4			11.6		
QSG	Qtz.	III	4	>90	-57.4			9.2		
QSG	Qtz.	III	4	>90	-59.2			-10.7		
QSG	Qtz.	III	4	>90	-58.5			-9.7		
QSG	Qtz.	III	4	>90	-58.5			-3.6		
QSG	Qtz.	III	4	>90	-58			2.1		
QSG	Qtz.	III	4	>90	-58.7			-2.1		
QSG	Qtz.	III	4	>90	-58			0.7		
QSG	Qtz.	III	4	>90	-57.8			2.5		
QSG	Qtz.	III	4	>90	-58.6			-7.4		
QSG	Qtz.	III	4	>90	-59.8			-34.2		
QSG	Qtz.	III	4	>90	-60.1			-41.2		
QSG	Qtz.	III	4	>90	-60.1			-40.5		
QSG	Qtz.	III	4	>90	-59.6			-18.8		
QSG	Qtz.	III	4	>90	-59			-19.4		
QSG	Qtz.	III	4	>90	-58.8			0.4		
SQS veins (Gold Hunter mine)										
SQS	Sid.	I	2	5		-13.9			-	18.2
SQS	Sid.	I	2	10		-20.1			144	22.8
SQS	Sid.	I	2	10		-14.4			202	18.4
SQS	Sid.	I	2	10		-17.1			144	20.6
SQS	Sid.	I	2	5		-7.4			165	11.1
SQS	Sid.	I	2	5		-10.6			187	14.8
SQS	Sid.	I	2	5		-7.5			160	11.3
SQS	Sid.	I	2	5		-10.3			165	14.5
SQS	Sid.	I	2	5		-10.3			160	14.5
SQS	Sid.	I	2	5		-12.1			173	16.3
SQS	Sid.	I	2	5		-10.3			145	14.5
SQS	Sid.	I	2	5		-7.3			203	11.0
SQS	Sid.	I	2	5		-16.1			150	19.8
SQS	Sid.	I	2	5		-15.9			125	19.6
SQS	Sid.	I	2	10		-10.7			184	14.9
SQS	Sid.	I	2	5		-12.2			158	16.4

Appendix I (Continued)

Vein Type	Host Min.	Stage	Incl. type	Volume % vapour	Tm_{CO_2} (C°)	Tm_{ice} (C°)	$Tm_{clath.}$ (C°)	Th_{CO_2} (C°) (to liquid)	Th_{total} (C°)	Eq. wt. % NaCl
SQS	Sid.	I	2	5		-10.9			158	15.1
SQS	Sid.	I	2	5		-16.1			145	19.8
SQS	Sid.	I	2	5		-12.1			158	16.3
SQS	Sid.	I	2	5		-13.7			158	17.8
SQS	Sid.	I	2	10		-17.3			160	20.7
SQS	Sid.	I	2	5		-15.6			160	19.4
SQS	Sid.	II	2	30		-7.9			232	11.7
SQS	Sid.	II	2	10		-7			221	10.6
SQS	Sid.	II	2	10		-8			196	11.9
SQS	Sid.	II	2	10		-8.5			212	12.5
SQS	Sid.	II	2	5		-6.5			250	10.0
SQS	Sid.	II	2	20		-7.7			230	11.5
SQS	Sid.	II	2	20		-7.8			232	11.6
SQS	Sid.	II	2	30		-6.8			257	10.4
SQS	Sid.	II	2	5		-8.6			223	12.6
SQS	Sid.	II	2	5		-7.4			223	11.1
SQS	Sid.	II	2	10		-9			245	13.0
SQS	Qtz.	III	3	30	-56.9		8.3	25.3	247	3.3
SQS	Qtz.	III	3	70	-57.1		8.3	20.7	-	3.3
SQS	Qtz.	III	3	55	-57.1		7.7	21.7	273	4.4
SQS	Qtz.	III	3	70	-57		7.6	21.2	-	4.6
SQS	Qtz.	III	3	35	-56.8		8.4	25	287	3.1
SQS	Qtz.	III	3	70	-57.1		8.5	21.1	-	3.0
SQS	Qtz.	III	3	10	-57		8	22.1	249	3.9
SQS	Qtz.	III	3	10	-57.1		8.2	25.3	278	3.5
SQS	Qtz.	III	3	20	-57.1		8.2	25.5	-	3.5
SQS	Qtz.	III	3	30	-56.8		7.9	25.3	289	4.1
SQS	Qtz.	III	3	50	-57.1		8.2	25.3	289	3.5
SQS	Qtz.	III	3	40	-57.1		7.4	25.2	292	5.0
SQS	Qtz.	III	3	50	-56.8		7.5	25.7	289	4.8
SQS	Qtz.	III	3	80	-56.9		7.3	25.9	-	5.2
SQS	Qtz.	III	3	50	-57.5		7.5	25.1	290	4.8
SQS	Qtz.	III	3	50	-56.8		7.9	25.1	289	4.1
SQS	Qtz.	III	3	40	-56.9		8.3	25.8	281	3.3
SQS	Qtz.	III	3	40	-57.2		8.1	25.8	280	3.7
SQS	Qtz.	III	4	>90	-57.4			12	-	
SQS	Qtz.	III	4	>90	-57.3			13.5	-	
SQS	Qtz.	III	4	>90	-57.3			11.3	-	
SQS	Qtz.	III	4	>90	-57.2			12	-	
SQS	Qtz.	III	4	>90	-56.9			12.1	-	
Coleman Au-quartz vein										
Au-Qtz.	Qtz.	n.a.	3	20	-57.1		9.4	20.8	-	3.0
Au-Qtz.	Qtz.	n.a.	3	50	-57		9.4	22.5	-	3.1
Au-Qtz.	Qtz.	n.a.	3	50	-57.2		9.6	23.2	-	2.2
Au-Qtz.	Qtz.	n.a.	3	45	-57.4		9.7	26.5	-	0.8
Au-Qtz.	Qtz.	n.a.	3	30	-57.3		9.2	26.6	-	3.0
Au-Qtz.	Qtz.	n.a.	3	35	-58.1		8.8	17.3	-	1.6
Au-Qtz.	Qtz.	n.a.	3	30	-57.5		8.6	22.8	-	1.2
Au-Qtz.	Qtz.	n.a.	3	50	-57.7		8.9	23	-	1.2
Au-Qtz.	Qtz.	n.a.	3	30	-57.6		7.4	17.8	-	0.8
Au-Qtz.	Qtz.	n.a.	3	40	-57.6		8.3	14.3	-	0.6

Appendix I (Continued)

Vein Type	Host Min.	Stage	Incl. type	Volume % vapour	Tm_{CO2} (C°)	Tm_{ice} (C°)	$Tm_{clath.}$ (C°)	Th_{CO2} (C°) (to liquid)	*Th_{total}* (C°)	Eq. wt. % NaCl
Au-Qtz.	Qtz.	n.a.	3	25	-57.4		8.4	25.3	-	1.6
Au-Qtz.	Qtz.	n.a.	3	30	-56.6		8.1	24.9	-	2.4
Au-Qtz.	Qtz.	n.a.	3	40	-57.6		9.4	27	-	2.8
Au-Qtz.	Qtz.	n.a.	3	30	-58.4		8.4	26	-	2.2
Au-Qtz.	Qtz.	n.a.	3	10	-56.9		8.6	21.8	-	5.0
Au-Qtz.	Qtz.	n.a.	3	50	-57.4		9.2	17.4	-	3.3
Au-Qtz.	Qtz.	n.a.	3	35	-57.5		9.2	18.8	-	3.1
Au-Qtz.	Qtz.	n.a.	3	60	-57.1		9.2	19.3	-	3.7
Au-Qtz.	Qtz.	n.a.	3	60	-57.6		9	16.9	-	1.2
Au-Qtz.	Qtz.	n.a.	3	60	-56.9		9	19.8	-	3.1
Au-Qtz.	Qtz.	n.a.	3	50	-57.3		9	17.6	-	2.8
Au-Qtz.	Qtz.	n.a.	3	35	-56.9		-	24.5	279.9	1.6
Au-Qtz.	Qtz.	n.a.	3	30	-56.9		9.2	22.8	277.9	1.6
Au-Qtz.	Qtz.	n.a.	3	10	-56.9		9.2	25	264.5	1.6
Au-Qtz.	Qtz.	n.a.	3	20	-57.1		9.2	22.6	261	2.0
Au-Qtz.	Qtz.	n.a.	3	15	-57.3		9.3	20.8	265	2.0
Au-Qtz.	Qtz.	n.a.	3	5	-57.3		9.1	16.9	193.2	2.0
Au-Qtz.	Qtz.	n.a.	3	50	-57		-	20.9	263.1	1.6
Au-Qtz.	Qtz.	n.a.	3	10	-57		-	19.4	278.7	1.6
Au-Qtz.	Qtz.	n.a.	3	35	-56.9		-	23	266	1.6
Au-Qtz.	Qtz.	n.a.	3	-	-57.1			20	255.8	1.4
Au-Qtz.	Qtz.	n.a.	3	30	-57.3			26.1	275	1.8
Au-Qtz.	Qtz.	n.a.	4	>90	-57.1			6.4		
Au-Qtz.	Qtz.	n.a.	4	>90	-57.4			9.2		
Au-Qtz.	Qtz.	n.a.	4	>90	-57.3			14.5		
Au-Qtz.	Qtz.	n.a.	4	>90	-57.2			10.8		
Au-Qtz.	Qtz.	n.a.	4	>90	-57.4			13.7		

APPENDIX II

Stable isotopic composition of siderite and quartz from the silver and base metal veins and also from the Coleman Au-quartz vein.

Sample No.	Mineral	Stage	$\delta^{18}O_{SMOW}$ (per mil)	$\delta^{13}C_{PDB}$ (per mil)
SQT-SUNSHINE MINE				
SSM-4b	Sid.	I	14.94	-7.02
SSM-40	Sid.	I	14.81	-6.94
SSM-41	Sid.	II	13.53	-7.27
SSM-4Q*	Qtz.	II	14.20	
SSM-4h	Sid. Alt.	I	14.12	-7.16
SSM-4m	Sid.	II	13.74	-7.16
SSM-8h	Sid. Alt.	I	14.72	-7.47
SSM-90	Sid.	II	15.20	-6.98
SSM-92	Sid.	I	13.55	-7.42
SSM-10	Sid.	I	14.82	-8.08
SSM-100	Sid.	I	15.17	-6.95
SSM-102	Sid.	II	13.54	-7.32
SSM-10*	Qtz.	II	14.97	
SSM-11	Sid.	I	16.91	-6.39
SSM-110	Sid.	I	17.33	-5.99
SSM-111	Sid.	I	16.07	-6.75
SSM-112	Sid.	I	16.07	-6.33
SSM-130	Sid.	I	16.84	-6.06
SSM-132	Sid.	II	13.51	-7.44
SSM-13	Qtz.	II	14.55	
SSM-14h	Sid. Alt.	I	13.57	-7.41
SSM-15	Sid.	I	15.83	-7.175
SSM-150	Sid.	I	14.86	-8.01
SSM-152	Sid.	II	13.27	-7.63
SSM-9h	Sid. Alt.	I	14.28	-7.26
SQT-COEUR MINE				
COM-1s	Sid.	?	13.25	-9.27
COM-1*	Sid.	?	15.03	
COM-22	Sid.	I	17.69	-5.82
COM-2	Qtz.	II	14.95	
COM-50	Sid.	I	20.21	-4.55
COM-51	Sid.	I	18.86	-4.86
COM-52a	Sid.	I	16.80	-6.17

Appendix II (Continued)

Sample No.	Mineral	Stage	$\delta^{18}O$ SMOW (per mil)	$\delta^{13}C$ PDB (per mil)
ЄCOM-52b	Sid.	I	17.25	-6.36
COM-5 d	Qtz.	II	14.61	
COM-92	Sid.	I	16.40	-6.43
LUCKY FRIDAY MINE				
LF-1h	Sid. Alt.	I	13.19	-7.41
LF-2h	Sid. Alt.	I	14.42	-8.26
LF-3h	Sid. Alt.	I	12.16	-7.29
LF-4h	Sid. Alt.	I	13.85	-7.34
LF-8 hsid	Sid. Alt.	I	13.60	-7.70
LF-7 qtz	Qtz.	II	14.54	
LF-7 sid 1	Sid.	I	16.45	-6.91
LF-7 ank	Ank.	II	12.74	-6.62
LF-10' qtz 2-3	Qtz.	III	13.24	
LF-10' sid 1	Sid.	I	16.35	-7.06
LF-10 sid 1	Sid.	I	16.01	-7.25
LF-10 ank	Ank.	II	14.25	-7.32
LF-10 ank	Ank.	II	14.28	-7.28
LF-11 hsid	Sid. Alt.	I	14.33	-7.36
LF-12 sid 1!	Sid.	I	15.15	-7.63
LF-14 qtz	Qtz.	II	14.09	
LF-14 sid	Sid.	II	12.72	-8.73
LF-15 qtz	Qtz.	II	13.79	
LF-15 sid	Sid.	II	13.27	-9.46
LF-19 qtz	Qtz.	II	14.02	
LF-18 sid	Sid.	I	15.88	-7.38
LF-18 hsid	Sid. Alt.	I	13.85	-7.40
SQS-GOLD HUNTER MINE				
LF 20	Qtz.	III	15.19	
LF-20 s	Sid.	III	13.99	-10.40
LF-20h	Sid. Alt.	I	15.15	-6.85
LF-21 sid	Sid.	I	16.27	-6.11
LF-26 sid	Sid.	I	15.90	-6.46
LF-261 sid	Sid.	I	15.48	-6.67
LF-262 sid	Sid.	II	14.22	-8.68
LF-22 sid	Sid.	II	14.55	-6.35
LF-22 qtz	Qtz.	II	14.43	
LF-23 ank	Ank.	II	13.44	-5.83
LF-24	Qtz.	II	16.17	
LF-251	Sid. Alt.	I	14.85	-7.71
LF-252	Sid. Alt.	I	15.04	-6.66
LF-253h	Sid. Alt.	I	15.08	-6.74

Appendix II (Continued)

Sample No.	**Mineral**	**Stage**	**$\delta^{18}O$** **SMOW (per mil)**	**$\delta^{13}C$** **PDB (per mil)**
COLEMAN AU-QUARTZ VEIN				
CV-1	Qtz.	Main	15.14	
CV-3	Qtz.	Main	14.80	
CV-5	Qtz.	Main	14.72	
CVU-4	Qtz.	Main	14.84	
CVU-5	Qtz.	Main	14.59	
CVU-6	Qtz.	Main	14.76	
CVU-7	host	Main	13.63	

APPENDIX III

Location and brief description of vein and host rock samples from Coeur d'Alene.

Sample no.	Approximate location	Vein type	Sample description
SUNSHINE MINE			
SSM-4	Sunshine mine (-3700 ft.)	SQT	Siderite vein
SSM-4q	As above	-	Quartz vein (subhorizontal)
SSM-4h	As above	-	Sericitic host rock (argillite) -
SSM-8h	Sunshine mine (-3100 ft.)	-	Sericitic host rock (argillite; footwall)*
SSM-9	As above	SQT	Siderite-quartz-tetrahedrite vein*
SSM-10	As above	As above	Siderite-quartz tetrahedrite vein*
SSM-11	As above	SQT	As above*
SSM-13	As above	As above	As above*
SSM-14h	As above	-	Sericitic host rock (argillite)*
SSM-15	As above	SQT	Siderite-quartz tetrahedrite vein*
SSM-16	As above	As above	Massive tetrahedrite with minor siderite and quartz (ore shoot)
SSM-9h	As above	-	Sericitic host rock (argillite; hangingwall)*
SSM-50s	Sunshine vein (unknown)	SQT	Sphalerite-galena vein
SSM-50g	As above	-	As above
	COEUR MINE		
COM-1	Coeur mine (-1300 ft.)	SQT	Quartz (siderite) vein (subvertical)
COM-2	As above	As above	Siderite-quartz tetrahedrite vein*
COM-5	Coeur mine (-1600 ft.)	As above	Quartz-siderite-tetrahedrite vein
COM-9	As above	As above	Siderite-quartz tetrahedrite vein*
COM-7	As above	As above	Siderite-quartz tetrahedrite vein*
COM-t	As above	As above	Massive tetrahedrite with minor siderite and quartz (ore shoot)
	LUCKY FRIDAY MINE		
LF-1h	Lucky Friday mine (-5500 ft.)	-	Quartzitic host rock
LF-2h	As above	-	Quartzitic host rock
LF-3h	As above	-	Quartzitic host rock (septa)
LF-4h	As above	-	Quartzitic host rock
LF-8 h	Lucky Friday mine (-5570 ft.)	-	Quartzitic host rock (hanging wall)
LF-7	As above	QSG	Galena-sphalerite-quartz-siderite vein
LF-10' q	As above	As above	Late euhedral quartz
LF-10	As above	As above	Galena-sphalerite-quartz-siderite vein
LF-11h	As above	-	Quartzitic host rock (footwall)
LF-12	Lucky Friday mine (-5560 ft.)	QSG	Galena-sphalerite-quartz-siderite vein
LF-14	As above	-	As above
LF-15	As above	-	As above
LF-19q	As above	-	As above
LF-18	As above	-	As above
LF-18h	As above	-	Quartzitic host rock
	GOLD HUNTER MINE		
LF 20	Gold Hunter mine (-4900 ft.)	-	Quartz vein (subhorizontal)
LF-20h	As above	-	Quartzitic host rock
LF-21	As above	SQS	Siderite-sphalerite vein
LF-26	As above	As above	As above

LF-22q	As above	-	Quartz vein (subhorizontal)
LF-22	As above	SQS?	Siderite vein (minor galena)
LF-23	As above	QSG	Galena-sphalerite-pyrite-quartz-siderite vein
LF-24	As above	SQS	Siderite-sphalerite vein
LF-251h	As above	-	Sericitic host rock
COLEMAN VEIN – NEW JERSEY MINE			
CV-1	Coleman vein – at the surface	Au-quartz	Quartz vein – Fe staining
CV-3	As above	As above	As above
CV-5	As above	As above	As above
CVU-1*	Coleman vein – (app. –180 ft.)	As above	As above
CVU-1	As above	As above	As above
CVU-4	As above	As above	As above
CVU-5	As above	As above	As above
CVU-6	As above	As above	As above
CVU-7	As above	As above	As above